

706

**ANALYSIS OF ELECTRON-ATOM AND ELECTRON-MOLECULE  
COLLISIONS**

by

**Osama Zaid Ibrahim Nagy  
M.Sc.**

Thesis submitted to the  
University of Stirling  
for the degree of  
Doctor of Philosophy

Department of Physics  
Atomic Physics Laboratory  
University of Stirling  
September, 1985

3/86

## ACKNOWLEDGEMENTS

It is a pleasure to acknowledge the advice, guidance and continuous encouragement given by my supervisor, Prof H. Kleinpoppen, throughout the course of my research and during the preparation of this thesis, who has at all times an interest in my work.

I would like particularly to thank Prof P. G. Burke, who by permitting me to work with his group and his help and encouragement, during my stay in the Department of Applied Mathematics and Theoretical Physics at the Queen's University of Belfast, has rendered possible to successful completion of this thesis.

I wish to record my indebtedness for the help received from other members of staff and research students in the Department of Applied Mathematics and Theoretical Physics at the Queen's University of Belfast and in the Department of Physics at Stirling University. Thanks also due to Dr's K. Blum and C. Noble for their useful discussion.

I must also offer my heart-felt thanks to my wife and all the members of my family in Egypt for their unfailing support and sincere love.

Last, but no means least, financial support by the Egyptian Government is gratefully acknowledged.

## CONTENTS

	Page
ABSTRACT	
INTRODUCTION	
CHAPTER I BASIC CONCEPTS	
I.1 Matrix Representation of the Density Operator	1
I.2 Stokes' Parameters	
I.3 Irreducible Spherical Tensors	
I.4 State and Integrated State Multipoles	
I.5 Orientation Vector and Alignment Tensor	
I.6 Spin Eigenvectors and Spin Tensors	
I.7 Vector Model and Symmetry Properties of Diatomic Molecules	
CHAPTER II RELATIVISTIC EFFECTS IN LOW ENERGY ELECTRON-ATOM SCATTERING AND SPIN POLARIZATION	13
II.1 Dirac Wave Equation and the Breit Interaction	
II.2 Choice of the Atomic Target States	
II.3 Calculation of R-Matrix and K-Matrix	
II.4 Description of Electron Spin Polarization, Cross sections and Scattering Asymmetry by Density Matrices	
CHAPTER III POLARIZATION PHENOMENAE OF RADIATION	33
III.1 Description of the Collision	
III.2 Expansion of the Integrated State Multipoles in Terms of the Reduced Density Matrix	
III.3 Effect of Perturbation on the Decaying Process	
III.4 Radiative Decay of an Excited Atom	
III.5 Stokes' Parameters Description of the Emitted Radiation	
CHAPTER IV ELECTRON SCATTERING BY DIATOMIC MOLECULES	55
IV.1 Born-Oppenheimer and Fixed-Nuclei Approximations	
IV.2 Representation of the Nuclear Motion (Rotation and Vibration)	
IV.3 Exchange and Polarization Potentials	
IV.4 Methods of solution of The Scattering Process	
CHAPTER V DISCUSSION AND NUMERICAL RESULTS	66
V.1 Low-Energy Scattering of Electrons by Caesium Atoms <sup>24,25</sup>	
V.2 Stokes' Parameter for Inelastic Electron-Caesium Scattering <sup>44</sup>	65
V.3 Vibrational Inelastic Scattering of Electron by N <sub>2</sub>	
REFERENCES	81

## ABSTRACT

The relativistic R-matrix method is used to calculate elastic and inelastic cross sections for electrons incident on caesium atoms with energies from 0 to 3 eV. In addition to the total cross sections, results are presented on the differential cross section,  $\sigma$ , and the spin polarization,  $P_y$ , of the scattered electrons as a function of energy at eight scattering angles ( $10^\circ$ ,  $30^\circ$ ,  $50^\circ$ ,  $70^\circ$ ,  $90^\circ$ ,  $110^\circ$ ,  $130^\circ$ ,  $150^\circ$ ). Also the differential cross section, spin polarization and the left-right asymmetry function,  $A_s$ , are calculated as a function of the scattering angles at a number of chosen values of energies. The calculation reveals a wealth of resonances around  $^2p_{1/2}$  and  $^2p_{3/2}$  thresholds. The resonances are analysed in detail and their role in the scattering process is discussed.

The density matrix formalism is used to derive expressions for the Stokes' Parameters to describe the state of the photons emitted in electron-atom collision experiment. Numerical results for the Stokes Parameters of the light emitted in the decay  $6p \ ^2p_{1/2, 3/2} \rightarrow 6s \ ^2S_{1/2}$  in atomic caesium after electron impact excitation are presented and compared with the available measurements. These results show what effects can be expected and may be useful for the planning of future experiments.

The angular distribution and the integrated cross sections have been calculated at incident electron energies 20, 25 and 30 eV, in  $e-N_2$  scattering. The calculations are based on the use of numerical basis functions in the R-Matrix method, and exchange and polarization effects are included. Also variation of the mixing parameter, between p- and f- partial waves and the individual eigenphases with the internuclear distance are presented. The mixing parameter has shown to be a rapidly varying function of the internuclear distance contradicting the assumption made by Chang (1977).

## INTRODUCTION

Electrons play a central part in atomic and molecular physics. Because of their small mass, electrons are much more active than the nuclei in this microscopic world. Knowledge of the behaviour of electrons is essential in understanding a large variety of problems such as gaseous electronics, fusion plasmas, ionospheres, auroras, stellar atmospheres and interstellar gases.

The outcome of electron-atom or electron-molecule collision processes is studied through scattering experiments under some suitable arrangements and physical conditions. Those physical conditions which determine what approximation scheme should be applied incorporating with the quantum theory of scattering. However, the theoretical treatment of electron-molecule collision has features as distinct from those of the electron-atom collision. This makes the solution of the electron-molecule system more complicated than the electron-atom one. These complications arise because the molecules have rotational and vibrational degrees of freedom, the electron-molecule interactions is essentially multicentered and nonspherical and lastly molecular targets can dissociate in collision with an electron.

In recent years there has been an increasing interest, both experimental and theoretical in the low energy scattering of electrons by heavy atoms and by molecules. In this contribution we present some recent theoretical results on the scattering of low energy electrons from heavy atomic targets, caesium, and on the scattering of electrons by  $N_2$ - molecule at intermediate energies.

Following some important concepts which form the basis of the theory in chapter I, chapter II contains a fuller discussion on the relativistic R-matrix theory and expressions for the total and

differential cross sections. Spin polarization and scattering asymmetry are also given. In chapter III the density matrix formalism is applied to describe the polarization state of the photons emitted from a heavy atom excited by electron impact. Methods of solution of the electron-molecule collision problem and the approximations used are briefly presented in chapter IV. In chapter V we discuss some implications of our work and illustrate their usefulness through numerical calculations.

## CHAPTER I

### BASIC CONCEPTS

Throughout this chapter we present some important concepts which form the basis of the theory.

#### I.1 Matrix Representation of The Density Operator

The dynamical state of a system must no longer be represented by a unique vector, but by a statistical mixture of vectors. If the dynamical state of a quantum system is completely known (one has succeeded in determining precisely the variables of one of the complete sets of compatible variable associated with the system) it is said to be in a pure state. States which are not pure are called mixed states or mixtures. Mixtures are states identified by less than maximum information, ie are not described by a single wavefunction. Therefore in order to describe mixed states the density operator is introduced<sup>1,2,3</sup> by the expression

$$\rho = \sum_i |\psi_i\rangle W_i \langle\psi_i| \quad i = 1, 2, \dots \quad (I.1-1)$$

where  $W_i$  are the probabilities for the system being in a set of pure states  $|\psi_i\rangle$ . In particular for a pure state  $|\psi\rangle$  the density operator turns out to be

$$\rho = |\psi\rangle \langle\psi| \quad (I.1-2)$$

In general the density matrix element can be deduced from equation (I.1-1), by sandwiching it between the two states of interest, as follows:

$$\begin{aligned} \rho_{ij} &= \langle\psi_i|\rho|\psi_j\rangle \\ &= \sum_k a_{ik} W_k a_{jk}^* \end{aligned} \quad (I.1-3)$$

where  $\psi_i$  can be expanded in terms of a set of orthogonal basis

$$|\psi_i\rangle = \sum_k a_{ik} |\phi_k\rangle \quad (1.1-4)$$

For our purpose we lay down some properties<sup>2</sup> of the density operator

(i) the density operator is a positive definite, hermitian operator of trace equal to unity.

(ii) For a mixed state, the following relation holds

$$\text{tr } \rho^2 < (\text{tr } \rho)^2,$$

whereas only for a pure state, we have

$$\text{tr } \rho^2 = (\text{tr } \rho)^2$$

(iii) For any observable quantity A the expectation value  $\langle A \rangle$  is related to  $\rho$  through the equation

$$\langle A \rangle = \frac{\text{tr } \rho A}{\text{tr } \rho} \quad (1.1-5)$$

(iv) In the  $|+\frac{1}{2}\rangle$  representation  $\rho$  is given by

$$\begin{aligned} \rho &= \frac{1}{2} \begin{pmatrix} 1 + P_z & P_x - iP_y \\ P_x + iP_y & 1 - P_z \end{pmatrix} \\ &= \frac{1}{2} [I + \mathbf{P} \cdot \boldsymbol{\sigma}] \end{aligned} \quad (1.1-6)$$

where  $P_x, P_y, P_z$  are the cartesian components of the polarization vector  $\underline{P}$ , and where the two-by-two unit matrix and the Pauli spin matrix are defined as

$$I = \begin{pmatrix} 1 & 0 \\ 0 & 1 \end{pmatrix} \quad \sigma_1 = \begin{pmatrix} 0 & 1 \\ 1 & 0 \end{pmatrix} \quad \sigma_2 = \begin{pmatrix} 0 & -i \\ i & 0 \end{pmatrix} \quad \sigma_3 = \begin{pmatrix} 1 & 0 \\ 0 & -1 \end{pmatrix} \quad (1.1.7)$$

The main virtue of the density matrix is its analytical power in the construction of general formulae and in proving general theorems. In fact, the specification of this operator is sufficient to determine all physically measurable quantities. This procedure has the advantage of providing uniform treatment for the pure states and the mixtures.

## 1.2 Stokes' Parameters

In the decay of an excited atomic state the emitted photons

may be observed in the direction of the unit vector  $\hat{n}_\gamma$  with polar angles  $\theta_\gamma, \phi_\gamma$  with respect to the collision system  $x, y, z$ , figure (1). Due to the transverse nature of the electromagnetic waves the polarization vector of photons is characterised by two linearly independent basis vectors  $e_1$ , and  $e_2$  in a plane perpendicular to  $\hat{n}_\gamma$ , as follows:

$$\begin{aligned}\hat{e}_1 &\equiv e_1(\theta_\gamma + 90, \phi_\gamma) \\ \hat{e}_2 &\equiv e_2(\theta_\gamma, \phi_\gamma + 90)\end{aligned}\tag{I.2-1}$$

where  $\hat{e}_1$ , and  $\hat{e}_2$  are pointing in the direction of increasing  $\theta_\gamma$  and  $\phi_\gamma$ , respectively.

The three basis vectors  $\hat{n}_\gamma, \hat{e}_1$ , and  $\hat{e}_2$  define a coordinate system called the detector frame with  $\hat{n}_\gamma$  as a quantization axis. The Stokes' parameters<sup>3,4,5</sup> are defined with respect to this detector frame in the following:

- (i) The total intensity  $I$  of the emitted photons

$$I = I(0^\circ) + I(90^\circ) = I(45^\circ) + I(135^\circ) = I(\text{RHS}) + I(\text{LHS})\tag{I.2-2}$$

- (ii) The degree of linear polarization  $\eta_3$  with respect to  $x$ - and  $y$ - axes

$$\eta_3 = \frac{I(0^\circ) - I(90^\circ)}{I(0^\circ) + I(90^\circ)}\tag{I.2-3}$$

- (iii) The degree of linear polarization  $\eta_1$ , with respect to two orthogonal axes oriented at 45 degrees to the  $x$ - axis

$$\eta_1 = \frac{I(45^\circ) - I(135^\circ)}{I(45^\circ) + I(135^\circ)}\tag{I.2-4}$$

where  $I(\alpha^\circ)$  is the fraction of intensity of a given beam which has passed a linear polarizer with transmission axis at angle  $\alpha^\circ$  to the axis  $e_1$ .

- (iv) The degree of circular polarization  $\eta_2$

$$\eta_2 = \frac{I(\text{RHS}) - I(\text{LHS})}{I(\text{RHS}) + I(\text{LHS})}\tag{I.2-5}$$

where  $I(\text{RHS})$  ( $I(\text{LHS})$ ) is the intensity of right (left) handed circularly polarized light.

In matrix notation the Stokes' parameters are grouped in the matrix form

$$\rho_{\lambda'\lambda} = \frac{I}{2} \begin{pmatrix} 1 + \eta_2 & -\eta_3 + i\eta_1 \\ -\eta_3 - i\eta_1 & 1 - \eta_2 \end{pmatrix} \quad (\text{I.2-6})$$

where  $\rho_{\lambda'\lambda}$  is the matrix element of the density operator  $\rho$ ,  $\lambda'(\lambda)$  is the helicity, taking values  $\pm 1$ . The normalization to the relevant intensity is chosen by the relation

$$\text{tr } \rho_{\lambda'\lambda} = I \quad (\text{I.2-7})$$

Using the normalization condition (I.2-7) and the fact that the matrix (I.2-6) is hermitian, we find only three parameters  $\eta_1, \eta_2, \eta_3$  are linearly independent.

### 1.3 Irreducible Spherical Tensors

The subject of irreducible tensor operators occupies a central position in the modern theory of angular momentum. When the angular symmetries of the ensemble of interest are important it is convenient to expand the density matrix operator  $\rho$  in terms of a basis set of operators defined by its transformation properties under changes of the coordinate system, these changes are rotations and inversions. Such a set of operators are the irreducible tensor operators. This method provides a well developed and efficient way of using the inherent symmetry of the system. It also enables the consequences of angular momentum conservation to be simply allowed for. Furthermore, one can separate the dynamical and geometrical factors in the equations of interest, without much effort, by using the "Wigner-Eckart Theorem".

A general tensor operator  $T_K$  of rank  $K$  is defined as a quantity represented by  $(2K + 1)$ - components,  $T_{KQ}$ , which transform according

to the irreducible representation of a rotation group by the transformation equation 6

$$\begin{aligned} T'_{KQ} &= R T_{KQ} R^{-1} \\ &= \sum_q T_{KQ} D(\alpha\beta\gamma)_{qQ}^{(K)} \end{aligned} \quad (1.3-1)$$

where  $(\alpha\beta\gamma)$  are the Euler angles, the rotation operator  $R$  takes the old system, unprimed, to the new system, primed, and  $D(\alpha\beta\gamma)_{qQ}^{(K)}$  are the matrix elements of  $R$  in the  $KQ$ -representation. Therefore, the tensor  $T_K$  transforms like a spherical harmonic of order  $K$ .

Consider now a degenerate energy level of the physical system which may include states with different angular momentum quantum numbers  $j, j', \dots$ . It is convenient to construct the set of tensor operators  $T(j'j)_{KQ}$  from the angular momentum states by applying the usual angular momentum coupling rules, in the form:

$$T(j'j)_{KQ} = \sum_{M_j M'_j} \sum_{j} (-1)^{j-M_j} (j' M'_j, j - M_j | KQ) | j' M'_j \rangle \langle j M_j | \quad (1.3-2)$$

where,

$$|j-j'| \leq K \leq j + j' \quad -K \leq Q \leq K$$

and  $(j' M'_j, j - M_j | KQ)$  is the well-known Clebsch-Gordan coefficient.

Beside the transformation property under rotation, equation (1.3-1), the irreducible tensor operators have the following important properties:

(i) the orthogonality property is defined as

$$\begin{aligned} \text{tr} T(j'j)_{KQ} T(j'j)_{kq}^\dagger &= \delta_{Kk} \delta_{Qq} \delta_{jj'} \\ T(j'j)_{KQ}^\dagger &= (-1)^{j'-j+Q} T(j'j)_{K,-Q} \end{aligned} \quad (1.3-3)$$

where  $T(j'j)_{KQ}^\dagger$  is the hermitian adjoint of  $T(j'j)_{KQ}$ .

(ii) Matrix elements of the irreducible tensor operators between any pair of desired states have a property known as the "Wigner-Eckart

Theorem". Namely, that the matrix elements with equal values of  $j$ ,  $j'$  and  $K$ , but with different  $M_j$  and  $M_j'$  and  $Q$  bear fixed ratios to one another. These ratios depend on  $j$ ,  $j'$  and  $K$  of the set of operators, but do not depend on the nature of the operators. This can be expressed in the equation

$$\langle j' M_j' | T(j' j)_{KQ} | j M_j \rangle = (-1)^{K-Q} (2j + 1)^{-\frac{1}{2}} (j' - M_j', KQ | j - M_j) \times \langle j' || T_K || j \rangle \quad (1.3-4)$$

In equation (1.3-4) the Clebsch-Gordan coefficient, geometrical factor, contains all the dependence on magnetic quantum numbers, whereas the reduced matrix element reflects the dynamics of the interaction.

#### 1.4 State and Integrated State Multipoles

The set of irreducible tensor operators  $T(j' j)_{KQ}$  is complete and hence any function of angular momentum operators can be expanded in terms of this set. Particularly, for the density matrix operator we get the expansion

$$\begin{aligned} \rho &= \sum_{KQ} \text{tr} [\rho T(j' j)_{KQ}^\dagger] T(j' j)_{KQ} \\ &= \sum_{KQ} \langle T(j' j)_{KQ}^\dagger \rangle T(j' j)_{KQ} \end{aligned} \quad (1.4-1)$$

where the mean values  $\langle T(j' j)_{KQ}^\dagger \rangle$  is called the state multipoles or the statistical tensor<sup>7</sup> which are closely related to the moments of the angular momentum operators. Thus the density operator is completely characterized in terms of the state multipoles. The matrix element of the density operator is given by

$$\langle j' M_j' | \rho | j M_j \rangle = \sum_{KQ} (-1)^{j-M_j} (j' M_j', j - M_j | KQ) \langle T(j' j)_{KQ}^\dagger \rangle. \quad (1.4-2)$$

Using the orthogonality property of the Clebsch-Gordan coefficients we have

$$\langle T(j'j)_{KQ}^{\dagger} \rangle = \sum_{M'_j} \sum_{M_j} (-1)^{j-M_j} \langle j'M'_j, j-M_j | KQ \rangle \langle j'M'_j | \rho | jM_j \rangle$$

(I.4-3)

In the following we sum up some of the properties of state multipoles.

(i) the number of independent state multipoles is restricted by the definition of its complex conjugate

$$\langle T(j'j)_{KQ}^{\dagger} \rangle^* = (-1)^{j'-j+Q} \langle T(j'j)_{K-Q}^{\dagger} \rangle$$

(I.4-4a)

In particular for states of well defined angular momentum ( $j' = j$ ) we have

$$\langle T(j)_{KQ}^{\dagger} \rangle^* = (-1)^Q \langle T(j)_{K-Q}^{\dagger} \rangle$$

(I.4-4b)

Some more restrictions on the state multipoles arise due to symmetry properties of the atomic systems.<sup>8</sup> Without spin polarization analysis before and after scattering the geometry of the experiment possesses reflection invariance in the scattering plane yielding the constraints

$$\langle T(j)_{KQ}^{\dagger} \rangle = (-1)^{K+Q} \langle T(j)_{K-Q}^{\dagger} \rangle$$

(I.4-5)

which give, after using equation (I.4-4b), the equation

$$\langle T(j)_{KQ}^{\dagger} \rangle^* = (-1)^K \langle T(j)_{KQ}^{\dagger} \rangle$$

(I.4-6)

If one of the incident beams has a component of the polarization vector in the scattering plane,  $xz$ -plane in figure 2a, equation (I.4-6) no more holds. But when both the polarization vectors of the incident beams lie perpendicular to the scattering plane,  $xz$ -plane in figure 2b, equation (I.4-6) stands again.

(ii) The transformation properties of the state multipoles under rotation obey the rule

$$\langle T(j'j)_{KQ}^{\dagger} \rangle = \sum_q \langle T(j'j)_{kq}^{\dagger} \rangle D(\alpha\beta\gamma)_{qQ}^{(K)*} \quad (\text{I.4-7a})$$

and the inverted form is

$$\langle T(j'j)_{kq}^{\dagger} \rangle = \sum_Q \langle T(j'j)_{KQ}^{\dagger} \rangle D(\alpha\beta\gamma)_{qQ}^{(K)} \quad (\text{I.4-7b})$$

This shows that state multipoles transform as irreducible tensors of rank  $K$  and component  $Q$ .

In measurements where the scattered electrons are not registered in coincidence with the emitted photons, we integrate equation (I.4-3) over all the electronic scattering angles,  $d\Omega_e$ , to get

$$\langle \mathcal{T}(j'j)_{KQ}^{\dagger} \rangle = \int d\Omega_e \langle T(j'j)_{KQ}^{\dagger} \rangle \quad (\text{I.4-8})$$

Due to this integration more restrictions<sup>9</sup> will be imposed on the integrated state multipoles (equation (I.4-8)). In chapter III we lay down these further restrictions.

### I.5 Orientation Vector and Alignment Tensor

The three components of the tensor  $\langle T(j)_{1Q}^{\dagger} \rangle$ , ( $Q = 0, \pm 1$ ), transform as the components of a vector and they are often called the components of the orientation vector. The tensor  $\langle T(j)_{2Q}^{\dagger} \rangle$ , ( $Q = 0, \pm 1, \pm 2$ ), is called the alignment tensor, whereas the tensor  $\langle T(j)_{00}^{\dagger} \rangle$  is merely a normalization constant.

In the state multipole language (for more detailed discussion see ref<sup>8</sup>) we call the system to be oriented if at least one of the components of the orientation vector is different from zero. Otherwise, we call the system to be aligned if at least one of the components of the alignment tensor is different from zero. More generally a system is said to be polarized if at least one multipole  $\langle T(j)_{KQ}^{\dagger} \rangle$  with  $K$  not equal to zero is nonvanishing.

### 1.6 Spin Eigenvectors and Spin Tensors

The set of basis vectors  $|jm\rangle$  of an angular momentum operator has a certain transformation properties under infinitesimal rotations,<sup>10</sup> and are normalized according to the equation

$$\langle j'm' | jm \rangle = \delta_{jj'} \delta_{mm'} \quad (1.6-1)$$

There is, however a useful notation for these eigenvectors, namely to write them as column vectors;

$$\begin{pmatrix} \delta_{j,m} \\ \delta_{j-1,m} \\ \vdots \\ \delta_{-j,m} \end{pmatrix}$$

In particular the spin- $\frac{1}{2}$  eigenvectors may be written as

$$|\frac{1}{2}\frac{1}{2}\rangle \sim \begin{pmatrix} 1 \\ 0 \end{pmatrix} \quad |\frac{1}{2}-\frac{1}{2}\rangle \sim \begin{pmatrix} 0 \\ 1 \end{pmatrix} \quad (1.6-2)$$

Using equation (1.4-2), we obtain the matrix element of a spin- $\frac{1}{2}$  particles as:

$$\langle \frac{1}{2}m' | \rho | \frac{1}{2}m \rangle = \sum_{kq} (-1)^{\frac{1}{2}-m} (\frac{1}{2}m', \frac{1}{2}-m | kq) \langle t(\frac{1}{2})_{kq}^+ \rangle \quad (1.6-3)$$

which give

$$\langle t(\frac{1}{2})_{kq}^+ \rangle = \sum_{mm'} (-1)^{\frac{1}{2}-m} (\frac{1}{2}m', \frac{1}{2}-m | kq) \langle \frac{1}{2}m' | \rho | \frac{1}{2}m \rangle \quad (1.6-3)$$

The state multipole,  $\langle t(\frac{1}{2})_{kq}^+ \rangle$ , is normally called the spin tensor and the Clebsch-Gordan coefficient in equations (1.6-2) and (1.6-3) restricts the values of  $k$  to be only 0 or 1.

### 1.7 Vector Model and Symmetry Properties of Diatomic Molecules

The classification of molecular states is very similar to that for atoms, except that the quantum numbers,  $J$  and  $L$  that describe atomic terms are replaced by quantum numbers  $\Omega$  and  $\Lambda$  that determine the component of angular momentum along the internuclear axis.

In a diatomic molecule, the electrons move in an electrostatic field that is symmetric about the internuclear axis connecting the two nuclei. If this field is weak, the vector  $\underline{L}$  representing the vector sum of the orbital angular momenta of all the individual electrons precesses about the internuclear axis, figure (3), with quantized component  $M_L$  about the axis where

$$M_L = L, L-1, \dots, -L \quad (1.7-1)$$

In most molecules, the electrostatic field due to the nuclei is so strong that  $\underline{L}$  precesses very rapidly, and only the component of orbital momentum along the axis is defined; to describe this a quantum number is introduced:

$$\Lambda = |M_L| = 0, 1, 2, \dots, L \quad (1.7-2)$$

The electronic states of the molecule are designated  $\Sigma, \pi, \Delta, \phi, \dots$ , as  $\Lambda = 0, 1, 2, 3, \dots$ , respectively.

Also as in atoms with LS-type coupling, the individual electron spins form a resultant  $\underline{S}$ . The multiplicity  $(2S + 1)$  of a term is designated by a superscript. For instance, the two electrons in the hydrogen molecule can form a series of singlet  $^1\Sigma, ^1\pi, \dots$ , and triplet  $^3\Sigma, ^3\pi, \dots$ , terms. The orbital motion of the electrons in states with  $\Lambda > 0$  produces a magnetic field directed along the internuclear axis which causes  $\underline{S}$  to precess about this axis with quantized component  $M_S$  where

$$M_S = S, S-1, \dots, -S \quad (1.7-3)$$

For  $\Sigma$ - electronic states there is no resultant magnetic field due to the orbital electron motion, and so the quantum number  $M_S$  is not defined, these states have only one component whatever the multiplicity is.

The sum of the components  $\underline{L}$  and  $\underline{S}$  along the internuclear axis gives the component of the total angular momentum about the axis with quantized component  $\Omega$

$$\Omega = |\Lambda + M_S| \quad (1.7-4)$$

where  $\Omega$  can have either integral or half-integral values and is written as a subscript to the term symbol.

The geometrical arrangement of the nuclei in a diatomic molecule exhibit certain symmetry operations, such as rotation by any angle about the internuclear axis and reflection in any plane passing through both nuclei. Neither of these operations alters the axially symmetric potential field in which the electrons move, the electronic energy is said to be invariant under the operations.

A plane of reflection is a two-way mirror. If such a plane can be placed in a molecule and the result of a double reflection looks the same as the original molecule, then we have

$$A_R^2 |\Psi\rangle = (+1) |\Psi\rangle \quad (1.7-5)$$

where  $A_R$  is the reflection operator and  $\Psi$  is the electronic wavefunction. This allows two possible eigenvalues (+1) and (-1) for the reflection operator with corresponding eigenfunctions which we distinguish as  $\Psi^+$  and  $\Psi^-$ , respectively. Each component of a doubly degenerate state with  $\Lambda > 0$  may be distinguished as  $\pi^+$ ,  $\pi^-$ ,  $\Delta^+$ ,  $\Delta^-$ , . . ., according to its behaviour upon reflection.  $\Sigma$ - states are not degenerate and have only one component, but can still be classified as either  $\Sigma^+$  or  $\Sigma^-$ .

For molecules which have a centre of symmetry, such as

homonuclear diatomic molecules, an additional symmetry operation for these is inversion through the midpoint of the internuclear axis. If the centre of symmetry is taken as the origin of the cartesian coordinate system and by carrying out the inversion operation twice in succession the original wavefunction is obtained. Therefore, the eigenvalue of the square of the inversion operator  $A_I^2$  is (+1), and so  $A_I$  itself has the eigenvalues (+1) or (-1); the wavefunction either remains unchanged upon inversion and is called 'even' or 'g' ('gerade'), or changes sign only and is called 'odd' or 'u' ('ungerade'). The symbols g and u are written as subscripts to the term symbol such as  $\Sigma_g$ ,  $\Sigma_u$ ,  $\pi_g$ ,  $\pi_u$ .

## CHAPTER II

RELATIVISTIC EFFECTS IN LOW ENERGY ELECTRON-ATOM  
SCATTERING AND SPIN-POLARIZATION

The study of relativistic effects in atomic structure theory have been done first by Sommerfeld<sup>10</sup> and the basic ideas were given in refs 11,12,13,14,15. Recently, with the help of the simplification encountered through the use of tensor operator techniques<sup>6</sup> and the very powerful electronic computers, the greater complexity of the scattering problem due to introducing the relativistic effects has been facilitated. Furthermore the increasing precision of experimental data, particularly that of hyperfine-structure, has progressively demonstrated the necessity of introducing relativistic effects into the study of atomic properties. Many detailed studies of this work have already been reviewed.<sup>16,17,18,19</sup>

Relativistic calculations are introduced into the electron-atom problem in several ways:

- (i) In the case of very heavy atoms, relativistic calculations<sup>20,21</sup> based on the Dirac wave equation are the only satisfactory way of proceeding.
- (ii) If the energy separations between fine-structure levels are small the parameters obtained from nonrelativistic calculations in LS-coupling scheme can be recoupled to account for these levels. For energies above all the threshold energies, the effects of intermediate coupling in the target can be included by this method. This method is used by Burke and Mitchel<sup>38</sup> to account for the cross sections when some of the channels are closed.
- (iii) For intermediate weight atoms, relativistic calculations<sup>22,23</sup> can be dealt with through the Breit-Pauli Hamiltonian.

In more recent publications<sup>24,25</sup> we reported our first results, using the third of these approaches combined with the R-matrix

method<sup>26</sup>, on the low energy scattering of electrons by caesium atoms.

Now we present a fuller account of the calculation, more detailed discussion of the results will be given in chapter V. We begin by viewing, in the next section, some concepts which are the starting point of any relativistic calculation of atomic properties.

## II.1 Dirac Wave Equation and the Breit Interaction

For an infinitely heavy nucleus of nuclear charge  $Z$ , concerning only with the motion of the electrons, Dirac approached the problem of finding a relativistic wave equation<sup>12</sup> by starting from the Hamiltonian

$$i \frac{\partial}{\partial t} \Psi = H \Psi \quad (\text{II.1-1})$$

which leads to the Dirac wave equation for an electron in a spherically symmetric potential (throughout this thesis we use atomic units)

$$(i \frac{\partial}{\partial t} - H_D) \Psi = 0 \quad , \quad (\text{II.1-2})$$

$$H_D = c(\underline{\alpha} \cdot \underline{p}) + \beta c^2 + V(\underline{r}) \quad , \quad (\text{II.1-3})$$

associated with the postulates:

- (i) It must satisfy the requirements of special relativity.
- (ii) In field free space it must agree with the Klein-Gordon equation.
- (iii) The Hamiltonian  $H_D$  must be linear in the space derivative.

In equation (II.1-3),  $V(\underline{r})$  is the potential energy,  $c$  is the speed of light and  $\underline{p}$  is the linear momentum operator. The operators  $\underline{\alpha}$  and  $\beta$  must be hermitians, as a consequence of the hermiticity of  $H_D$ , and their matrix representations are related to the two-by-two unit matrix and the Pauli spin matrix, defined in equation (I.1-7), through the relations

$$\underline{\alpha} = \begin{pmatrix} 0 & \sigma \\ \sigma & 0 \end{pmatrix} \quad \beta = \begin{pmatrix} I & 0 \\ 0 & I \end{pmatrix} \quad (\text{II.1-4})$$

A characteristic feature of the Dirac wave equation is that the spin of the particle is intrinsically included into the theory from the beginning. Moreover, the Dirac Hamiltonian, equation (II.1-3), is invariant under rotation and reflection,

$$[H_D, \hat{J}] = 0 \quad [H_D, \beta_P] = 0 \quad (\text{II.1-5})$$

where  $\hat{J}$  is the total angular momentum operator and  $\beta_P$  is the Dirac equivalent of the parity operator. Therefore solutions of the Dirac wave equation in a central field may be classified in terms of eigenstates of  $\underline{J}^2$ ,  $J_z$  and parity.

Concerning with interacting electrons, the Dirac wave equation is not sufficient. The Breit Hamiltonian<sup>19,27</sup> is the most commonly used approximation to account for this interaction. For N- electrons moving in the field of a point heavy nucleus of charge Z, the Breit Hamiltonian takes the form:

$$(H_P - \sum_{i=1}^N H_{D_i} - \sum_{i<j} \frac{1}{r_{ij}}) \psi = - [ \sum_{i<j} \frac{(\underline{\alpha}_i \cdot \underline{\alpha}_j)}{2r_{ij}} + \frac{(\underline{\alpha}_i \cdot \underline{r}_{ij})(\underline{\alpha}_j \cdot \underline{r}_{ij})}{2r_{ij}^3} ] \psi \quad (\text{II.1-6})$$

where

$$r_{ij} = |\underline{r}_i - \underline{r}_j|$$

The sum over the Dirac Hamiltonians is the one-body part in equation (II.1-6). The RHS represents the two-body part of the problem and is called the Breit interaction which accounts for perturbations due to magnetic and retardation effects.

Assuming that the interaction of more than two electrons do not simultaneously contribute, then equation (II.1-6) may be generalised to the (N + 1)- electron problem. Reduction of the corresponding Hamiltonian to the Pauli form by expanding the expectation value in

$\alpha^2$  ( $\equiv \frac{c^2}{u}$  in a u) by a valid perturbation expansion results in the Breit Pauli Hamiltonian.

Thus, for an electron incident upon an N-electron atom the Breit-Pauli Hamiltonian is written as

$$H_{BP}^{N+1} = H^{N+1} + \underline{H}^{N+1} \quad (\text{II.1-7})$$

where  $H^{N+1}$  refers to a summation over the nonrelativistic single particle Hamiltonian.  $\underline{H}^{N+1}$  stands for the relativistic perturbations, which is given by

$$\underline{H}^{N+1} = H_{SS}^{N+1} + H_{SO}^{N+1} + H_{OO}^{N+1} + H_{SOO}^{N+1} + H_{SSC}^{N+1} + H_m^{N+1} + H_{D_1}^{N+1} + H_{D_2}^{N+1} \quad (\text{II.1-8})$$

where the relativistic Hamiltonians are defined as follows:

- Spin-spin interaction

$$H_{SS}^{N+1} = \alpha^2 \left[ \sum_{i < j}^{N+1} \frac{(\underline{S}_i \cdot \underline{S}_j)}{r_{ij}^3} - \frac{3}{r_{ij}^5} (\underline{S}_i \cdot \underline{r}_{ij})(\underline{S}_j \cdot \underline{r}_{ij}) \right] \quad (\text{II.1-9})$$

which can be viewed as arising from the magnetic interaction between the spins of two electrons

- Spin-orbit interaction

$$H_{SO}^{N+1} = \alpha^2 \cdot \frac{Z}{2} \cdot \sum_{i=1}^{N+1} \frac{\underline{l}_i \cdot \underline{S}_i}{r_i^3} \quad (\text{II.1-10})$$

It refers to the familiar interaction between the spin of an electron and its orbit.

- Orbit-orbit interaction

$$H_{OO}^{N+1} = -\alpha^2 \sum_{i < j}^{N+1} \left[ \frac{\underline{P}_i \cdot \underline{P}_j}{2r_{ij}} + \frac{(\underline{r}_{ij} \cdot \underline{P}_i)(\underline{r}_{ij} \cdot \underline{P}_j)}{2r_{ij}^3} \right], \quad (\text{II.1-11})$$

this arises classically from the magnetic interaction between the orbits of two electrons.

- Spin-other orbit interaction

$$H_{\text{SOO}}^{N+1} = -\alpha^2 \sum_{i \neq j}^{N+1} \frac{(\underline{r}_{ij} \times \underline{p}_i) \cdot (\underline{s}_i \cdot 2\underline{s}_j)}{2r_{ij}^3} \quad (\text{II.1-12})$$

this describes the magnetic interaction between the spin of one electron and the orbit of another

- Spin contact interaction

$$H_{\text{SCC}}^{N+1} = -8\pi\alpha^2 \sum_{i < j}^{N+1} (\underline{s}_i \cdot \underline{s}_j) \delta(\underline{r}_{ij}) \quad (\text{II.1-13})$$

The interaction arising from the spins of two electrons that are touching.

- Mass correction term

$$H_{\text{m}}^{N+1} = -\left(\frac{\alpha^2}{8}\right) \sum_{i=1}^{N+1} v_i^4, \quad (\text{II.1-14})$$

it is the mass correction due to relativistic velocities.

Lastly the two terms,

$$H_{\text{D}_1}^{N+1} = -\left(\frac{\alpha^2 Z}{8}\right) \sum_{i=1}^{N+1} \left(\frac{v_i}{r_i}\right)^2, \quad (\text{II.1-15})$$

$$H_{D_2}^{N+1} = \left(\frac{\alpha}{4}\right)^2 \sum_{i=1}^{N+1} \left(\frac{\nabla_i^2}{r_{ij}}\right),$$

(II.1-16)

are the one- and two-body Darwin terms, respectively.

We note that the fine structure terms in equations (II.1-9), (II.1-10) and (II.1-12) commute with  $\underline{J}^2$ ,  $J_z$  and parity. Thus it is convenient to choose a representation which is diagonal in  $\underline{J}^2$ ,  $J_z$  and parity.

Another formulae<sup>19,27</sup> are given to express the interactions felt by the relativistic electrons as a product of a radial function and an angular function. Furthermore the angular dependence is given in terms of spherical tensors.

## II.2 Choice of the Atomic Target States

The accuracy of the R-matrix method<sup>26</sup> depends essentially upon the quality of the atomic target states introduced into the calculation. This is because, as is to be seen later, the radius of the boundary of the internal region is defined by these states. Adding to that the bound state orbitals, which are used to represent these states, are also used in the representation of the electron-atom collision wavefunction.

For a heavy atom containing N-electrons the atomic wave functions, which must be eigenfunctions of  $\underline{J}^2$ ,  $J_z$  and parity, are expanded<sup>26,28</sup> in the form

$$\phi_i = \sum_j b_{ij} \phi_j \quad (\text{II.2-1})$$

where the summation over j includes all configurations and where the total

orbital angular momentum  $\underline{L}$  and the total spin angular momentum  $\underline{S}$  add vectorially to give  $\underline{J}$ . All configurations are built-up from one-electron orbitals coupled together to give a function which is completely antisymmetric with respect to interchange of the space and spin coordinates of any two electrons. Each orbital is a product of a radial function, a spherical harmonic and a spin function

$$U_{n\ell m_\ell}(\underline{r}, m_s) = r^{-1} P_{n\ell}(r) Y_{\ell}^{m_\ell}(\theta, \phi) \chi(\frac{1}{2}m_s), \quad (\text{II.2-2})$$

where the radial functions themselves are required to satisfy the orthonormality relations

$$\langle P_{n\ell} | P_{n'\ell} \rangle = \delta_{nn'}, \quad (\text{II.2-3})$$

Assuming that the changes induced on the radial functions, felt by the relativistic electrons, are of negligible importance, which is true for intermediate weight atoms. Then the radial functions  $P_{n\ell}$  can be determined in the LS-coupling scheme.<sup>29</sup> Therefore equation (II.2-1) can be replaced by

$$\psi_i = \sum_{j=1}^k a_{ij} \psi_j, \quad (\text{II.2-4})$$

where in this case the index  $j$  must then represent the coupling of the  $N$ -orbitals to form eigenfunctions of  $L^2$ ,  $S^2$ ,  $L_z$  and  $S_z$ . The coefficients  $a_{ij}$  are determined by diagonalising the nonrelativistic atomic Hamiltonian

$$\langle \psi_i | H^N | \psi_j \rangle = \epsilon_i^N \delta_{ij} \quad (\text{II.2-5})$$

The radial functions are expanded in the Slater form

$$P_{n\ell}(r) = \sum_j C_{jn\ell} r^{I_{jn\ell}} \text{EXP}(-\xi_{jn\ell} r) \quad .$$

(II.2-6)

The radial functions are now refined by varying the nonlinear parameters  $\xi_{jn\ell}$  and recalculating the linear expansion coefficients  $C_{jn\ell}$  so the orthonormality conditions (II.2-3) are satisfied. The atomic Hamiltonian is then rediagonalized and the process repeated until the required eigen-energies  $\epsilon_i^N$  are minimized. Once we obtain the radial functions the coefficients  $b_{ij}$  in equation (II.2-1) can be determined by diagonalizing the Breit-Pauli Hamiltonian

$$\langle \phi_i | H_{BP}^N | \phi_j \rangle = E_i^N \delta_{ij} \quad \text{(II.2-7)}$$

### II.3 Calculation of R-matrix and K-matrix

The essential idea of the R-matrix method is that configuration space describing the scattered particle and the target is divided into two regions. In the internal region ( $r < a$  where  $r$  is the relative coordinate of the colliding particles) there is a strong many-body interaction and the collision process is difficult to calculate. In the external region ( $r > a$ ), on the other hand, the interaction is weak and in many cases is exactly solvable in terms of plane waves or of Coulomb waves. In the internal region a complete discrete set of states describing all the particles is defined by imposing logarithmic boundary conditions on the surface of this region. This R-matrix basis can then be used to expand the collision wavefunction at any energy and in particular to obtain the logarithmic derivative of this wavefunction on the boundary. From this information and the known solution in the external region the K-matrix can be calculated.

We are now in a position to define the (N+1)-electron R-matrix basis functions as follows

$$\psi_k = \sum_{ij} c_{ijk} \phi_i U_j + \sum_j d_{jk} \phi_j \quad ,$$

(II.3-1)

for each  $\underline{J}$  and parity combination, the functions  $\phi_i$ , are a finite set of atomic eigenstates or pseudostates satisfying equation (II.2-7), which are coupled with the angular and spin functions of the incident electron to form a channel eigenstates of  $\underline{J}^2$ ,  $J_z$  and parity. The  $\phi_j$  are (N+1)-electron configurations formed from the atomic orbital basis and are included to fulfil completeness of the total wave function and to allow for short range calculation.  $U_j$  are the finite set of continuum orbitals, which is the eigensolutions of the following second order differential equation,

$$\left( \frac{d^2}{dr^2} - \frac{l(l+1)}{r^2} + v(r) + k_i^2 \right) U_i(r) = \sum_j \lambda_{ij} P_j(r)$$

(II.3-2)

for each angular momentum, subject to the R-matrix boundary conditions

$$U_i(0) = 0$$

$$a U_i^{-1}(a) \frac{dU_i(a)}{dr} = b \quad \text{(II.3-3)}$$

$$\int_0^a dr U_i(r) U_j(r) = \delta_{ij} \quad \text{for all } i, j$$

where Lagrangian multipliers  $\lambda_{ij}$  allow the orthogonality constrains

$$\langle U_i | P_j \rangle = 0 \quad \text{for all } j \quad \text{(II.3-4)}$$

$P_j$  are the set of radial atomic wavefunctions, equation (II.2-6).

It follows that the functions  $U_i(r)$  together with the atomic orbitals form a complete set in the range  $0 \leq r \leq a$  for any potential

$V(r)$  and logarithmic boundary condition b.

The coefficients  $c_{ijk}$  and  $d_{jk}$  in equation (II.3-1) are determined by diagonalizing the (N+1)-Breit-Pauli Hamiltonian

$$\langle \psi_k | H_{BP}^{N+1} | \psi_{k'} \rangle = E_k^{N+1} \delta_{kk'} \quad (\text{II.3-5})$$

It is now assumed that the states  $\psi_k$  form a basis for the expansion of the total wavefunction  $\psi_E$  for any energy  $E$  in the region of configuration space where all electron coordinates  $r \leq a$ . Then, we write

$$\psi_E = \sum_k A_{Ek} \psi_k \quad (\text{II.3-6})$$

and the equivalent relation

$$y_i(r) = \sum_k A_{Ek} \psi_{ik} \quad (\text{II.3-7})$$

By applying Green's theorem the logarithmic derivative of the channel functions (II.3-7) on the boundary is given by

$$y_i(a) = \sum_j R_{ij} \left[ a \frac{dy_j(a)}{dr} - by_j(a) \right] \quad (\text{II.3-8})$$

where the R-matrix element is written as

$$R_{ij} = (2a)^{-1} \sum_k \frac{W_{ik}(a)W_{jk}(a)}{E_k^{N+1} - E}, \quad (\text{II.3-9})$$

$$W_{ik} = \sum_j c_{ijk} U_j \quad (\text{II.3-10})$$

The truncation of equation (II.3-9) to a finite, numerically manageable, number of terms represents a source of error in the calculation. For instance if we retained in our original expansion (II.3-1) those  $U_i$  corresponding to the lowest few eigenvalues  $k_i^2$  in each channel, the error in the expansion (II.3-9) corresponds to the neglect of an infinite number of distant levels. These play an important role in the diagonal elements of  $R_{ij}$ , where they add coherently. The

correction to the diagonal elements of  $R_{ij}$  at the energy  $k_i^2$  is given<sup>30</sup> by

$$R_{ij}^C = \left( \frac{a}{U_i(a)} \cdot \frac{dU_i(r)}{dr} \Big|_{r=a} - b \right)^{-1} - \frac{1}{a} \sum_j \frac{U_{ij}^2(a)}{k_{ij}^2 - k_i^2}$$

(II.3-11)

where the summation over  $j$  subtracts out those levels which have already been included in the expansion (II.3-9),  $U_i(r)$  is the solution of equation (II.3-2) at the channel energy in question. This energy is related to the total energy through the equation (for nonrelativistic incident electrons):

$$k_i^2 = 2(E - E_i^N) \quad (\text{II.3-12})$$

Having been determined the R-matrix from the solution in the internal region, we proceed to consider the solution of the coupled differential equations

$$\left( \frac{d^2}{dr^2} - \frac{l_i(l_i+1)}{r^2} + \frac{2Z}{r} + k_i^2 \right) y_i(r) = 2 \sum_{j=1}^n V_{ij}(r) y_j(r)$$

$$i = 1, n \quad (\text{II.3-13})$$

in the region of  $r > a$ , where  $a$  is chosen so that the exchange terms are small enough to be neglected but the potential terms in this region are still important. The potential matrix in equation (II.3-13) is defined by

$$V_{ij}(r) = \langle \phi_i | \sum_{k=1}^N r_{k,N+1}^{-1} | \phi_j \rangle \quad (\text{II.3-14})$$

where the integration is taken over all electron coordinates except the

radial coordinate of the scattered electron.

Our basic problem is to relate the solution obtained in the inner region with the solution at very large distances and thus to relate the R-matrix and the K-matrix.

Making use of the expansion

$$\sum_{k=1}^N r_{k,N+1}^{-1} = \sum_{\lambda=0}^{\infty} r_{N+1}^{-\lambda-1} \sum_{k=1}^N r_k^{\lambda} P_{\lambda}(\cos \theta_{k,N+1}) \quad (\text{II.3-15})$$

where,

$$\cos \theta_{k,N+1} = \hat{r}_k \cdot \hat{r}_{N+1}$$

we then define the coefficients

$$a_{ij}^{\lambda} = \langle \phi_i | \sum_{k=1}^N r_k^{\lambda} P_{\lambda}(\cos \theta_{k,N+1}) | \phi_j \rangle \quad (\text{II.3-16})$$

Now equation (II.3-13) becomes

$$\left( \frac{d^2}{dr^2} - \frac{\ell_i(\ell_i+1)}{r^2} + \frac{2(Z-N)}{r} + k_i^2 \right) y_i(r) = \sum_{\lambda=1}^M \sum_{j=1}^n a_{ij}^{\lambda} r^{-\lambda-1} y_j(r)$$

$$i = 1, n ; \quad r > a \quad (\text{II.3-17})$$

where M being the maximum value of  $\lambda$  allowed by the triangular relations imposed by the angular integrals (II.3-16).

The K-matrix is defined by the asymptotic form of the solutions of equation (II.3-17).

We assume that at the energy of interest the open and closed channels being defined as follows:

$$k_i^2 > 0 \quad i = 1, n_a \quad \text{open channels}$$

$$k_i^2 < 0 \quad i = n_a + 1, n \quad \text{closed channels}$$

we then have

$$y_{ij}(r) \underset{r \rightarrow \infty}{\sim} k_i^{-\frac{1}{2}} (\sin \theta_i \delta_{ij} + \cos \theta_{ij} K_{ij})$$

$$i = 1, n_a \quad ; \quad j = 1, n_a$$

(II.3-18)

$$y_{ij}(r) \underset{r \rightarrow \infty}{\sim} O(r^{-2})$$

$$i = n_a + 1, n \quad ; \quad j = 1, n_a$$

(II.3-19)

where,

$$\theta_i = k_i r - \frac{1}{2} \ell_i \pi - \eta_i \ln 2k_i r + \sigma_{\ell_i}$$

$$\eta_i = -(Z-N)k_i^{-1}$$

$$\sigma_{\ell_i} = \arg \Gamma(\ell_i + 1 + i \eta_i)$$

(II.3-20)

To relate the  $n$ -by- $n$  dimensional R-matrix to the  $n_a$ -by- $n_a$  dimensional K-matrix, defined in equation (II.3-18), we introduce the  $(n + n_a)$ - linearly independent solutions,  $v_{ij}$ , of equation (II.3-13), satisfying the boundary conditions

$$v_{ij} \underset{r \rightarrow \infty}{\sim} k_i^{-\frac{1}{2}} \sin \theta_i \delta_{ij} + O(r^{-1})$$

$$j = 1, n_a \quad ; \quad i = 1, n$$

$$v_{ij} \underset{r \rightarrow \infty}{\sim} k_i^{-\frac{1}{2}} \cos \theta_i \delta_{ij - n_a} + O(r^{-1})$$

$$j = n_a + 1, 2n_a \quad ; \quad i = 1, n$$

$$v_{ij} \underset{r \rightarrow \infty}{\sim} \text{EXP}(-\phi_i) \delta_{ij-n_a}$$

$$j = 2n_a + 1, n + n_a ; \quad i = 1, n \quad (\text{II.3-21})$$

where,

$$\phi_i = |k_i| r - \frac{Z-N}{|k_i|} \ln(2|k_i|r)$$

$$(\text{II.3-22})$$

Then, the required solutions  $y_{ij}(r)$  is expanded<sup>30,31</sup> in terms of the linearly independent solutions  $v_{ij}(r)$ ,

$$y_{ij}(r) = \sum_{\ell=1}^{n+n_a} v_{i\ell}(r) X_{\ell j}$$

$$i = 1, n ; \quad j = 1, n_a ; \quad a \leq r \leq \infty$$

$$(\text{II.3-23})$$

Using equations (II.3-8), (II.3-18) and (II.3-19) we obtain

$$X_{\ell j} = \delta_{\ell j} \quad \ell = 1, n_a$$

$$\sum_{\ell=1}^{n+n_a} [v_{i\ell}(a) - \sum_{m=1}^n R_{im} \left( a \frac{dv_{m\ell}(r)}{dr} - bv_{m\ell}(r) \right)_{r=a}] X_{\ell j} = 0$$

$$i = 1, n$$

$$(\text{II.3-24})$$

which is solved for each  $j = 1, n_a$ .

The K-matrix element is then given by

$$K_{ij} = X_{i+n_a, j} \quad i, j = 1, n_a \quad (\text{II.3-25})$$

It should be noted to mention that the K-matrix is related to the scattering matrix, S, by the relation

$$S = (I + iK)(I - iK)^{-1} \quad (\text{II.3-26})$$

where  $I$  is an  $n_a$ -by- $n_a$  unit matrix.

Since one is usually only interested in transitions between different states it is convenient to extract from the  $S$ -matrix the unit operator  $I$  and to define the transition operator  $T$  by

$$T = S - I \quad (\text{II.3-27})$$

#### II.4 Description of Electron Spin Polarization, Cross Sections and Scattering Asymmetry by Density Matrices

Early theoretical investigations on electron spin polarization, by applying the relativistic effects, have been carried out by Mott, Massey and Mohr<sup>32,33</sup>. Recently, various authors<sup>34,35,36</sup> summarized the progress of theoretical and experimental studies of spin effects in electron-atom scattering. The spin analysis, neglecting the spin-orbit interaction, has been investigated<sup>37</sup> where either the incoming electrons or the target atom or both of them are spin polarized. Over the last ten years there has been considerable experimental and theoretical interest in the low-energy scattering of electrons by caesium atoms.<sup>37,38</sup> This interest has been further stimulated by recent advances in experimental techniques which permit the use of polarized electron beams with a high energy resolution. Besides the measurement of total and differential, elastic and inelastic cross sections these techniques also allow the determination of observables such as spin polarization, asymmetry function and Stokes' parameters which provide a detailed test of the theoretical model.

In this section, combined with the previous sections, we stimulate our fuller account of the calculation encountered in refs.<sup>24,25</sup>

The scattering process can be described by the following reaction

$$\bar{e} : | \ell_0 m_{\ell_0} \frac{1}{2} m_0 ; \vec{k}_0 \rangle + A : | n_0 j_0 M_{j_0} \rangle \rightarrow A^* : | n_1 j_1 M_{j_1} \rangle + \bar{e} : | \ell_1 m_{\ell_1} \frac{1}{2} m_1 ; \vec{k}_1 \rangle ,$$

(II.4-1)

where for elastic scattering one can write  $A: |n_0 j_0 M_{j_0}\rangle$  instead of  $A^*: |n_1 j_1 M_{j_1}\rangle$ .

The target atoms are assumed to be in their ground state  $|n_0 j_0 M_{j_0}\rangle$  and after excitation to be in the state  $|n_1 j_1 M_{j_1}\rangle$ ,  $n$  being introduced to distinguish states with the same  $j$  but different energy. The incident and scattered electrons are described by the states  $|\ell_0 m_{\ell_0} \frac{1}{2} m_0; \vec{k}_0\rangle$ ,  $|\ell_1 m_{\ell_1} \frac{1}{2} m_1; \vec{k}_1\rangle$ , respectively, where  $\ell_0 m_{\ell_0}$  ( $\ell_1 m_{\ell_1}$ ) are the orbital momentum and its third component of the incident (scattered) electron,  $\vec{k}_0$  ( $\vec{k}_1$ ) is the linear momentum of the incident (scattered) electron and  $m_0$  ( $m_1$ ) is the third component of the spin angular momentum of the incident (scattered) electron.

The density matrix  $\rho_{out}$ , in which all the information on the scattered states alone are contained, is obtained by operating on the initial density matrix  $\rho_{in}$ , which describes the system (electron + atom) before interaction, by the transition operator and its hermitian adjoint

$$\rho_{out} = T \rho_{in} T^\dagger \quad (II.4-2)$$

The electronic and atomic states are not correlated before interaction, then  $\rho_{in}$  can be written as

$$\rho_{in} = \rho_A \times \rho_e \quad (II.4-3)$$

where  $\times$  refers to the outer product, and  $\rho_A$  and  $\rho_e$  are related to the unit operator and the Pauli-spin matrix, equation (I.1-7), through the equation

$$\rho = \sum_i \frac{1}{2} (I + P_i \cdot \sigma_i) \quad i = 1, 2, 3 \quad (II.4-4)$$

$P_i$  are the cartesian components of the polarization vector of any of the initial beams.

By sandwiching equation (II.4-2) between the final states and then introducing the completeness relation of the initial states twice, we obtain the density matrix elements describing the states of the scattered particles: (we suppress terms, which are fixed by the

experimental conditions, where it is convenient)

$$\langle j_1 M_1' m_1' | \rho_{out} | j_1 M_1 m_1 \rangle = \int \sum_{\substack{M_0' M_0 \\ m_0' m_0}} \langle n_1 j_1 M_1' : \ell_1 m_1' m_1' | T | n_0 j_0 M_0' m_0' \rangle \times$$

$$\times \langle n_0 j_0 M_0' m_0' | \rho_{in} | n_0 j_0 M_0 m_0 \rangle \langle n_0 j_0 M_0 m_0 | T^\dagger | n_1 j_1 M_1 : \ell_1 m_1 m_1 \rangle$$

(II.4-5a)

$$= \int \sum_{\substack{M_0' M_0 \\ m_0' m_0}} f(n_1 j_1 M_1' m_1' : n_0 j_0 M_0' m_0' : \theta_e) \times$$

$$\times f^*(n_1 j_1 M_1 m_1 : n_0 j_0 M_0 m_0 : \theta_e) \langle M_0' m_0' | \rho_{in} | M_0 m_0 \rangle$$

(II.4-5b)

where,  $\theta_e$  is the electronic scattering angle. On the right hand side of equation (II.4-5b) we perform averages over initial internal states, sum over final unobserved states and integrate over continuous variables.

The scattering amplitudes in equation (II.4-5b) take the form:<sup>39</sup>

$$f(n_1 j_1 M_1' m_1' : n_0 j_0 M_0' m_0' : \theta_e) = \left[ \frac{\pi}{k_1 k_0} \right]^{\frac{1}{2}} i \sum_{\substack{\ell_1 K_1 \ell_0 K_0 \\ J \pi'}} (2\ell_0 + 1)^{\frac{1}{2}} Y_{\ell_1}^{m_1}(\theta_e, \phi_e)$$

$$\times \left\{ i^{\ell_0 - \ell_1} \right\} (j_0 M_0 \ell_0 0 | K_0 M_0) (K_0 M_0 \frac{1}{2} m_0 | J M_0) (j_1 M_1 \ell_1 m_1 | K_1 M_1) \times$$

$$\times (K_1 M_1 \frac{1}{2} m_1 | J M_1) T_{n_1 j_1 K_1 \ell_1 : n_0 j_0 K_0 \ell_0}^{J \pi'}$$

(II.4-6)

In deriving equation (II.4-6) a pair-coupling scheme has been adopted. In this coupling scheme we first couple the total angular momentum of the atom with the orbital angular momentum of the electron to obtain  $\underline{K}$  which is then coupled with the spin angular momentum of the electron to give  $\underline{J}$  ie

$$\underline{J}_0 + \underline{\ell}_0 = \underline{K}_0 ; \underline{K}_0 + \frac{1}{2} = \underline{J}$$

$$\underline{J}_1 + \underline{\ell}_1 = \underline{K}_1 ; \underline{K}_1 + \frac{1}{2} = \underline{J}$$

(II.4-7)

It should be noted that the appearance of zero as the last index of the string  $j_o M_j \ell_o 0$  on  $(j_o M_j \ell_o 0 | K_o M_j)$  in equation (II.4-6) is a reminder that the direction of the incident electron,  $k_o$ , is chosen as the z-axis; therefore the incident plane wave is expanded simply in terms of  $Y_{\ell_o}^0(\theta)$ . The assumptions made allow for the total angular momentum of the system  $J$ , its projection over the z-axis  $M_j$  and the parity  $\pi'$  to be conserved during collision. Moreover, the z-axis has been defined as both the quantization axis and the axis of the incident beam.

The number of independent amplitudes is reduced by the requirement that the interaction dynamics must be invariant against reflection in the scattering plane,<sup>40</sup> defined by  $\vec{k}_0$  and  $\vec{k}_1$ .

$$f(n_1 j_1 M_j m_1 : n_o j_o M_j m_o : \theta_e) = (-1)^{\pi + j_1 - M_j + j_o - M_j + \frac{1}{2} - m_1 + \frac{1}{2} - m_o} \\ \times f(n_1 j_1 -M_j -m_1 : n_o j_o -M_j -m_o : -\theta_e) \quad (\text{II.4-8})$$

Now, we project our density matrix element equation (II.4-5b) onto the subspace of interest to eliminate all nonessential indices, that is by taking the matrix elements of the total density matrix  $\rho_{out}$  which are diagonal in the unobserved variables and summing these elements over all these unobserved variables. The matrix  $\langle M_j' m_o' | \rho_{in} | M_j m_o \rangle$  in equation (II.4-5b) contains all information about the spin polarization of the initial state of the system. Then, the general form, for polarized or unpolarized initial beams, of the resulting reduced density matrix of the scattered electrons with unobserved final atomic states looks like

$$\langle m_1' | \rho_{out} | m_1 \rangle = \sum_{\substack{M_j' M_j \\ j_o' j_o \\ m_o' m_o \\ M_j = M_j'}} f(j_1 M_j m_1 : j_o M_j' m_o' : \theta_e) f^*(j_1 M_j m_1 : j_o M_j m_o : \theta_e) \times \\ \times \langle M_j' m_o' | \rho_{in} | M_j m_o \rangle \quad (\text{II.4-9})$$

and the differential cross section is given by summing over all terms diagonal in  $m_1$ ,

$$\sigma(\theta_e) = \sum_{m_1} \langle m_1 | \rho_{out} | m_1 \rangle \quad (\text{II.4-10a})$$

By integrating equation (II.4-10a) over all the electronic scattering angles we get the total scattering cross section.

$$\sigma_{tot} = \int d\Omega_e \sigma(\theta_e) \quad (\text{II.4-10b})$$

Making use of equations (I.1-5), (II.4-9) and (II.4-10a), the cartesian components of the polarization vector of the scattered electrons are given by

$$\begin{aligned} \sigma(\theta_e) P_i^{out} &= \text{tr } \rho_{out} \sigma_i \\ &= \sum_{m_1, m_1'} \langle m_1' | \rho_{out} | m_1 \rangle \langle m_1 | \sigma_i | m_1' \rangle \quad i = x, y, z \end{aligned} \quad (\text{II.4-11})$$

In case of unpolarized initial beams equation (II.4-11) reduces to (using equations (II.4-8) and (II.4-9)):

$$\begin{aligned} \sigma_{un}(\theta_e) P_y^{out} &= \frac{1}{2(2j_o+1)} \sum_{\substack{m_o, M_{j_o} \\ M_{j_1}}} (-2) \text{Im} [ f(j_1 M_{j_1} - \frac{1}{2}; j_o M_{j_o} m_o; \theta_e) \times \\ &\quad \times f^*(j_1 M_{j_1} \frac{1}{2}; j_o M_{j_o} m_o; \theta_e) ] , \end{aligned} \quad (\text{II.4-12})$$

$$\sigma(\theta_e) P_x^{out} = \sigma(\theta_e) P_z^{out} = 0 \quad (\text{II.4-13})$$

in this case  $P_y^{out}$  is called the polarizing power.

If polarized electrons are scattered, as a result of collision, there will be a left-right asymmetry in the differential cross section which is characterised by a function  $A_s(\theta_e)$ . These effects have been extensively studied by Kessler.<sup>36</sup> Assuming that the incoming electrons are polarized in the y- direction and the target atoms are unpolarized. The differential cross section can be written in terms of unpolarized and polarized parts, given by

$$\sigma(\theta_e) = \sigma_{\text{un}}(\theta_e) + \sigma_{\text{pol}}(\theta_e) \quad (\text{II.4-14})$$

where usually we choose our normalization in such a way that

$$\begin{aligned} \sigma_{\text{un}}(\theta_e) &= \frac{1}{2(2j_o+1)} \sum_{\substack{m_o M_{j_o} \\ m_1 m_{j_1}}} |f(j_1 M_{j_1} m_1 : j_o M_{j_o} m_o : \theta_e)|^2 \\ &= \text{tr } \rho_{\text{out}} \end{aligned} \quad (\text{II.4-15})$$

and the polarized part is

$$\begin{aligned} \sigma_{\text{pol}}(\theta_e) &= \frac{1}{2(2j_o+1)} P_y \sum_{\substack{m_1 m_{j_o} \\ M_{j_1}}} (-2) \text{Im}[f(j_1 m_{j_1} m_1 : j_o M_{j_o} -\frac{1}{2} : \theta_e)] \times \\ &\quad \times f^*(j_1 M_{j_1} m_1 : j_o M_{j_o} \frac{1}{2} : \theta_e) \end{aligned} \quad (\text{II.4-16})$$

The unpolarized and the polarized terms (equations (II.4-15) and (II.4-16)) are related by the scattering asymmetry (analysing power) through the equation

$$\sigma_{\text{un}}(\theta_e) A_s(\theta_e) = \sigma_{\text{pol}}(\theta_e) \quad (\text{II.4-17})$$

Comparing equations (II.4-12) and (II.4-17) and using equation (II.4-16) we find that the polarizing power,  $P_y^{\text{out}}$ , is equal to the analysing power,  $A_s(\theta_e)$ , under the condition

$$f(j_1 M_{j_1} -m_1 : j_o M_{j_o} m_o : \theta_e) = f(j_1 M_{j_1} m_1 : j_o M_{j_o} -m_o : \theta_e) \quad (\text{II.4-18})$$

Condition (II.4-18) holds for elastic scattering as a consequence of time reversal invariance whereas in inelastic scattering condition (II.4-18) is, in general, not satisfied.

**CHAPTER III**  
**POLARIZATION PHENOMENAE OF RADIATION**

The angular distribution and polarization of the emitted radiation have been studied very extensively in literatures.<sup>3,8,41,42,43</sup> However most of these cases have been set for atoms that are well described in the LS-coupling scheme. If we allowed for the spin-orbit interaction to take a place during collision (such as the case of heavy atoms) LS-coupling is violated in the collision. In case of LS-coupling is violated in the collision we presented our numerical calculation<sup>44</sup> for the Stokes' parameters of the light emitted in the decay of excited cassium atom. This calculation follows closely a recent one<sup>45</sup> on mercury.

In this chapter we present the details of the calculation, the numerical results and discussion will be found in chapter V.

**III.1 Description of the Collision**

The excitation and decay processes can be described by the following reactions:

$$e^- : |\ell_0 m_{\ell_0} \frac{1}{2} m_{s_0}; \vec{k}_0\rangle + A : |n_0 j_0 M_{j_0}\rangle \rightarrow A^* : |n_1 j_1 M_{j_1}\rangle + e^- : |\ell_1 m_{\ell_1} \frac{1}{2} m_{s_1}; \vec{k}_1\rangle$$

(III.1-1)

$$A^* : |n j M_j\rangle + \omega$$

(III.1-2)

where  $\omega$  is the frequency of the emitted radiation and in case of decaying to the ground state we replace  $A^* : |n j M_j\rangle$  by  $A : |n_0 j_0 M_{j_0}\rangle$ .

To find the reduced density matrix describing the state of  $A^*: |n_1 j_1 M_{j_1}\rangle$  alone, just after collision, we follow as the same procedure as to get equation (II.4-9), but instead of making summation over  $M_{j_1}' = M_{j_1}$  we sum over  $m_1' = m_1$ , to obtain:

$$\langle j_1 M_{j_1}' | \rho_{\text{out}} | j_1 M_{j_1} \rangle = \sum_{\substack{M_{j_1}' M_{j_1} \\ m_1' m_1 \\ m_1' = m_1}} f(j_1 M_{j_1}' m_1 : j_1 M_{j_1} m_1 : \theta_e) f^* (j_1 M_{j_1} m_1 : j_1 M_{j_1}' m_1 : \theta_e) \times \\ \times \langle M_{j_1}' m_1' | \rho_{\text{in}} | M_{j_1} m_1 \rangle \quad (\text{III.1-3})$$

once again it is trivial to find that

$$f(j_1 M_{j_1}' m_1 : j_1 M_{j_1} m_1 : \theta_e) f^* (j_1 M_{j_1} m_1 : j_1 M_{j_1}' m_1 : \theta_e) = \\ (-1)^{\pi + \pi' + 2j_1 + 2j_1' - M_{j_1}' - M_{j_1} - M_{j_1}' - M_{j_1}} f(j_1 -M_{j_1}' -m_1 : j_1 -M_{j_1} -m_1 : -\theta_e) \times \\ \times f^* (j_1 -M_{j_1} -m_1 : j_1 -M_{j_1}' -m_1 : -\theta_e) \quad (\text{III.1-4})$$

and the normalization condition is expressed by equation (II.4-15).

In our calculation we are interested only in measurements without detection of the scattered electron. In this way we integrate the bilinear combination of the scattered amplitudes in equation (III.1-3) over all the electronic scattering angles. Using equation (II.4-6) and the orthogonality relation of the spherical harmonics

$$\int d\Omega_e Y_{\ell_1}^{m_{\ell_1}}(\theta_e, \phi_e) Y_{\ell_1'}^{m_{\ell_1}'}(\theta_e, \phi_e) = \delta_{\ell_1 \ell_1'} \delta_{m_{\ell_1} m_{\ell_1}'} \quad (\text{III.1-5})$$

we obtain

$$\begin{aligned}
F(j_1 M_1' m_1 : j_0 M_0' m_0') F^* (j_1 M_1 m_1 : j_0 M_0 m_0) &= \int d\Omega_e f(j_1 M_1' m_1 : j_0 M_0' m_0' : \theta_e) \times \\
&\times f^* (j_1 M_1 m_1 : j_0 M_0 m_0 : \theta_e) \\
&= \frac{\pi}{k_1 k_0} \sum_{\ell_1 m_1} \sum_{\ell_0 m_0} \sum_{\substack{K_1 M_1' \ell_1 K_0' \\ J_1 M_1' \ell_1 K_0'}} \sum_{\substack{K_1 M_1 \ell_0 K_0 \\ J M_J}} \{i_0^{\ell_0 - \ell_0'}\} (2\ell_0 + 1)(2\ell_0' + 1) \times \\
&\times (j_0 M_0' m_0' : \ell_0' 0 | K_0' M_0' m_0') (K_0' M_0' m_0' : \frac{1}{2} m_0' | J_1 M_1' m_1) (j_1 M_1' m_1 : \ell_1 m_1 | K_1 M_1' m_1) (K_1 M_1' m_1 : \frac{1}{2} m_1 | J_1 M_1' m_1) \times \\
&\times (j_0 M_0 m_0 : \ell_0 0 | K_0 M_0 m_0) (K_0 M_0 m_0 : \frac{1}{2} m_0 | J M_J) (j_1 M_1 m_1 : \ell_1 m_1 | K_1 M_1 m_1) (K_1 M_1 m_1 : \frac{1}{2} m_1 | J M_J) \times \\
&\times T_{j_1 \ell_1 K_1' : j_0 \ell_0' K_0'}^{J_1 \pi'} T_{j_1 \ell_1 K_1 : j_0 \ell_0 K_0}^{* J \pi} \tag{III.1-6}
\end{aligned}$$

### III.2 Expansion of the Integrated State Multipoles in Terms of the Reduced Density Matrix

We expand the spherical tensor operators, equation (I.4-9), in terms of the reduced density matrix (III.1-3). The relevant integrated state multipoles are given by the relation, using equation (III.1-6):

$$\begin{aligned}
\langle \mathcal{J}(j_1)_{KQ}^+ \rangle &= (2K+1)^{\frac{1}{2}} \sum_{\substack{M'_1 M_1 m_1 \\ M'_0 M_0 m'_0 m_0}} (-1)^{j_1 - M'_1} (j_1 M'_1, j_1 - M_1 | KQ) \times \\
&\times \langle M'_0 m'_0 | \rho_{in} | M_0 m_0 \rangle F(j_1 M'_1 m_1 : M'_0 m'_0) F^*(j_1 M_1 m_1 : M_0 m_0)
\end{aligned}
\tag{III.2-1}$$

where we assume transitions between two well defined energy levels.

As we mentioned before the matrix  $\langle M'_0 m'_0 | \rho_{in} | M_0 m_0 \rangle$  in the above equation contains all the dependence of the integrated state multipoles on the initial polarization vectors of the colliding partners. For instance the following physical situations may arise:

(i) For unpolarized initial beams the excitation process is axially symmetric around the z-axis (we choose z-axis as the direction of the incoming beams). Applying the transformation operator  $D(0 \ 0 \ \gamma)_{qQ}^{K*}$  and making use of equation (I.4-7a), we have

$$\langle \mathcal{J}(j_1)_{KQ}^+ \rangle = \langle \mathcal{J}(j_1)_{KQ}^+ \rangle e^{-iQ\gamma}$$

then

$$\langle \mathcal{J}(j_1)_{KQ}^+ \rangle = 0 \quad Q \neq 0 \tag{III.2-2}$$

Furthermore, according to reflection invariance in any plane through z-axis we get in particular, using equation (I.4-6):

$$\langle \mathcal{J}(j_1)_{10}^+ \rangle = 0 \tag{III.2-3}$$

In this case the residual nonzero multipoles are the monopole

$$\langle \mathcal{J}(j_1)_{00}^+ \rangle_{un} \text{ and the alignment parameter } \langle \mathcal{J}(j_1)_{20}^+ \rangle_{un}.$$

(ii) If one of the polarization vectors of the incoming beams or both of them has a component lies along z-axis, reflection invariance in planes through the z-axis no more holds, this gives:

$$\langle \mathcal{J}(j_1)_{10}^+ \rangle \neq 0 \tag{III.2-4}$$

but the process is axially symmetric around the z-axis and as a consequence equation (III.2-2) is still required.

(iii) In case of transversally polarized initial beams, one can choose the direction of the polarization vector as y-axis and x-axis perpendicular to y- and z- axes, the excitation process, described in figure (2b), is invariant under reflection in the x-z plane and consequently equation (I.4-6) holds. Because of summation of the bilinear combination of the scattered amplitudes over all the electronic scattering angles further restrictions<sup>9</sup> should be imposed to reduce the number of independent parameters. These restrictions can be noted from equation (III.1-6) in the following.

The total angular momentum of the system is conserved during the collision, which give for unpolarized initial beams:

$$\begin{aligned} M'_{j_1} + m_{\lambda_1} + m_1 &= M_{j_0} + m_0 \\ M_{j_1} + m_{\lambda_1} + m_1 &= M_{j_0} + m_0 \end{aligned} \quad \text{(III.2-5)}$$

As a consequence we obtain nonzero multipoles if the following condition is satisfied

$$M'_{j_1} = M_{j_1} \quad \text{(III.2-6)}$$

combining equation (III.2-6) with equation (III.2-1) results in

$$Q = 0 \quad \text{(III.2-6)}$$

Therefore, we have

$$\langle \mathcal{J}(j_1)_{KQ}^+ \rangle_{un} = 0 \quad Q \neq 0 \text{ or } M'_{j_1} \neq M_{j_1} \quad \text{(III.2-7)}$$

and

$$\langle \mathcal{J}(j_1)_{KQ}^+ \rangle = \langle \mathcal{J}(j_1)_{KQ}^+ \rangle_{pol} \quad Q \neq 0 \quad \text{(III.2-8)}$$

If the incident electrons are transversally polarized equation (III.2-5) is replaced by

$$\begin{aligned} M'_{j_1} + m_{\lambda_1} + m_1 &= M_{j_0} + m'_0 \\ M_{j_1} + m_{\lambda_1} + m_1 &= M_{j_0} + m_0 \end{aligned} \quad \text{(III.2-9)}$$

then

$$M'_{j_1} - M_{j_1} = m'_0 - m_0 = \pm 1 \quad (\text{III.2-10})$$

Inserting equations (III.2-7), (III.2-8) and (III.2-10) into equation (I.4-6)

we end up with the four nonvanishing independent parameters

$$\langle \mathcal{J}(j_1)_{00}^{\dagger} \rangle = \langle \mathcal{J}(j_1)_{00}^{\dagger} \rangle_{\text{un}} \quad (\text{III.2-11})$$

$$\langle \mathcal{J}(j_1)_{20}^{\dagger} \rangle = \langle \mathcal{J}(j_1)_{20}^{\dagger} \rangle_{\text{un}} \quad (\text{III.2-12})$$

$$\langle \mathcal{J}(j_1)_{11}^{\dagger} \rangle = \langle \mathcal{J}(j_1)_{11}^{\dagger} \rangle_{\text{pol}} \quad (\text{III.2-13})$$

$$\langle \mathcal{J}(j_1)_{21}^{\dagger} \rangle = \langle \mathcal{J}(j_1)_{21}^{\dagger} \rangle_{\text{pol}} \quad (\text{III.2-14})$$

We note that in case of transversally polarized initial target atoms and unpolarized electrons the condition (III.2-10) is replaced by

$$M'_{j_1} - M_{j_1} = M'_{j_0} - M_{j_0}, \quad (\text{III.2-15})$$

and we follow the same procedure as before to reduce the number of independent multipoles according to the case under consideration.

Now we are in a position to expand the integrated state multipoles in terms of the bilinear combination of the scattered amplitudes.

### III.2A Excitation From the $S_{\frac{1}{2}}$ to the $P_{\frac{1}{2}}$ State

#### Case 1 Unpolarized Initial Beams

The only nonzero multipole is

$$\begin{aligned} \langle \mathcal{J}(\frac{1}{2})_{00}^{\dagger} \rangle_{\text{un}} &= \frac{1}{2\sqrt{2}} \sum_{i=1}^8 |F_i|^2 \\ &= \frac{\sigma_{\text{un}}(\frac{1}{2})}{2\sqrt{2}} \end{aligned} \quad (\text{III.2A-16})$$

where  $\sigma_{\text{un}}(M_{j_1})$  is the total cross section for the excitation of the magnetic sublevel  $M_{j_1}$ .

#### Case 2 Longitudinally Polarized Electrons and Unpolarized Target Atoms

Only two parameters are required, the monopole

$$\langle \mathcal{J}(\frac{1}{2})_{00}^+ \rangle = \langle \mathcal{J}(\frac{1}{2})_{00}^+ \rangle_{\text{un}} \quad (\text{III.2A-17})$$

and the orientation parameter

$$\begin{aligned} \langle \mathcal{J}(\frac{1}{2})_{10}^+ \rangle_{\text{pol}} &= \frac{P_z}{2\sqrt{2}} \left[ \sum_i (|F_i|^2 - |F_{i+2}|^2) \right] ; \quad i = 1, 3, 5 \\ &= \frac{P_z}{2\sqrt{2}} \left[ \sigma(\frac{1}{2}; m_0 = \frac{1}{2}) - \sigma(\frac{1}{2}; m_0 = -\frac{1}{2}) \right] \end{aligned} \quad (\text{III.2A-18})$$

where  $\sigma(M_{j_1}; m_0)$  is the total cross section for excitation of magnetic sublevel  $M_{j_1}$  with a definite electronic quantum number  $m_0$ .

### Case 3 Transversally Polarized Electrons and Unpolarized Target Atom

In this case we have again

$$\langle \mathcal{J}(\frac{1}{2})_{00}^+ \rangle = \langle \mathcal{J}(\frac{1}{2})_{00}^+ \rangle_{\text{un}} \quad (\text{III.2A-19})$$

and the nonvanishing component of the orientation vector

$$\langle \mathcal{J}(\frac{1}{2})_{11}^+ \rangle_{\text{pol}} = (i) \frac{P_y}{2} \text{Re}[F_1 F_7^* + F_3 F_5^*] \quad (\text{III.2A-20})$$

It is clear that, from equation (III.2A-20), the component of the orientation vector is purely imaginary.

The set of scattered amplitudes is referred as

$$\begin{aligned} F_1 &= F(\frac{1}{2}; \frac{1}{2}; \frac{1}{2}; \frac{1}{2}) & F_5 &= F(\frac{1}{2}; \frac{1}{2}; -\frac{1}{2}; \frac{1}{2}) \\ F_2 &= F(\frac{1}{2}; \frac{1}{2}; \frac{1}{2}; -\frac{1}{2}) & F_6 &= F(\frac{1}{2}; \frac{1}{2}; -\frac{1}{2}; -\frac{1}{2}) \\ F_3 &= F(\frac{1}{2}; \frac{1}{2}; -\frac{1}{2}; \frac{1}{2}) & F_7 &= F(\frac{1}{2}; \frac{1}{2}; -\frac{1}{2}; -\frac{1}{2}) \\ F_4 &= F(\frac{1}{2}; \frac{1}{2}; -\frac{1}{2}; -\frac{1}{2}) & F_8 &= F(\frac{1}{2}; \frac{1}{2}; -\frac{1}{2}; -\frac{1}{2}) \end{aligned}$$

### III.2B Excitation From the $S_{\frac{1}{2}}$ - to the $P_{\frac{3}{2}}$ - state

#### Case 1

The relevant multipoles are

$$\begin{aligned} \langle \mathcal{J}(\frac{3}{2})_{00}^+ \rangle_{\text{un}} &= \frac{1}{4} \sum_{i=1}^{16} |F_i|^2 \\ &= \frac{1}{4} \left[ \sigma_{\text{un}}(\frac{3}{2}) + \sigma_{\text{un}}(\frac{1}{2}) \right] \end{aligned} \quad (\text{III.2B-21})$$

and

$$\begin{aligned} \langle \mathcal{J}(\frac{3}{2})_{20}^+ \rangle_{\text{un}} &= \frac{1}{4} \left[ \sum_{i=1}^8 |F_i|^2 - \sum_{i=9}^{16} |F_i|^2 \right] \\ &= \frac{1}{4} \left[ \sigma_{\text{un}}(\frac{3}{2}) - \sigma_{\text{un}}(\frac{1}{2}) \right] \end{aligned}$$

(III.2B-22)

**Case 2:**

There are three independent parameters, defined as follows:

$$\langle \mathcal{J}(\frac{3}{2})_{00}^+ \rangle = \langle \mathcal{J}(\frac{3}{2})_{00}^+ \rangle_{\text{un}} \quad , \quad \text{(III.2B-23)}$$

$$\langle \mathcal{J}(\frac{3}{2})_{20}^+ \rangle = \langle \mathcal{J}(\frac{3}{2})_{20}^+ \rangle_{\text{un}} \quad , \quad \text{(III.2B-24)}$$

and

$$\begin{aligned} \langle \mathcal{J}(\frac{3}{2})_{10}^+ \rangle_{\text{pol}} &= \frac{P_z}{4\sqrt{5}} \left[ 3 \sum_{i=1}^7 (|F_i|^2 - |F_{i+1}|^2) + \sum_{i=9}^{15} (|F_i|^2 - |F_{i+1}|^2) \right] \\ &\quad , \quad i \text{ takes odd values only} \\ &= \frac{P_z}{4\sqrt{5}} \left[ 3\sigma(\frac{3}{2}; m_0 = \frac{1}{2}) + \sigma(\frac{1}{2}; m_0 = \frac{1}{2}) - 3\sigma(\frac{3}{2}; m_0 = -\frac{1}{2}) - \sigma(\frac{1}{2}; m_0 = -\frac{1}{2}) \right] \end{aligned}$$

(III.2B-25)

**Case 3:**

In general we have four independent parameters

$$\langle \mathcal{J}(\frac{3}{2})_{00}^+ \rangle = \langle \mathcal{J}(\frac{3}{2})_{00}^+ \rangle_{\text{un}} \quad , \quad \text{(III.2B-26)}$$

$$\langle \mathcal{J}(\frac{3}{2})_{20}^+ \rangle = \langle \mathcal{J}(\frac{3}{2})_{20}^+ \rangle_{\text{un}} \quad , \quad \text{(III.2B-27)}$$

$$\begin{aligned} \langle \mathcal{J}(\frac{3}{2})_{11}^+ \rangle_{\text{pol}} &= (i) \frac{P_y}{\sqrt{10}} \text{Re} \left[ \sqrt{3} (F_1 F_{10}^* + F_3 F_{12}^* + F_5 F_{14}^* + F_7 F_{16}^*) + \right. \\ &\quad \left. + 2(F_9 F_{12}^* + F_{11} F_{13}^*) \right] \quad , \end{aligned}$$

(III.2B-28)

and

$$\langle \mathcal{J}(\frac{3}{2})_{21}^+ \rangle_{\text{pol}} = -\frac{P_y}{2\sqrt{2}} \text{Im} [F_1 F_{10}^* + F_3 F_{12}^* + F_5 F_{14}^* + F_7 F_{16}^*] \quad \text{(III.2B-29)}$$

Equation (III.2B-29) confirms that the alignment parameter,

$\langle \mathcal{J}(j)_1^+ \rangle_{\text{pol}}$ , is a real quantity.

The set of scattered amplitudes in this transition is written as

$$\begin{aligned}
 F_1 &= F\left(\frac{3}{2}; \frac{3}{2}; \frac{1}{2}; \frac{1}{2}\right) & F_9 &= F\left(\frac{3}{2}; \frac{1}{2}; \frac{1}{2}; \frac{1}{2}\right) \\
 F_2 &= F\left(\frac{3}{2}; \frac{3}{2}; \frac{1}{2} - \frac{1}{2}\right) & F_{10} &= F\left(\frac{3}{2}; \frac{1}{2}; \frac{1}{2}; \frac{1}{2} - \frac{1}{2}\right) \\
 F_3 &= F\left(\frac{3}{2}; \frac{3}{2}; -\frac{1}{2}; \frac{1}{2}\right) & F_{11} &= F\left(\frac{3}{2}; \frac{1}{2}; \frac{1}{2}; -\frac{1}{2}; \frac{1}{2}\right) \\
 F_4 &= F\left(\frac{3}{2}; \frac{3}{2}; -\frac{1}{2} - \frac{1}{2}\right) & F_{12} &= F\left(\frac{3}{2}; \frac{1}{2}; \frac{1}{2}; -\frac{1}{2} - \frac{1}{2}\right) \\
 F_5 &= F\left(\frac{3}{2}; \frac{3}{2} - \frac{1}{2}; \frac{1}{2}; \frac{1}{2}\right) & F_{13} &= F\left(\frac{3}{2}; \frac{1}{2} - \frac{1}{2}; \frac{1}{2}; \frac{1}{2}\right) \\
 F_6 &= F\left(\frac{3}{2}; \frac{3}{2} - \frac{1}{2}; \frac{1}{2} - \frac{1}{2}\right) & F_{14} &= F\left(\frac{3}{2}; \frac{1}{2} - \frac{1}{2}; \frac{1}{2} - \frac{1}{2}\right) \\
 F_7 &= F\left(\frac{3}{2}; \frac{3}{2} - \frac{1}{2}; -\frac{1}{2}; \frac{1}{2}\right) & F_{15} &= F\left(\frac{3}{2}; \frac{1}{2} - \frac{1}{2}; -\frac{1}{2}; \frac{1}{2}\right) \\
 F_8 &= F\left(\frac{3}{2}; \frac{3}{2} - \frac{1}{2}; -\frac{1}{2} - \frac{1}{2}\right) & F_{16} &= F\left(\frac{3}{2}; \frac{1}{2} - \frac{1}{2}; -\frac{1}{2} - \frac{1}{2}\right)
 \end{aligned}$$

### III.3 Effect of Perturbations on the Decaying Process

The time evolution of an atomic states, where LS- or jj-coupling holds during collision, under the influence of fine structure and hyperfine structure interactions has been adequately considered elsewhere.<sup>3,42,43,46</sup> But for the sake of completeness we briefly consider the effect of perturbations in this section when the collision is describable in jj-coupling scheme.

When LS-coupling does not hold during collision two somewhat different situations may occur.

#### (i) Excited Atoms Violating LS-coupling

In this situation the spin-orbit interaction has an appreciable effect during the collision, ie the collision time  $t_c$  is comparable with the precession time  $\tau_{j_1' j_1}$  of the fine structure states

$$t_c \sim \frac{1}{E_{j_1'} - E_{j_1}} = \tau_{j_1' j_1} \quad \text{(III.3-1)}$$

The characteristic times  $\tau_{j_1' j_1}$  is just the precession period of the spin angular momentum and the orbital angular momentum vectors around the total angular momentum of the excited atom.

As a result the scattered amplitudes and as will the integrated

state multipoles, being a function of the scattered amplitudes, referring to different fine structure states are no longer correlated, but are treated as independent parameters. Even in case of light emitted from different fine structure levels is not resolved, the breakdown of LS-coupling implies that the splittings,  $E_{j_1}^i - E_{j_1}$ , are large compared to the level widths  $\gamma$ , i.e. the precession times of the fine structure states are smaller than the atomic life time  $\tau = \frac{1}{\gamma}$ . This result can be understood by saying that many precessions will take place during the atomic life time. Since we are interested in quantities averaged over a time interval  $0 \rightarrow t_R$  (where  $t_R$  is the resolution time and practically we have  $t_R \gg \tau$ ) all interference terms with  $j_1^i \neq j_1$  cancel each other and only the time independent terms  $j_1^i = j_1$  will survive. Therefore the radiation intensities from different fine structure levels add incoherently and only interference of radiation from different hyperfine structure levels need be considered.

We then have the density matrix of the excited atom just after collision,  $t = 0$ , in the form ( $I$  is the nuclear spin):

$$\rho(0) = \rho_{j_1}(0) \times \rho_I(0) \quad \text{(III.3-2)}$$

(ii) Nonradiating Atom Violating LS-Coupling

In this case the total electronic spin is not a good quantum number of the system. This arises when the target atom or any atom formed in the collision violates LS-coupling, even though the radiating atom obeys them. For instance, the Ly- $\alpha$  radiation resulting from charge transfer of protons on Xe originates from the 2p-state of the hydrogen atom, which obeys LS-coupling, however the states of Xe and Xe<sup>+</sup> do not.

In view of the above mentioned, three different situations may occur:

- (a) The transition operator  $T$  may depend explicitly upon the spin.

(b) The initial and final states of the collision partners, describing the internal states of the collision partners before and after collision, respectively, may not obey LS-coupling rules.

(c) The initial and final state vectors defined above may approximately obey LS-coupling, but some of the substates of their multiplets may not be energetically accessible.

In all the three cases the amplitudes of scattering  $f\{j_1 M_{j_1}\}$  and as well as the reduced density matrix elements in  $j_1 M_{j_1}$  - representation, where  $j_1 M_{j_1}$  refers to the state of the radiating atom, can still be related to those in the  $L_1 M_{L_1}, S_1 M_{S_1}$  - representation by a Clebsch-Gordan transformation. As a consequence to spin-orbit interaction, the scattering amplitudes referring to different  $M_{S_1}$  states can interfere yielding no reduction in the number of unknown parameters ensues from the transformation to the  $L_1 M_{L_1}, S_1 M_{S_1}$  - representation. Hence, the scattering amplitudes describing the formation of the radiating atom may be expressed in  $j_1 M_{j_1}$  - representation.

Keeping in mind the above mentioned concepts, one can classify the effect of fine and hyperfine structures on the decay process according to the relation between the line widths and energy separations of the relevant structure.

#### - Energy Separations and Line Widths are Comparable

Accordingly we have

$$\tau \sim \tau_{jj} \quad (\text{III.3-3})$$

and the scattered amplitudes referring to different fine structure levels interfere. If also the fine structure splittings are large compared to the hyperfine structure splittings, then

$$\tau \sim \tau_{jj} \ll \tau_{jF'F} \quad (\text{III.3-4})$$

and the excited ensemble decays before the hyperfine structure

interaction takes place.

The total density matrix, which only describes the excited orbital states, just after collision, is then given by (no need to couple  $\rho_1(0)$  under this circumstance):

$$\rho(0) = \rho_{j_1' j_1} (0) . \quad (\text{III.3-5})$$

Using equation (I.4-1) we obtain

$$\rho(0) = \sum_{K_j Q_j} \langle \mathcal{T}(j_1' j_1)_{K_j Q_j}^\dagger \rangle \mathcal{T}(j_1' j_1)_{K_j Q_j} \quad (\text{III.3-6})$$

At time  $t$  the system is represented by a density matrix  $\rho(t)$  which has evolved from the density matrix  $\rho(0)$  governed by the time evolution operator  $U(t)$

$$\rho(t) = U(t) \rho(0) U(t)^\dagger \quad (\text{III.3-7})$$

where,

$$U(t) = \text{Exp}(-iHt) , \quad (\text{III.3-8})$$

$$H = H_0 + H' \quad (\text{III.3-9})$$

and where the interaction term  $H'$  couples the spin and orbital states of the system and  $H_0$  is the unperturbed Hamiltonian.

Inserting equation (III.3-6) into equation (III.3-7) yields

$$\rho_{j_1' j_1}(t) = \sum_{K_j Q_j} \langle \mathcal{T}(j_1' j_1)_{K_j Q_j}^\dagger \rangle U(t) \mathcal{T}(j_1' j_1)_{K_j Q_j} U(t)^\dagger \quad (\text{III.3-10})$$

The integrated state multipoles describing the orbital states at time  $t$  is defined<sup>3</sup> as

$$\langle \mathcal{T}(j_1' j_1; t)_{K_j Q_j}^\dagger \rangle = \text{tr} \{ \rho_{j_1' j_1}(t) \mathcal{T}(j_1' j_1)_{K_j Q_j} \} \quad (\text{III.3-11})$$

Using equation (III.3-10) we get:

$$\langle \mathcal{T}(j_1' j_1; t)_{K_j Q_j}^\dagger \rangle = \sum_{K_j Q_j} \langle \mathcal{T}(j_1' j_1)_{K_j Q_j}^\dagger \rangle \text{tr} \{ U(t) \mathcal{T}(j_1' j_1)_{K_j Q_j} U(t)^\dagger \times \\ \times \mathcal{T}(j_1' j_1)_{K_j Q_j} \} \quad (\text{III.3-12})$$

$$= \sum_{K_j Q_j} \langle \mathcal{T}(j_1' j_1)_{K_j Q_j}^\dagger \rangle G(j_1' j_1; t)_{K_j Q_j} \quad (\text{III.3-13})$$

where  $G(j_1' j_1; t)_{K_j Q_j}$  are the perturbation coefficients in this new multipole expansion.

Comparing equations (III.3-12) and (III.3-13), we have

$$G(j_1' j_1; t)_{K_j Q_j} = \text{tr} \{ U(t) \mathcal{T}(j_1' j_1)_{K_j Q_j} U(t)^\dagger \mathcal{T}(j_1' j_1; t)_{K_j Q_j} \} \quad (\text{III.3-14})$$

Applying the Wigner-Eckart theorem, equation (I.3-4), and a standard formulae<sup>6</sup> of angular momentum theory for determination of matrix elements of irreducible tensor operators with the help of the symmetry properties of the Clebsch-Gordan coefficients, we obtain:

$$G(j_1' j_1; t)_{K_j Q_j} = e^{-\gamma t} \sum_{j_1' j_1} \cos \omega_{j_1' j_1} t \delta_{K_j K} \delta_{Q_j Q} \quad (\text{III.3-15})$$

where,  $\gamma_{j_1'} = \gamma_{j_1} = \gamma = \frac{1}{\tau}$   $\omega_{j_1' j_1} = E_{j_1'} - E_{j_1}$

The Kronecker symbols in equation (III.3-15) indicate that multipoles with different ranks and components can not be mixed, in this case, by the interaction.

#### - Energy Separations are Large Compared to the Level Widths

Opposite to the previous case, interference between amplitudes referring to different fine structure levels are not allowed. Therefore the total density matrix describing the orbital states of the excited system, just after collision, is given by equation (III.3-2).

Using equation (I.4-1),  $\rho(0)$  can be written in the form

$$\rho(0) = \sum_{K_I j_1} \langle \mathcal{T}(j_1)_{K_I}^\dagger \rangle \times \langle \tau(I)_{K_I 0}^\dagger \rangle \mathcal{T}(j_1)_{K_I} \times \langle \tau(I)_{K_I 0} \rangle \quad (\text{III.3-16})$$

where  $\chi_{j_1}$  are the components of the integrated state multipoles  $\langle \mathcal{J}(j_1)_{K_j \chi_{j_1}}^\dagger \rangle$  in the spin polarization frame (defined by taking the spin polarization direction of the scattered atom,  $\hat{n}_s$ , as a quantization axis) and we assume that the nuclear spins of the excited ensemble are polarized along the quantization axis.

Applying a similar procedure as in the previous case, we get

$$\begin{aligned} \langle \mathcal{J}(j_1; t)_{K_j \chi_{j_1}}^\dagger \rangle &= \text{tr} \{ \rho_{j_1}(t) \mathcal{J}(j_1; t)_{K_j \chi_{j_1}} \times \underline{I} \} \\ &= \sum_{K_j \chi_{j_1}} \langle \mathcal{J}(j_1)_{K_j \chi_{j_1}}^\dagger \rangle \langle t(I)_{K_I 0}^\dagger \rangle \times \\ &\times \text{tr} \{ U(t) \mathcal{J}(j_1)_{K_j \chi_{j_1}} \times t(I)_{K_I 0}^\dagger U(t) \mathcal{J}(j_1; t) \} \times \underline{I} \} \end{aligned} \quad (\text{III.3-17})$$

$$= \sum_{K_j \chi_{j_1}} \langle \mathcal{J}(j_1)_{K_j \chi_{j_1}}^\dagger \rangle G(j_1; t)_{K_j \chi_{j_1}} \quad (\text{III.3-18})$$

where  $\underline{I}$  is a unit operator in the spin space. Comparing equations (III.3-17) and (III.3-18) we obtain for the perturbation coefficient

$$\begin{aligned} G(j_1; t)_{K_j \chi_{j_1}} &= \sum_{K_I F F'} (-1)^{j_1 + I + F + K} \langle t(I)_{K_I 0}^\dagger \rangle \times \\ &\times (2F+1)(2F'+1) [(2K_I+1)(2K_j+1)]^{\frac{1}{2}} (K_I 0, K_j \chi_{j_1} | K \chi_{j_1}) \begin{Bmatrix} F' & F & K \\ j_1 & j_1 & I \end{Bmatrix} \times \\ &\times \begin{Bmatrix} K_I & K_j & K \\ I & j_1 & F' \\ I & j_1 & F \end{Bmatrix} \text{EXP} \{ -i(E_{j_1 F'} - E_{j_1 F})t - \gamma_{j_1} t \} \end{aligned} \quad (\text{III.3-19})$$

where the symbols  $\begin{Bmatrix} \cdot & \cdot & \cdot \\ \cdot & \cdot & \cdot \\ \cdot & \cdot & \cdot \end{Bmatrix}$  and  $\begin{Bmatrix} \cdot & \cdot & \cdot \\ \cdot & \cdot & \cdot \\ \cdot & \cdot & \cdot \end{Bmatrix}$  are the

6j- and 9j- symbols, respectively.

Under the condition that atomic and nuclear spins are both polarized along the same direction,  $\hat{k}_o$ , we replace  $\chi_{j_1}$  by  $Q_{j_1}$ .

The Clebsch-Gordan coefficient, 6j- and 9j- symbols, in equation (III.3-19), put the necessary restrictions due to the angular momentum

coupling rules:

$$\begin{aligned} 0 \leq K_{j_1} \leq 2j_1 & & -K_{j_1} \leq \chi_{j_1} \leq K_{j_1} \\ 0 \leq K_I \leq 2I & & |K_{j_1} - K_I| \leq K \leq K_{j_1} + K_I \end{aligned}$$

These restrictions limit the number of possible perturbation coefficients for each  $j_1$ .

Now, if the splittings,  $E_{j_1 F'} - E_{j_1 F}$ , are comparable with the line widths, ie  $\tau_{j_1 F' F} \sim \tau$ , interference between states of different hyperfine structure levels (the time dependent terms in equation (III.3-19)) are significant. For some physical situations it may happen that the splittings are smaller than the line widths, then the oscillatory terms with  $F' \neq F$ , in equation (III.3-19), average out during the comparatively long life time and are neglected.

In the physical situation of interest where the nuclear spins are initially unpolarized ( $K_I = 0$ ) and the precession time  $\tau_{j_1 F' F}$  much smaller than the life time  $\tau$ , equation (III.3-19) reduces to

$$\bar{G}(j_1; t)_{K_{j_1}} = \frac{1}{2I+1} \sum_F (2F+1)^2 \left\{ \begin{matrix} j_1 & F & I \\ F & j_1 & K_{j_1} \end{matrix} \right\}^2 \text{EXP} \{-\gamma t\} \quad (\text{III.3-20})$$

#### III.4 Radiative Decay of an Excited Atom

The decaying process have been considered under the following assumptions.<sup>47</sup>

- The atoms have been instantaneously excited at time  $t = 0$  and their states are specified by a density operator  $\rho(0)$  which is assumed to be known.
- The excited atomic ensemble is considered as a statistical mixture of states  $|j_1 M_{j_1}\rangle$  (here we suppress all quantum numbers which are necessary to describe the state in addition to the angular momentum quantum number, for sake of simplicity) which are assumed to be degenerate in  $M_{j_1}$  but not in  $j_1$ .

- At a later time  $t$  the ensemble decays to lower levels  $|jM_j\rangle$  by emitting photons.
- The excitation and decay processes do not change the atomic and nuclear spins.
- The density matrix  $\rho(\hat{n}_\gamma, t)$ , which contains all information about the system (atoms and emitted photons) at time  $t$ , is given by:

$$\rho(\hat{n}_\gamma, t) = U(t) \rho(0) U(t)^\dagger \quad (\text{III.4-1})$$

where the operator  $U(t)$  describes the time evolution under the influence of the interaction between the excited ensemble and the electromagnetic field,  $V_\gamma(t)$ , of the virtual photons.

In the first order perturbation theory this time evolution operator is written as:

$$U(t) = U_0(t) \{1 - i \int_0^t dt U_0(t)^\dagger V_\gamma(t) U_0(t)\}, \quad (\text{III.4-2})$$

where  $U_0(t)$  is the free time evolution operator corresponding to the unperturbed Hamiltonian.

In view of these assumptions the elements of the polarization density matrix of photons observed in the direction  $\hat{n}_\gamma$  in the interval  $0 \rightarrow t$  and in the photon detector frame are given by<sup>3</sup>

$$\begin{aligned} \rho(\hat{n}_\gamma, t)_{\lambda'\lambda} &= C(\omega) \sum_{j_1 M_{j_1}} \langle j M_j | \underline{r}_{\lambda'} | j_1 M_{j_1} \rangle \langle j_1 M_{j_1} | \rho(0) | j_1 M_{j_1} \rangle \times \\ &\times \langle j_1 M_{j_1} | \underline{r}_\lambda^\dagger | j M_j \rangle \times \frac{j_1 M_{j_1} \langle j_1 M_{j_1} | j_1 M_{j_1} \rangle}{1 - \text{EXP} \left[ \frac{-i(E_{j_1} - E_{j_1})t - \frac{1}{2}(\gamma_{j_1} + \gamma_{j_1})t}{i(E_{j_1} - E_{j_1}) + (\gamma_{j_1} + \gamma_{j_1})} \right]} \end{aligned}$$

(III.4-3)

where  $C(\omega) = \frac{\omega^4}{2\pi c^3} d\Omega_\gamma$ ,  $c$  is the velocity of light in atomic units,  $d\Omega_\gamma$  is the element of the solid angle into which photons are emitted.

The quantities  $\underline{r}_{\lambda'}$  and  $\underline{r}_\lambda$  ( $\lambda', \lambda = \pm 1$  for right- and left-handed circularly polarized light) are the spherical components of the dipole vector  $\underline{r}$  in the "helicity-frame" spanned by the three basis vectors

$$\hat{e}_{\pm 1} = \mp \frac{1}{2} \{\hat{e}_1 \pm i \hat{e}_2\}; \quad \hat{e}_0 = \hat{n}_\gamma \quad (\text{III.4-4})$$

where  $\hat{e}_0$ ,  $\hat{e}_1$  and  $\hat{e}_2$  have polar angle  $(\theta_\gamma, \phi_\gamma)$ ,  $(\theta_{\gamma+90}, \phi_\gamma)$  and  $(\theta_\gamma, \phi_\gamma+90)$ , respectively, in the collision system, figure (1).

Then,

$$\underline{r} = r_{+1}^* \hat{e}_{+1} + r_{-1}^* \hat{e}_{-1} + r_0^* \hat{n}_\gamma$$

Using equation (I.4-1), equation (III.4-3) becomes

$$\rho(\hat{n}_\gamma, t) = C(\omega) \sum_{\substack{Kq j_1' M_1' \\ j_1 M_1 j_1 M_1}} \langle j_1 M_1 | \underline{r}_\lambda | j_1' M_1' \rangle \langle j_1' M_1' | \mathcal{J}(j_1' j_1)_{Kq} | j_1 M_1 \rangle \times$$

$$\times \langle \mathcal{J}(j_1' j_1)_{Kq}^\dagger \rangle \langle j_1 M_1 | \underline{r}_\lambda^\dagger | j_1 M_1 \rangle \times$$

$$\times \frac{1 - \text{EXP}[-i(E_{j_1'} - E_{j_1})t - \frac{1}{2}(\gamma_{j_1'} + \gamma_{j_1})t]}{i(E_{j_1'} - E_{j_1}) + \frac{1}{2}(\gamma_{j_1'} + \gamma_{j_1})}$$

(III.4-5)

$$= C(\omega) \sum_{Kq j_1' j_1} \text{tr}(\underline{r}_\lambda, \mathcal{J}(j_1' j_1)_{Kq} \underline{r}_\lambda^\dagger) \langle \mathcal{J}(j_1' j_1)_{Kq}^\dagger \rangle \times$$

$$\times \frac{1 - \text{EXP}[-i(E_{j_1'} - E_{j_1})t - \frac{1}{2}(\gamma_{j_1'} + \gamma_{j_1})t]}{i(E_{j_1'} - E_{j_1}) + \frac{1}{2}(\gamma_{j_1'} + \gamma_{j_1})}$$

(III.4-6)

Comparing equation (III.4-5) with equation (III.4-6), we have

$$\begin{aligned} \text{tr}\{\underline{r}_\lambda, \mathcal{J}(j_1' j_1)_{Kq} \underline{r}_\lambda^\dagger\} &= \sum_{\substack{j M_j \\ j_1' M_{j_1}' \\ j_1 M_{j_1}}} \langle j M_j | \underline{r}_\lambda | j_1' M_{j_1}' \rangle \times \\ &\times \langle j_1' M_{j_1}' | \mathcal{J}(j_1' j_1)_{Kq} | j_1 M_{j_1} \rangle \langle j_1 M_{j_1} | \underline{r}_\lambda^\dagger | j M_j \rangle \end{aligned} \quad (\text{III.4-7})$$

Applying the Wigner-Eckart theorem, equation (I.3-4), on equation (III.4-7) three times, and taking into account that  $\underline{r}$  is a tensor of rank one, allows us to separate the geometrical parts (represented in the Clebsch-Gordan coefficients) from the dynamical parts (represented in the reduced matrix elements).

$$\begin{aligned} \text{Hence} \quad \text{tr}\{\underline{r}_\lambda, \mathcal{J}(j_1' j_1)_{Kq} \underline{r}_\lambda^\dagger\} &= \sum_{\substack{j M_j \\ j_1' M_{j_1}' \\ j_1 M_{j_1}}} \frac{1}{3} (-1)^{j+j_1+j_1'+M_j} \times \\ &\times (j M_j, j_1' - M_{j_1}' | 1 - \lambda') (j M_j, j_1 - M_{j_1} | 1 - \lambda) (j_1' M_{j_1}', j_1 - M_{j_1} | Kq) \times \\ &\times \langle j || \underline{r} || j_1' \rangle \langle j || \underline{r} || j_1 \rangle^* \end{aligned} \quad (\text{III.4-8})$$

More simplification of equation (III.4-8) can be done by using the relation 48,

$$\begin{aligned} (c\gamma, a\alpha | f - \phi) \begin{Bmatrix} a & b & e \\ d & c & f \end{Bmatrix} &= \sum_{\beta \delta \epsilon} (-1)^{f+\alpha+\delta+b+d-a-c-e} \times \\ &\times \frac{1}{(2e+1)} \cdot (a\alpha, b\beta | e\epsilon) (d\delta, c\gamma | e-\epsilon) (b\beta, d\delta | f\phi) \end{aligned} \quad (\text{II.4-9})$$

then we obtain

$$\begin{aligned} \text{tr}\{\underline{r}_\lambda, \mathcal{J}(j_1' j_1)_{Kq} \underline{r}_\lambda^\dagger\} &= \sum_j \langle j || \underline{r} || j_1' \rangle \langle j || \underline{r} || j_1 \rangle^* (-1)^{j+j_1+\lambda'} \times \\ &\times (1-\lambda', 1\lambda | K-q) \begin{Bmatrix} 1 & 1 & K \\ j_1 & j_1' & j \end{Bmatrix} \end{aligned} \quad (\text{III.4-10a})$$

In case of decay from a well defined energy level to the same final state, we have

$$\text{tr} \{ \underline{r}_\lambda, \mathcal{J}(j_1)_{Kq} \underline{r}_\lambda^\dagger \} = | \langle j_1 | | \underline{r}_\lambda | | j_1 \rangle |^2 (-1)^{j+j_1+\lambda'} \times$$

$$\times (1-\lambda', 1\lambda | K-q) \begin{Bmatrix} 1 & 1 & K \\ j_1 & j_1 & j \end{Bmatrix} \quad (\text{III.4-10b})$$

Now by differentiating equation (III.4-6), with respect to time, one gets the reduced density matrix of those photons emitted at instant  $t$ .

$$\dot{\rho}(\hat{n}_\gamma, t) = C(\omega) \sum_{Kq} \text{tr} \{ \underline{r}_\lambda, \mathcal{J}(j_1' j_1)_{Kq} \underline{r}_\lambda^\dagger \} \langle \mathcal{J}(j_1' j_1; t)_{Kq}^\dagger \rangle \quad (\text{III.4-11})$$

where

$$\langle \mathcal{J}(j_1' j_1; t)_{Kq}^\dagger \rangle = \langle \mathcal{J}(j_1' j_1)_{Kq}^\dagger \rangle \text{EXP}[-i(E_{j_1'} - E_{j_1})t - \frac{1}{2}(\gamma_{j_1'} + \gamma_{j_1})t] \quad (\text{III.4-12})$$

The exponential factor in equation (III.4-12) describes the time evolution of the excited states, between excitation and decay, whereas the multipoles  $\langle \mathcal{J}(j_1' j_1)_{Kq}^\dagger \rangle$  contain all information about the excitation process.

It is more appropriate to transform the multipoles from the photon detector frame to the collision frame using equation (I.4-7b)

$$\langle \mathcal{J}(j_1' j_1; t)_{Kq}^\dagger \rangle = \sum_Q \langle \mathcal{J}(j_1' j_1; t)_{KQ}^\dagger \rangle D(\hat{n}_\gamma \rightarrow \hat{k}_0)_{qQ}^{(K)}, \quad (\text{III.4-13})$$

$D(\hat{n}_\gamma \rightarrow \hat{k}_0)_{qQ}^{(K)}$  is the relevant transformation operator.

Substituting equation (III.4-13) in equation (III.4-11), we have

$$\dot{\rho}(\hat{n}_\gamma, t) = C(\omega) \sum_{KQq} \text{tr} \{ \underline{r}_\lambda, \mathcal{J}(j_1' j_1)_{Kq} \underline{r}_\lambda^\dagger \} \langle \mathcal{J}(j_1' j_1; t)_{KQ}^\dagger \rangle D(\hat{n}_\gamma \rightarrow \hat{k}_0)_{qQ}^{(K)} \quad (\text{III.4-14})$$

Using equations (III.3-18) and (III.4-13) in equation (III.4-14), yields

$$\dot{\rho}(\hat{n}_\gamma, t) = C(\omega) \sum_{K_j, KqQ, j_1} \text{tr} \{ \underline{r}_\lambda, \mathcal{J}(j_1' j_1)_{Kq} \underline{r}_\lambda^\dagger \} \times$$

$$\times \langle \mathcal{J}(j_1' j_1)_{K_j, Q_j}^\dagger \rangle G(j_1' j_1; t)_{K_j, K}^{Q_j, Q_j} D(\hat{n}_\gamma \rightarrow \hat{k}_0) \quad (\text{III.4-15})$$

where the trace is given by equation (III.4-10a) and the perturbation coefficients are given by equation (III.3.19).

In the special case of interest, where the energy separations are large compared to the level widths and the atomic and nuclear spins are unpolarized, equation (III.4-15) reduces to

$$\begin{aligned} \dot{\rho}(\hat{n}_\gamma, t) = & \sum_{\substack{K=K_{j_1} \\ qQ_{j_1}}} \text{tr} \{ \underline{r}_\lambda \mathcal{J}(j_1, ; t)_{K_{j_1} q_{j_1}}^{\dagger} \} \langle \mathcal{J}(j_1)_{K_{j_1} Q_{j_1}}^{\dagger} \rangle \times \\ & \times \bar{G}(j_1; t)_{K_{j_1} q_{j_1}}^{(K_{j_1})} D(\hat{n}_\gamma \rightarrow \hat{k}_0)_{qQ_{j_1}} \end{aligned} \quad \text{(III.4-16)}$$

where now the trace is given by equation (III.4.10b) and the perturbation coefficients are given by equation (III.3-20).

### III.5 Stokes' Parameters Description of the Emitted Radiation

The integrated Stokes' parameters are calculated by comparing equation (III.4-16) with equation (I.2-6). Keeping in mind that, according to our previous assumption the decaying process does not change the spins of the excited atoms and consequently the dynamical factor appearing in equation (III.4-10b) does not change if it is calculated in the LS- or jj-coupling scheme.

#### III.5A The Decay Process $P_{\frac{1}{2}} \rightarrow S_{\frac{1}{2}}$

##### Case 1 Unpolarized Initial Beams

$$I = C(\omega) |\langle 0 || \underline{r} || 1 \rangle|^2 \left[ \frac{\sqrt{2}}{3} \bar{G}_0(\frac{1}{2}) \langle \mathcal{J}(\frac{1}{2})_{00}^{\dagger} \rangle_{\text{un}} \right] \quad \text{(III.5A-1)}$$

$$I\eta_1 = I\eta_2 = I\eta_3 \quad \text{(III.5A-2)}$$

##### Case 2 Longitudinally Polarized Initial Electrons and Unpolarized Target Atoms

Equation (III.5A-1) still holds, but we have for the circular polarization

$$I\eta_2 = C(\omega) |\langle 0 || \underline{r} || 1 \rangle|^2 \left[ \frac{\sqrt{2}}{3} \cos \theta \bar{G}_1(\frac{1}{2}) \langle \mathcal{J}(\frac{1}{2})_{10}^{\dagger} \rangle_{\text{pol}} \right] \quad \text{(III.5A-3)}$$

and

$$I\eta_1 = I\eta_3 = 0 \quad (\text{III.5A-4})$$

**Case 3** Transversally polarized electrons and unpolarized target atoms

Again equation (III.5A-1) still survive whereas  $I\eta_2$  now takes the form

$$I\eta_2 = C(\omega) | \langle 0 || \underline{r} || 1 \rangle |^2 \left[ \frac{2}{3} \sin \theta_\gamma \sin \phi_\gamma \bar{G}_1(\frac{1}{2}) \text{Im} \langle \mathcal{J}(\frac{1}{2})^+_{11} \rangle_{\text{pol}} \right]$$

(III.5A-5)

If one considers excitation by a steady flux of incoming electrons the time at which the photons are emitted is no longer uniquely defined with respect to the excitation time, and the time dependent exponential in the perturbation coefficient, equation (III.3-20), may be integrated from  $t = 0$  to  $t = \infty$  with negligible error. In case of caesium atom we have,

$$\begin{aligned} \bar{G}_0(\frac{1}{2}) &= \frac{1}{\gamma} = \tau \\ \bar{G}_1(\frac{1}{2}) &= 0.34375 \tau \end{aligned}$$

**III.5B** The Decay Process  $P_{\frac{3}{2}} \rightarrow S_{\frac{1}{2}}$

**Case 1:**

$$\begin{aligned} I &= C(\omega) | \langle 0 || \underline{r} || 1 \rangle |^2 \left\{ \frac{1}{3} [\bar{G}_0(\frac{3}{2}) \langle \mathcal{J}(\frac{3}{2})^+_{00} \rangle_{\text{un}} + \right. \\ &\quad \left. + \frac{1}{4} (3 \cos^2 \theta_\gamma - 1) \bar{G}_2(\frac{3}{2}) \langle \mathcal{J}(\frac{3}{2})^+_{20} \rangle_{\text{un}} ] \right\} \end{aligned}$$

(III.5B-6)

$$I\eta_3 = -C(\omega) | \langle 0 || \underline{r} || 1 \rangle |^2 \left[ \frac{1}{4} \sin^2 \theta_\gamma \bar{G}_2(\frac{3}{2}) \langle \mathcal{J}(\frac{3}{2})^+_{20} \rangle_{\text{un}} \right] \quad (\text{III.5B-7})$$

$$I\eta_1 = I\eta_2 = 0 \quad (\text{III.5B-8})$$

**Case 2:**

The intensity  $I$  and  $\eta_3$  are given by equations (III.5B-6) and (III.5B-7), respectively, but  $\eta_2$  is given by

$$I\eta_2 = C(\omega) | \langle 0 || \underline{r} || 1 \rangle |^2 \left[ \frac{\sqrt{5}}{6} \cos \theta_\gamma \bar{G}_1 \left( \frac{3}{2} \right) \langle \mathcal{J} \left( \frac{3}{2} \right)_{10}^+ \rangle_{\text{pol}} \right] \quad (\text{III.5B-9})$$

and

$$I\eta_1 = 0 \quad (\text{III.5B-10})$$

**Case 3:**

In this case we have, in general, nonvanishing values for all the integrated Stokes' parameters

$$I = C(\omega) | \langle 0 || \underline{r} || 1 \rangle |^2 \left[ \frac{1}{3} \bar{G}_0 \left( \frac{3}{2} \right) \langle \mathcal{J} \left( \frac{3}{2} \right)_{00}^+ \rangle_{\text{un}} + \frac{1}{12} (3 \cos^2 \theta_\gamma - 1) \bar{G}_2 \left( \frac{3}{2} \right) \right. \\ \left. \times \langle \mathcal{J} \left( \frac{3}{2} \right)_{20}^+ \rangle_{\text{un}} - \frac{1}{2\sqrt{6}} \sin 2\theta_\gamma \cos \phi_\gamma \bar{G}_2 \left( \frac{3}{2} \right) \text{Re} \langle \mathcal{J} \left( \frac{3}{2} \right)_{21}^+ \rangle_{\text{pol}} \right] \quad (\text{III.5B-11})$$

$$I\eta_1 = C(\omega) | \langle 0 || \underline{r} || 1 \rangle |^2 \left[ \frac{1}{\sqrt{6}} \sin \theta_\gamma \sin \phi_\gamma \bar{G}_2 \left( \frac{3}{2} \right) \text{Re} \langle \mathcal{J} \left( \frac{3}{2} \right)_{21}^+ \rangle_{\text{pol}} \right] \quad (\text{III.5B-12})$$

$$I\eta_2 = C(\omega) | \langle 0 || \underline{r} || 1 \rangle |^2 \left[ \frac{\sqrt{10}}{6} \sin \theta_\gamma \sin \phi_\gamma \bar{G}_1 \left( \frac{3}{2} \right) \text{Im} \langle \mathcal{J} \left( \frac{3}{2} \right)_{11}^+ \rangle_{\text{pol}} \right] \quad (\text{III.5B-13})$$

$$I\eta_3 = -C(\omega) | \langle 0 || \underline{r} || 1 \rangle |^2 \left[ \frac{1}{2\sqrt{2}} \sin^2 \theta_\gamma \bar{G}_2 \left( \frac{3}{2} \right) \langle \mathcal{J} \left( \frac{3}{2} \right)_{20}^+ \rangle_{\text{un}} + \right. \\ \left. + \frac{1}{2\sqrt{6}} \sin 2\theta_\gamma \cos \phi_\gamma \bar{G}_2 \left( \frac{3}{2} \right) \text{Re} \langle \mathcal{J} \left( \frac{3}{2} \right)_{21}^+ \rangle_{\text{pol}} \right] \quad (\text{III.5B-14})$$

and the set of perturbation coefficients is

$$\begin{aligned} \bar{G}_0 \left( \frac{3}{2} \right) &= \tau \\ \bar{G}_1 \left( \frac{3}{2} \right) &= 0.37 \tau \\ \bar{G}_2 \left( \frac{3}{2} \right) &= 0.21869 \tau \end{aligned}$$

## CHAPTER IV

ELECTRON SCATTERING BY DIATOMIC MOLECULES

The theory of electron collision with molecules, in several areas of current research interest, is the demand for increasing understanding of detailed mechanism of scattering in molecular physics. Important applications<sup>50,51</sup> of this theory provide a strong incentive for development of accurate methods of ab initio calculation. Besides the formidable challenge in treating the electron-atom collision process,<sup>52,53</sup> new difficulties arise in dealing with electron-molecule scattering:

- (i) The strong nonspherical character of the target molecule complicates the partial-wave analysis resulting in very slowly convergent.
- (ii) The dynamics of the target molecule possess internal degrees of freedom due to the nuclear motion.
- (iii) As there are two nuclei or more, acting as sources of the field, multi-centre integrals may required to be performed.

Alternative theories of electron-molecule scattering simply reflect different approaches to calculate wavefunctions, or any measurable quantity, which are eigenfunctions of the electron-molecule Hamiltonian

$$H = H_{\text{rot}} + H_{\text{v}} + H_{\text{N}} - \frac{1}{2}\nabla_{\text{N+1}}^2 + V_{\text{N+1}} \quad , \quad (\text{IV-1})$$

defined by solving the Schrodinger equation, at total energies E

$$(H - E)|\psi_{\text{E}}\rangle = 0 \quad (\text{IV-2})$$

where  $H_{\text{rot}}$ ,  $H_{\text{v}}$  and  $H_{\text{N}}$  are the rotational, vibrational and electronic parts of the molecular Hamiltonian ;  $-\frac{1}{2}\nabla_{\text{N+1}}^2$  is the kinetic energy operator of the scattered electron;  $V_{\text{N+1}}$  refers to the potential interaction between the incident electron and the target molecule and in case of diatomic molecule is written as

$$V_{N+1} = \sum_{i=1}^N \frac{1}{|\underline{r}_{N+1} - \underline{r}_i|} - \frac{Z_A}{|\underline{r}_{N+1} - \underline{r}_A|} - \frac{Z_B}{|\underline{r}_{N+1} - \underline{r}_B|} \quad (\text{IV-3})$$

where we assume a target molecule of  $N$ -electrons,  $r_i$  are their coordinates and  $Z_A$  and  $Z_B$  are the nuclear charges located at  $\underline{r}_A$  and  $\underline{r}_B$ .

Similar to equation (II.3-6), the total wavefunction  $\Psi_E$  is expanded at each internuclear separation  $R$  as follows

$$|\Psi_E\rangle = \sum_k A_{Ek} |\Psi_k\rangle, \quad (\text{IV-4})$$

$$|\Psi_k\rangle = \int \sum_i c_{ki} \phi_i F_i(N+1) + \sum_j \xi_j(x_1, \dots, x_{N+1}; R) d_{jk} \quad (\text{IV-5})$$

where  $\phi_i$ , in general, involves rotational, vibrational and electronic states;  $F_i$  describes the motion of the scattered electron and  $\xi_j$  are  $N+1$ -electron antisymmetrized functions which allow for the delocalization and correlation effects.

Because of the complications encountered in solving equation (IV-2) we require taking advantage of any simplifying feature<sup>54</sup> that may be available in each range of electron-molecule distances. For instance at large distances the interaction is weak and nearly central and the angular momenta of the electron and the molecule need not to be coupled. At short distances, the total angular momentum  $\underline{L}$  and the internuclear distance  $\underline{R}$  couple strongly and  $\Lambda = \underline{L} \cdot \underline{R}$  is a well defined quantum number. In such case the Body-Fixed frame of reference (fixed with the molecule) is a natural choice to carry out calculation. At some carefully chosen boundary<sup>54,55</sup> one transforms the solution from the Body-Fixed frame to the LAB frame (in which the molecule is rotating) and by introducing the nuclear Hamiltonian, continues the solution of the resulting equations into the asymptotic region. Hopefully one can find such transformation radius where all short range interactions can be ignored in the outer region. The entire problem can be solved in the BF frame under the following conditions:<sup>56,57</sup>

- The energy of the incident electron is very large compared to the threshold energy.
- Strong long range interaction is not dominant.
- Nonresonant scattering.

We now sum up, very briefly, in the following sections some important concepts which form the basis of the electron-molecule scattering theory, limiting ourselves as much as possible to the scope of the problem of interest.

#### **IV.1 Born-Oppenheimer and Fixed-Nuclei Approximations**

The great disparity of electronic and nuclear masses allows one to consider separately the motions of the electrons and the nuclei in a molecule. So, in principle, the properties of the molecule could be determined by calculating the electron motions for each possible configuration of the nuclei, whose relative positions would enter these calculations only as a parameter. This is the essence of the Born-Oppenheimer approximation, therefore one can first solve the electronic problem with the nuclei fixed. The nuclei are then assumed to move in response to the adiabatic potential energy corresponding to the stationary electronic state. However, corrections should be taken into account for the breakdown of the Born-Oppenheimer approximation due to the small electron velocities, large nuclear velocities or where two or more electronic energy curves cross or come very close to one another.

If the collision time is small compared with the characteristic rotational and vibrational times, ie the incident electron passes the potential area before any vibrational or rotational coupling takes place,

we need only consider the electronic Hamiltonian for the electron-molecule system as the nuclei are then assumed to be fixed. This is the Fixed-Nuclei approximation<sup>55,57</sup> where any measurable quantity will correspond to an average of all the possible molecular geometries over the relevant molecular states.

#### IV.2 Representation of the Nuclear Motion (Rotation and Vibration)

As mentioned before the Born-Oppenheimer approximation enables the electronic and nuclear motions in a molecule to be separated from each other. The molecule persists in a particular electronic state with a corresponding electronic energy during nuclear motion. The electronic energy and the energy due to the electrostatic repulsion of the nuclei both vary with the internuclear separation, and together provide the potential that determines the rotational and vibrational motions.

Inclusion of rotational and vibrational motions obeys the following classification:

If the collision time  $t_c$  is small compared with the characteristic rotational times  $\tau_{j'j}$ ,  $t_c \ll \frac{1}{E'_{rot} - E_{rot}} = \tau_{j'j}$ ,

one can find an orthogonal transformation<sup>54,55,57</sup> which connect the two sets of wavefunctions and as well the T-matrices calculated in the Body-Fixed (molecular rotation is neglected) and Laboratory (molecular rotation is included) frames. Then, the relevant scattering amplitudes and cross sections for transitions between rotational states can be obtained.

For slow electron collision compared with the characteristic rotational times,

$$t_c \gg \frac{1}{E'_{rot} - E_{rot}},$$

the rotational Hamiltonian can no longer be neglected and the Body-

Fixed frame treatment may be replaced by a Laboratory frame treatment. However, a simplification of this treatment, given by Chang and Fano,<sup>54</sup> showed that for slow electron collisions, the electron and molecule interaction energy will still dominate the rotational Hamiltonian for sufficiently small electron-molecule distances. The Body-Fixed frame wavefunctions can be used in this internal region, and then transformed at the boundary of this region (using a unitary transformation). This procedure provides the boundary conditions for the solution of the Laboratory frame equations in the outer region including the rotational Hamiltonian.

Similarly if the collision time is small compared with characteristic vibrational times,

$$t_c \ll \frac{1}{E'_v - E_v} = \tau_{v'v} ,$$

an adiabatic transformation<sup>58</sup> of the T-matrices can be applied, we obtain

$$T_{i'v'l';ivl}^\Lambda = \langle X_{v'} | T_{i'l';il}^\Lambda | X_v \rangle \quad (\text{IV.2-1})$$

where  $\Lambda$  is the molecular symmetry; the integration of equation (IV.2-1) is carried out over the nuclear coordinate corresponding to the initial and final vibrational states  $X_v, X_{v'}$ .

A hybrid expansion<sup>59,60</sup> can be used if the time of collision is not short compared with the characteristic vibrational times but is short compared with the characteristic rotational times.

Finally if the collision time is large compared with both the characteristic vibrational and rotational times

$$\frac{1}{E'_v - E_v} \ll t_c \gg \frac{1}{E'_v - E_v}$$

an expansion in terms of the rotational and vibrational eigenfunctions may be used. This increases the size of the system of equations and thus tends to make its practical solution much more difficult. However, this difficulty might not be great by using the simplification

of the frame transformation approach. Luckily we seldom meet this type of situation, we then do not attempt this problem.

### IV.3 Exchange and Polarization Potentials

The scattering electron is indistinguishable from the molecular electrons. Hence the system wavefunction must obey the Pauli principle, ie  $\Psi_E$  must be antisymmetric under interchange of any two electrons. This requirement gives rise to exchange effects.

Combining equations (IV-1) and (IV-5) yields, after some straightforward calculation,

$$\left(\frac{d^2}{dr^2} - \frac{\ell(\ell+1)}{r^2} + k^2\right)U_{ik}(r) = 2 \sum_j (V_{ij} + W_{ij})U_{jk}(r) \quad (\text{IV.3-1})$$

where all correlation terms in equation (IV-5) are neglected, and  $U_{ik}(r)$  is the set of radial parts of equation (IV-5), and where the direct matrix elements are written as

$$V_{ij} = \langle \phi_i | V_{ij} | \phi_j \rangle \quad (\text{IV.3-2})$$

and the exchange matrix elements, which interchange bound orbitals in  $\phi_j$  with continuum orbitals  $U_{jk}$  to the right of equation (IV.3-1), are defined by

$$W_{ij}U_{jk}(r) = - \int dr' K(ij|r'r)U_{jk}(r'), \quad (\text{IV.3-3})$$

$$K(ij|r'r) = \sum_{m=1}^{N_{\text{occ}}} \sum_{ij\lambda} \psi_{\ell}^{(m)}(r) \psi_{\ell'}^{(m)}(r') \times$$

$$\times g_{\lambda}(ij\ell\ell'; \Lambda\Lambda_m) \frac{[\min(r, r')]^{\lambda}}{[\max(r, r')]^{\lambda+1}} \quad (\text{IV.3-4})$$

where the target orbitals are expanded as

$$\phi^{(m)}(\underline{r}) = \frac{1}{r} \sum_{\ell} \psi_{\ell}^{(m)}(r) Y_{\ell\Lambda_m}(\hat{r}) \quad (\text{IV.3-5})$$

and  $g_\lambda$  are coefficients given by the product of four coupling coefficients.

Solution of equation (IV.3-1) represents a formidable challenge, therefore a number of approximate models to remove the nonlocality of the exchange operator have been developed to treat the exchange term. Such an operator is said to be 'nonlocal' (because it requires knowledge of the integrand throughout space, rather than only at a single point). Consequently, the exchange operator in equations (IV.3-1) and (IV.3-3) is replaced by a simple local exchange potential energy function, ie representing the electron-molecule static exchange by an approximate local potential made up of static and exchange contributions. Recent applications to treat exchange terms have been focused on either the Free-Electron-Gas<sup>61,62,63</sup> (FEG) or the semiclassical<sup>62</sup> (SC) exchange models.

Burke and Chandra<sup>64</sup> proposed a totally different approach to the problems posed by exchange. This approach is based on the fact that in the exact static exchange theory of electron scattering from a closed-shell molecule, the radial scattering functions are necessarily orthogonal to the bound orbitals of the target molecule. In a sense, one can think of this condition as imposing constraints on the scattering functions. These constraints are not the only effect of the exact nonlocal exchange terms on the scattering functions, but Burke and Chandra argued that they may be the most important ones. One can derive the scattering equations of their procedure by starting in the static approximation, in which exchange is completely neglected, and then imposing suitable orthogonality constraints on the solutions of these equations. This method of solution is called the orthogonalised static method.

So far we did not include any correlation terms, in particular no polarization of the target molecule due to the slow approach of the

incident electron to the bound electrons in the target is considered. Electrostatic and exchange effects dominate the near-target region. Further from the molecule, a new interaction that becomes important is the induced polarization interaction. The adiabatic change in energy felt by the field of the incident electron in the dipole approximation is written asymptotically as

$$V_p(\underline{r}) \underset{r \rightarrow \infty}{\sim} - \frac{\alpha(\hat{r})}{2r^4} \quad (\text{IV.3-6})$$

In this equation,  $\alpha(r)$  is the polarizability of the molecule which is a measure for the molecular capability to distort in response to an electric field directed along  $r$ . Equation (IV.3-6) breaks down if the electron closely approaches the molecule and also the adiabatic picture breaks down at high energies and near the nuclei.<sup>57</sup>

To properly take account of non-adiabatic effects and deviations from the simple asymptotic form (IV.3-6), a model potential has been introduced. The form of this model polarization potential is

$$V_p(\underline{r}) \underset{r \rightarrow \infty}{\sim} - \frac{\alpha(\hat{r})}{r^4} [1 - \text{EXP}(-\frac{r}{r_c})^6] \quad (\text{IV.3-7})$$

where  $r_c$  is an adjustable parameter which is usually chosen to give the best agreement with experiment.

#### **IV.4 Methods of Solution of the Scattering Process**

Many alternative techniques have been widely introduced to have an approximate solution of equation (IV-2). In this section a very short overview is presented on the approximations used in solving the scattering process, a little more detailed survey is also presented on the R-matrix method which is used in our calculation.<sup>65</sup>

One approach which has been widely used (for details see refs

66-71) is to make a single-centre expansion of the scattered electron wavefunction and the target orbitals. This common centre of expansion is usually chosen as the centre of gravity of the molecule. This approach is appropriate at large distances where the electron-molecule interaction is weak and nearly central, but convergence problems do arise for all molecules except the lightest ones due to the presence of nuclear singularities. These nuclear singularities provide a strong coupling of a large number of partial waves at short distances.

Due to the slow convergence, associated with the single-centre expansion method, other techniques,<sup>72,73</sup> so called multi-centre expansion methods, are introduced. In these methods the collision wavefunction is written in terms of a multi-centre expansion using a set of square integrable functions.

One of these methods is the T-matrix method,<sup>74,75</sup> in which no partitioning of configuration space into different regions is explicitly involved.

Another method is the R-matrix expansion technique. Following the frame transformation approach<sup>54</sup> the configuration space is partitioned into different regions, figure 4, now a further partitioning<sup>76</sup> into a core region  $r \leq a_c$  and a potential field region  $r \geq a_c$ , is appropriate. Under conditions such that the adiabatic nuclei approximation is valid for rotation, vibration, or both, then the relevant frame transformation radii can be taken to be infinite ie the frame transformation reduces to a constant transformation. The power of the R-matrix technique derives from the fact that in the inner region a fixed-nuclei, Body frame calculation of the R-matrix is sufficient followed by a relatively straight forward integration of the scattering equations in the outer region.

Briefly speaking (for details see ref <sup>76</sup>) in the internal region, assuming an incident electron upon an N-electron target molecule, the Schrodinger equation is written as

$$(H - E + L_b) \Psi_E = L_b \Psi_E \quad (\text{IV.4-1})$$

where  $\Psi_E$  is expanded, using equations (IV-4) and (IV-5), in the form

$$\begin{aligned} \Psi_E = & \sum_k A_{Ek} \left\{ \sum_i c_{ki} \phi_i(x_1, \dots, x_N; \sigma_{N+1}; R) F_i(r_{N+1}) + \right. \\ & \left. + \sum_j \xi_j(x_1, \dots, x_{N+1}; R) d_{jk} \right\} \end{aligned} \quad (\text{IV.4-2})$$

where the unperturbed target wave functions are denoted by  $\phi_j$ , the spatial one-electron continuum orbitals are denoted by  $F_j$ , while  $c_{ki}$  and  $d_{jk}$  are coefficients to be determined by diagonalization procedure.

The surface projection operator  $L_b$  in equation (IV.4-1) is introduced<sup>77</sup>

$$L_b = \sum_i |\phi_i\rangle \delta(r-a_c) \left[ \frac{d}{dr} - \frac{b}{a_c} \right] \langle \phi_i| \quad , \quad (\text{IV.4-3})$$

to remove the non-hermitian components of H in the inner region and also ensures that the wavefunctions (IV.4-2) satisfy the required logarithmic boundary condition at the R-matrix surface.

Following a procedure similar to section (II.3), the R-matrix is related to the radial wafunctions  $U_i$  of the scattered electron, in channel i, by the equation

$$U_i = \sum_j R_{ij} \left[ a_c \frac{dU_j}{dr} - b_j U_j \right]_{r=a_c} \quad (\text{IV.4-4})$$

in which  $a_c$  is the distance from the centre of mass of the diatomic molecule to the spherical R-matrix surface.

Therefore,

$$R_{ij} = \frac{1}{2a_c} \sum_k \frac{\gamma_{ki}^+ \gamma_{kj}}{E_k - E} \quad (\text{IV.4-5})$$

where  $\gamma_{ki}$  is defined on the R-matrix surface by

$$\gamma_{ki} = \langle \phi_i | \Psi_k \rangle_{r=a_c} \quad (\text{IV.4-6})$$

Given the R-matrix at  $r = a_c$  and assuming the usual asymptotic boundary conditions, the set of second order coupled differential equations,

$$\left[ \frac{d^2}{dr^2} - \frac{\ell(\ell+1)}{r^2} + k^2 \right] U_{i\ell}(r) = 2 \sum_{i'\ell'} V_{ii'\ell\ell'}(r) U_{i'\ell'}(r) \quad ,$$

(IV.4-7)

can be integrated in the outer region to determine the K-matrix for each  $E_i = k_i^2/2$ , where  $V_{ii'\ell\ell'}(r)$  is the local asymptotic potential coupling the channels  $i$  and  $i'$ .

## CHAPTER V

### DISCUSSION AND NUMERICAL RESULTS

#### V.1 Low-Energy Scattering of Electrons by Caesium Atoms<sup>24,25</sup>

The study of the low-energy scattering of electrons by caesium atoms has received much attention over the last ten years.<sup>37,38,78</sup> Recent advances in experimental techniques, together with the development of powerful numerical methods, have further stimulated work on this process. Not only can total and differential, elastic and inelastic cross-sections be measured but the use of high-resolution polarized electron beams enable observables such as spin polarization, the asymmetry function and the Stokes' parameters to be determined. Advances in numerical methods which now allow the inclusion of relativistic effects directly into the scattering equations have enabled theoretical calculations of these observables to be made. A stringent test of the theoretical model is therefore available. It is hoped that these results will be helpful to the various experiments which are currently in progress or under preparation in Munster<sup>79</sup> and Stirling.<sup>80</sup>

#### V.1A The Scattering Calculation

The dynamical calculations were performed using the relativistic R-matrix method first described by Scott and Burke<sup>81</sup> and programmed in ref.<sup>82</sup> This method, as discussed in chapter II, augments the non-relativistic electrostatic Hamiltonian with operators from the Breit-Pauli Hamiltonian thereby enabling some relativistic effects to be included into the scattering equations which describe the collision. Consequently the method allows the various effects which are important in low-energy electron scattering by heavy atoms to be accounted for. These effects resulting from strong-channel coupling, electron exchange,

relativistic effects and the influence of resonances.

As in recent calculations<sup>45,83</sup> we use a model potential to represent the closed-shell core of the target atom. In our model we therefore assume that one valence electron and the colliding electron are interacting with each other in the average field of the 54 core electrons. The R-matrix basis functions used to expand the total wavefunction are defined, using equation (II.3-1), as follows,

$$\psi_k = \sum_{ij} c_{ijk} \phi_i(1)u_{ij}(2) + \sum_j d_{jk} \phi_j(1,2) \quad (\text{V.1A-1})$$

where the unknown coefficients  $c_{ijk}$  and  $d_{jk}$  were determined by diagonalising the following model Hamiltonian,

$$H^2 = -\frac{1}{2} \left( \sum_{i=1}^2 \nabla_i^2 + V(r_i) - \alpha^2 Z \frac{(\ell_i \cdot s_i)}{r_i^3} \right) + \sum_{i>j} \frac{1}{r_{ij}} \quad (\text{V.1A-2})$$

$\alpha$  is the fine-structure constant,  $Z$  is the nuclear charge and  $V(r)$  is a model potential representing the core electrons. This is defined as

$$V(r) = V_H + \frac{\alpha_d}{r^4} [1 - \text{EXP}(-\frac{r}{r_c})]^6 + \frac{\alpha_q}{r^6} [1 - \text{EXP}(-\frac{r}{r_c})]^{10} \quad (\text{V.1A-3})$$

Here  $V_H$  is a Hartree potential constructed from Thomas-Fermi Core orbitals,  $\alpha_d$  is the static dipole polarizability of the core, while  $\alpha_q$  and  $r_c$  are treated as adjustable parameters for each orbital angular momentum. Values for these adjustable parameters were found by calculating the negative eigen-energies of the following equation,

$$\left( \frac{d^2}{dr^2} - \frac{\ell(\ell+1)}{r^2} + V(r) + k^2 \right) U(r) = 0 \quad (\text{V.1A-4})$$

The values of  $\alpha_q$  and  $r_c$  were varied until the eigen-energies of equation (V.1A-4) gave energy splittings in good agreement with experiment. The values used in the scattering calculation together with the corresponding eigen-energies are given in table 1.

We include the following five target eigenstates in expansion

$$(\text{V.1A-1}), \quad 6s \ ^2S_{\frac{1}{2}} \quad 6p \ ^2P_{\frac{1}{2}, \frac{3}{2}} \quad 5d \ ^2D_{\frac{3}{2}, \frac{5}{2}} \quad . \quad (\text{V.1A-5})$$

Each of these states was represented by a single configuration one-electron function which, together with the core functions form the Hartree potential, were calculated using the SUPERSTRUCTURE program.<sup>84</sup>

The R-matrix continuum orbitals were determined by imposing a logarithmic derivative of zero at the R-matrix radius of 40.3555 a.u. This radius  $r_a$ , was chosen automatically by the code to ensure that for  $r \geq r_a$  exchange between the incident electron and the target could be neglected. These orbitals were orthogonalised to the core and valence orbitals. Sixteen continuum orbitals were retained in the expansion for each orbital angular momentum in order to guarantee convergence over the energy range considered in these calculations.

All quadratically integrable correlation functions were included in the expansion (V.1A-1) which could be constructed from the 6s, 6p and 5d orbitals with the appropriate symmetry as discussed in the next section. The diagonal elements of the Hamiltonian matrix were adjusted so that the theoretical target energy splittings were in good agreement with experiment.

K-matrices were calculated for each of the total angular momentum from  $J = 0$  to 10 for both even and odd parities. This ensured that converged scattering amplitudes could be calculated over the energy range from 0 to 3 eV. The inclusion of five target states gave rise to up to 18 coupled channels.

#### **V.1B Analysis of the resonances**

In an earlier work<sup>37</sup> a two-state (6s-6p) calculation was employed which accounts for almost all the static dipole polarizability of the ground state. They obtained a total cross section which was in reasonable accord with experiment and the present calculation in energy

regions which were not close to the 6p and 5d excited-state thresholds. However, inclusion of the 5d state in the present work introduces a large number of additional resonances, particularly in the neighbourhood of the 6p  $^2P_{\frac{1}{2},\frac{3}{2}}$  and 5d  $^2D_{\frac{3}{2},\frac{5}{2}}$  thresholds. Inclusion of this state is therefore important if accurate results are to be obtained close to these excited-state thresholds. These resonances have a pronounced effect on the angular distributions and their number and complexity explains the difficulty that Gehenn and Reichert<sup>78</sup> experienced in analysing their experimental measurement of these cross sections.

Most of the resonances are associated with the inclusion of the quadratically integrable function in equation (V.1A-1). These allow physically for the situation where the incident electron is captured into a state whose lifetime is long compared with the collision time. We included the following 35 quadratically integrable functions:

$$\begin{aligned}
 &6s^2 \ ^1S_0^e, \ 6s6p \ ^3P_{0,1,2}^0, \ 6s6p \ ^1P_1^0, \ 6p \ ^2_3P_{0,1,2}^e, \ 6p^2 \ ^1D_2^e, \\
 &6p^2 \ ^1S_0^e, \ 6s5d \ ^3D_{1,2,3}^0, \ 6s5d \ ^1D_2^e, \ 6p5d \ ^3P_{0,1,2}^e, \\
 &6p5d \ ^1P_1^0, \ 6p5d \ ^3D_{1,2,3}^0, \ 6p5d \ ^1D_2^0, \ 6p5d \ ^3F_{2,3,4}^0, \\
 &6p5d \ ^1F_3^0, \ 5d^2 \ ^1S_0^e, \ 5d^2 \ ^3P_{0,1,2}^e, \ 5d^2 \ ^1D_2^e, \ 5d^2 \ ^3F_{2,3,4}^e, \\
 &5d^2 \ ^1G_4^e.
 \end{aligned}$$

(V.1B-1)

Of course not all of these give rise to observable resonances. For example, the  $6s^2 \ ^1S_0^e$  is not seen since its energy is below the  $6s \ ^2S_{\frac{1}{2}}$  threshold and this corresponds to a bound state of  $Cs^-$ . Also many of the others lie at too high an energy and are too broad to noticeably affect the cross section.

A further class of resonance which we observe corresponds to the situation where the incident electron is temporarily captured at very large distances in the long-range field of the target in an excited state. This is most likely in our calculation near the strongly polarizable

$6p \ 2P_{\frac{1}{2}, \frac{3}{2}}^0$  states of the target, since our inclusion of the  $5d \ 2D_{\frac{3}{2}, \frac{5}{2}}^e$  states allows to account for most of the strong long-range polarization potential in this case.

One of the most satisfactory ways of analysing and describing the resonances is by reference to the eigenphase sums. It is well known<sup>85</sup> that near an isolated resonance this quantity has the following behaviour

$$\delta(E) = \delta_0(E) + \tan^{-1} \frac{\frac{1}{2}\Gamma}{E_r - E} \quad (\text{V.1B-2})$$

where  $\delta_0(E)$  is a slowly varying background phase shift and  $\Gamma$  and  $E_r$  are the width and position of the resonance, respectively. Hence the phaseshift increases by  $\pi$  rad in the neighbourhood of  $E_r$ . However, in practice, particularly in a complex situation such as we are considering in this discussion, this simple picture is often obscured. Firstly, the rate of change of the background phaseshift can be as large or larger than the resonance term itself, and can either be increasing, due to attractive polarization potentials, or decreasing just above a threshold involving a virtual or bound state. Secondly, several resonances with different widths can be overlapping. Finally, strong configuration interaction effects mean that identifying a resonance with a single configuration in (V.1B-1) can only be an approximate description.

With these qualifications in mind, we present, in figures (5-14), the eigenphase sums for the resonant symmetries which from (V.1B-1) are seen to be  $J = 0$  to  $4$  with odd and even parities. In an attempt to assign a configuration to each resonance we performed a number of additional calculations. We begin by calculating the eigenphases in LS-coupling neglecting the relativistic terms in the Hamiltonian defined by equation (V.1A-2). We carried out three such calculations, in the one-state (6s), two-state (6s-6p) and three-state (6s-6p-5d) approximations. This enabled us to observe how the resonances appeared and changed in

character as additional states and closed channels were added. The three-state eigenphases together with the corresponding R-matrix poles were analysed in detail. This allowed us to assign each resonance with a configuration. The five-state relativistic calculation was then performed and we were able to observe how each LS-coupled resonance was split by the spin-orbit interaction and distributed into different total angular momentum symmetries. These assignments were confirmed further by an analysis of the relativistic R-matrix poles.

In figures (5-14) each resonance is designated by a letter. The corresponding configurations are presented in table (2). The lowest-lying odd parity resonance is located close to the  ${}^2P_{\frac{1}{2}}$  threshold in  $J = 2$  symmetry, figure (7). It clearly has the configuration  $6p5d {}^3F_2^o$  and can also be seen at slightly higher energies in the  $J = 3$  and  $J = 4$  symmetries, figures (8,9). We find this resonance at a lower energy than Burke and Mitchell<sup>37</sup> which is in good agreement with Gehenn and Reichert.<sup>78</sup> This resonance is simply a consequence of the inclusion of the 5d state in our calculations. It is the influence of this resonance which is responsible for the broad 'bump' just below the  ${}^2P_{\frac{1}{2}}$  threshold in the  ${}^2S_{\frac{1}{2}} + {}^2S_{\frac{1}{2}}$  cross section shown in figure (15). Lying very close to the  ${}^2P_{\frac{1}{2}}$  threshold we find a narrow resonance to which we have assigned the configuration  $6p\bar{n}s {}^3p^o$ . This is clearly seen in the  $J = 0,1$  and 2 symmetries, figures (5-7). This resonance cannot be associated with any of the quadratically integrable functions in (V.1B-1) so we have concluded that it is the result of the capture of the incident electron in the long-range potential field of Cs as discussed above. Near the  ${}^2P_{\frac{3}{2}}$  threshold a number of resonances are found. Below the threshold there is a  $6s6p {}^1p_1^o$  and a  $6p5d {}^1D_2^o$ . In both these cases the rapid increase in the eigenphase sum is cut short by the onset of the  ${}^2P_{\frac{3}{2}}$  threshold. Between the  ${}^2P_{\frac{3}{2}}$  and  ${}^2D_{\frac{3}{2}}$  thresholds we find a broad

6p5d  $^1F_3^0$  resonance and a distinctive feature in the  $J = 0, 1$  and  $2$  symmetries, figures (5-7), which is attributable to the 6p5d  $^3P^0$  configuration. Because of the near degeneracy of the  $^2D_{3/2}$  and  $^2D_{5/2}$  thresholds resonance structure in this energy region are difficult to resolve. However, we believe there are indications of a 6p5d  $^3D^0$  resonance in the  $J = 1, 2$  and  $3$  symmetries, figures (6-8), close to these thresholds.

We are turning our attention now to the even symmetries. Here we only observe resonance structure in the  $J = 0, 1, 2$  and  $3$  symmetries, figures (10-13). The rise in the eigenphase sum above the  $^2P_{3/2}$  threshold in the  $J = 4$  symmetry, figure (14), is probably due to the polarizability of the 6p state which is accounted for by inclusion of the 5d state. In the even symmetries the lowest-lying resonance occurs below 0.5 eV where a broad feature with configuration 6s5d  $^3D^e$  is observed in the  $J = 1, 2$  and  $3$  symmetries, figures (11-13). Close to the  $^2P_{1/2}$  threshold in the  $J = 0$  symmetry, figure (10), we find a distinctive resonance which is the combined effect of two resonances, the  $6p^2 \ ^1S^e$  and the  $6p^2 \ ^3P^e$ . The  $6p^2 \ ^3P^e$  is also observed above the  $^2P_{1/2}$  threshold in the  $J = 1$  and  $2$  symmetries, figures (11,12). As in the odd symmetry we find evidence for the capture of the incident electron by the long-range potential field of Cs. This time it occurs at the  $^2P_{3/2}$  threshold in the  $J = 1, 2$  and  $3$  symmetries, figures (11-13), with configuration  $6p\bar{n}p \ ^3D^e$ . There are no indications of any resonances around the  $^2D_{3/2}$  and  $^2D_{5/2}$  thresholds in the even symmetries, figures (10-14).

Despite the large number of resonances identified from the eigenphase sums only a few sharp features appear in the cross sections for the transitions  $^2S_{1/2} \rightarrow ^2S_{1/2}$ ,  $^2P_{1/2}$ ,  $^2P_{3/2}$ , figures (15-17). This is because many of the resonances in different symmetries overlap in energy and strongly interfere with each other in the total cross sections.

### V.1C Differential Cross section, Spin Polarization and Scattering Asymmetry

We described in section (II.4) how to calculate differential cross section, spin polarization and scattering asymmetry for a general transition from an initial state  $|j_0 M_{j_0}\rangle$  to a final state  $|j_1 M_{j_1}\rangle$ . Here we discuss our numerical calculation for these quantities.

In figures (18,19) we show the elastic differential cross section  $\sigma$  and the scattering asymmetry  $A_s = p_y$  for the three energies (0.816 eV, 1.632 eV, 2.04 eV). Absolute values of  $A_s$  up to 20% are found near the minima in the elastic cross sections around  $125^\circ$ ; the relation of high absolute values of  $A_s$  to the minima in the cross sections is a well known feature in the elastic Mott scattering process.<sup>36</sup>

In figures (20-25) we show the functions  $P_y$  and  $A_s$  and the differential cross sections for inelastic scattering (transitions  $6s \ ^2S_{\frac{1}{2}} \rightarrow 6p \ ^2P_{\frac{1}{2}, \frac{3}{2}}$ ). The first notable feature of the curves is the high absolute values of  $P_y$  and  $A_s$  even for very small scattering angles (ie less than or equal to  $20^\circ$ ); these high values are not necessarily combined with minima in the cross sections. The second interesting feature to be noted is the following approximate symmetry relation in the form

$$P_y\left(\frac{1}{2}\right) \approx -2P_y\left(\frac{3}{2}\right) \quad (\text{V.1C-1})$$

$$A_s\left(\frac{1}{2}\right) \approx -2A_s\left(\frac{3}{2}\right) \quad (\text{V.1C-2})$$

where the arguments  $\frac{1}{2}$  and  $\frac{3}{2}$  indicate the final states  $^2P_{\frac{1}{2}}$  and  $^2P_{\frac{3}{2}}$  respectively. Relations (V.1C-1) and (V.1C-2) are very well fulfilled for 2.04 eV and are a clear indication of the validity of the so-called 'fine-structure' effect discussed by Hanne.<sup>86</sup> In this effect the spin-orbit coupling within the target and the spin-orbit interaction of the scattered electron are assumed to be weak and the spin-dependent effects then arise from the transformation from LS-coupling to a

representation determining transitions between fine-structure levels. The only qualitative agreement for 1.632 eV is due to close vicinity of resonances and thresholds, where Hanne's approximation cannot be expected to be valid.

In figures (26-37) we present results for the differential cross section and spin polarization of the scattered electrons as a function of energy at eight scattering angles ( $10^\circ$ ,  $30^\circ$ ,  $50^\circ$ ,  $70^\circ$ ,  $90^\circ$ ,  $110^\circ$ ,  $130^\circ$ ,  $150^\circ$ ). Expressing these quantities as a function of energy at a fixed angle involves a lengthy calculation. Since there are as yet no experimental results available to compare with we only used a small number of energy points to give an indication of the structure involved. These figures are only intended as a guide to experimentalists until more data become available.

In figures (26-29) the differential cross section for unpolarized initial beams is plotted as a function of the incident electron energy for different scattering angles  $\theta_e$ . As expected dominant structures can be seen in the resonance region, especially around the  $^2P_{\frac{1}{2}}$  and  $^2P_{\frac{3}{2}}$  thresholds at 1.39 and 1.46 eV. Figures (30-33) show the spin polarization  $P_y$  of the scattered electrons, again for initially unpolarized beams and for the transition  $^2S_{\frac{1}{2}} \rightarrow ^2S_{\frac{1}{2}}$ . It should be noted that, apart from the resonance region, the absolute values of  $P_y$  are rather small ( $\leq 15\%$ ). In figures (34-37) we show the spin polarization  $P_y$  of the scattered electron beam when the electrons are initially fully transversally polarized.

## V.2 Stokes' Parameter for Inelastic Electron-Caesium Scattering<sup>44</sup>

In chapter III we described the polarization properties of light detected from an excited atom. In view of that description the Stokes'

parameter of the light emitted in the decay  $6p \ ^2P_{\frac{1}{2}, \frac{3}{2}} \rightarrow 6s \ ^2S_{\frac{1}{2}}$  in atomic caesium after electron impact excitation are given by the following:

**Case A Incident electrons are initially transversally polarized in the y-direction with polarization  $P_y$  and photons detected in the y-direction**

$$(i) \text{ Cs : } 6p \ ^2P_{\frac{1}{2}} \rightarrow 6s \ ^2S_{\frac{1}{2}}$$

$$\eta_2 = \sqrt{2} \frac{\bar{G}_1(\frac{1}{2}) \operatorname{Im}[\langle \mathcal{J}(\frac{1}{2})_{11}^+ \rangle_{\text{pol}}]}{\bar{G}_0(\frac{1}{2}) \langle \mathcal{J}(\frac{1}{2})_{00}^+ \rangle_{\text{un}}} \quad ; \quad \eta_1 = \eta_3 = 0 \quad (\text{V.2A-1})$$

$$(ii) \text{ Cs : } 6p \ ^2P_{\frac{3}{2}} \rightarrow 6s \ ^2S_{\frac{1}{2}}$$

$$\eta_1 = \frac{\frac{1}{2} \bar{G}_2(\frac{3}{2}) \operatorname{Re}[\langle \mathcal{J}(\frac{3}{2})_{21}^+ \rangle_{\text{pol}}]}{\frac{1}{\sqrt{6}} [4\bar{G}_0(\frac{3}{2}) \langle \mathcal{J}(\frac{3}{2})_{00}^+ \rangle_{\text{un}} - \bar{G}_2(\frac{3}{2}) \langle \mathcal{J}(\frac{3}{2})_{20}^+ \rangle_{\text{un}}]} \quad (\text{V.2A-2})$$

$$\eta_2 = \frac{4/\sqrt{5}}{\sqrt{2}} \cdot \frac{\bar{G}_1(\frac{3}{2}) \operatorname{Im}[\langle \mathcal{J}(\frac{3}{2})_{11}^+ \rangle_{\text{pol}}]}{4\bar{G}_0(\frac{3}{2}) \langle \mathcal{J}(\frac{3}{2})_{00}^+ \rangle_{\text{un}} - \bar{G}_2(\frac{3}{2}) \langle \mathcal{J}(\frac{3}{2})_{20}^+ \rangle_{\text{un}}} \quad (\text{V.2A-3})$$

$$\eta_3 = -3 \frac{\bar{G}_2(\frac{3}{2}) \langle \mathcal{J}(\frac{3}{2})_{20}^+ \rangle_{\text{un}}}{4\bar{G}_0(\frac{3}{2}) \langle \mathcal{J}(\frac{3}{2})_{00}^+ \rangle_{\text{un}} - \bar{G}_2(\frac{3}{2}) \langle \mathcal{J}(\frac{3}{2})_{20}^+ \rangle_{\text{un}}} \quad (\text{V.2A-4})$$

**Case B Incident electrons are initially longitudinally polarized with polarization  $P_z$  and photons detected in the forward direction**

$$(i) \text{ Cs : } 6p \ ^2P_{\frac{1}{2}} \rightarrow 6s \ ^2S_{\frac{1}{2}}$$

$$\eta_2 = \frac{\bar{G}_1(\frac{1}{2}) \langle \mathcal{J}(\frac{1}{2})_{10}^+ \rangle_{\text{pol}}}{\bar{G}_0(\frac{1}{2}) \langle \mathcal{J}(\frac{1}{2})_{00}^+ \rangle_{\text{un}}} \quad ; \quad \eta_1 = \eta_3 = 0 \quad (\text{V.2B-1})$$

$$(ii) \text{ Cs : } 6p \ ^2P_{\frac{3}{2}} \rightarrow 6s \ ^2S_{\frac{1}{2}}$$

$$\eta_2 = \sqrt{5} \frac{\bar{G}_1(\frac{3}{2}) \langle \mathcal{J}(\frac{3}{2})_{10}^+ \rangle_{\text{pol}}}{2\bar{G}_0(\frac{3}{2}) \langle \mathcal{J}(\frac{3}{2})_{00}^+ \rangle_{\text{un}} + \bar{G}_2(\frac{3}{2}) \langle \mathcal{J}(\frac{3}{2})_{20}^+ \rangle_{\text{un}}} \quad (\text{V.2B-2})$$

Before we discuss these coefficients we make the following remarks:

(i) As can be shown by general symmetry arguments,<sup>3</sup>  $\eta_1$  and  $\eta_2$  are proportional to the polarization component of the incoming electrons, whereas  $\eta_3$  (and the total intensity) is independent of the electron polarization.

(ii) For the transition  $6p \ ^2P_{\frac{1}{2}} \rightarrow 6s \ ^2S_{\frac{1}{2}}$  only  $\eta_2$  can be different from zero;  $\eta_1$  and  $\eta_3$  are proportional to integrated state multipoles with rank  $K = 2$ , which cannot appear in an excited state with  $J = \frac{1}{2}$  (in general  $2j \leq K$ ).

(iii) Integrated state multipoles with rank  $K = 3$  which can appear in the description of an excited state with  $j = \frac{3}{2}$  cannot be measured in this type of experiment.

It can be seen from the values of the perturbation coefficients, written in section III.5, that the large nuclear spin  $I = \frac{7}{2}$  in Caesium causes a significant depolarization of the emitted radiation. With  $\overline{G}_2(\frac{7}{2}) = 0.219$  a rough estimate has shown that for example values of  $|\eta_3|$  or  $|\eta_1/P_y|$  greater than 20% seem to be very unlikely.

In figures (38-41) we present our numerical results for the integrated Stokes' parameters  $\eta_1$ ,  $\eta_2$  and  $\eta_3$  in case of transversally polarized incoming electrons. The polarization dependent components  $\eta_1$  and  $\eta_2$  are normalised to an initial electron polarization of 100%. As expected from the values of the perturbation coefficients, the absolute values of the Stokes' parameters are rather small, and it should be noted that the polarizations  $\eta_1$  and  $\eta_2$ , which can be measured in an experiment, become even smaller if  $P_y$  is less than 100%.

Also in figure (42) we show our numerical results compared with the only available measurement.<sup>87</sup> In this case the incident electrons were polarized with polarization vector along the z-axis and the photons detected in the forward direction. This shows a fairly good agreement of our calculation with experiment.

### V.3 Vibrational Inelastic Scattering of Electrons by N<sub>2</sub>

In previous papers by Chang<sup>89,90</sup> it was shown that, using the frame transformation formulation of Chang and Fano,<sup>54</sup> the resonant differential cross section, at intermediate energies, in electron scattering from N<sub>2</sub>-molecule is due to <sup>2</sup>Σ<sub>u</sub> in symmetry with a dominant f component. He admits also p component to take a place in the former.

In our work,<sup>65</sup> we used the same technique as Burke et al<sup>91</sup> to extract the transition matrix, which contains all information about the scattering process, in the static exchange plus polarization approximation, SEP. We carried out calculation for <sup>2</sup>Σ<sub>u</sub> symmetry and only contributions from p- and f-partial waves, as in Chang's paper,<sup>90</sup> were included.

According to these assumptions the differential cross section for excitation from a vibrational state v<sub>i</sub> to state v<sub>f</sub> is given by<sup>55,90,92</sup>

$$\begin{aligned} \frac{\partial \sigma(v_i \rightarrow v_f)}{\partial \Omega} = & \frac{1}{4k_{v_i}} \sum_{L,j} (2J+1) [9 \cdot (10,10|L0)]^2 \begin{Bmatrix} 1 & 1 & j \\ 1 & 1 & L \end{Bmatrix} \times \\ & \times |M_{v_i 1; v_f 1}^{(j)}|^2 + 49 \cdot (30,30|L0)^2 \begin{Bmatrix} 3 & 3 & j \\ 3 & 3 & L \end{Bmatrix} |M_{v_i 3; v_f 3}^{(j)}|^2 + \\ & + 42 \cdot (10,10|L0)(30,30|L0) \begin{Bmatrix} 3 & 3 & L \\ 1 & 1 & j \end{Bmatrix} |M_{v_i 1; v_f 3}^{(j)}|^2 P_L(\cos \theta) \end{aligned} \quad (V.3-1)$$

where P<sub>L</sub>(cos θ) is the Legendre polynomial and M-matrix is defined, in general, by the relation

$$\begin{aligned} M_{v_i l; v_f l'}^{(j)} = & \sum_{\Lambda} (-1)^{l-l'+\Lambda} \cdot \frac{1}{(2j+1)^{\frac{1}{2}}} (l\Lambda, l'-\Lambda|j0) \times \\ & \times T_{v_i l; v_f l'}^{(\Lambda)}, \end{aligned} \quad (V.3-2)$$

$l, l'$  are the angular momentum of the incident and scattered electron and  $\Lambda$  is the component of the angular momentum along the internuclear axis.

The vibrational transition matrix in equation (V.3-2), in the adiabatic approximation, may be written as ( $\alpha$  is appended to distinguish different target eigenstates with the same  $\Lambda$ )

$$T_{v_i l; v_f l'}^{(\Lambda)} = \frac{2}{1 + \delta_{\Lambda 0}} \cdot \langle X_{v_f}(R) | \sum_{\alpha} (C_{l\alpha}^{(\Lambda)}(R) e^{2i\delta_{\alpha\Lambda}(R)} \tilde{C}_{\alpha l'}^{(\Lambda)}(R) | X_{v_i}(R) \rangle \quad (\text{V.3-3})$$

In the present calculation, eleven equally spaced values of  $R$  define the mesh of the internuclear distances and a theoretical vibrational wavefunctions,  $X_v(R)$ , are used where only the first four vibrational levels are treated. In this two channels problem, C-matrix has the form

$$\underline{C}^{(\Lambda)}(R) = \begin{pmatrix} \cos \beta(R) & \sin \beta(R) \\ -\sin \beta(R) & \cos \beta(R) \end{pmatrix}, \quad (\text{V.3-4})$$

where  $\beta(R)$  is the mixing parameter which relates p- and f- waves contributions to the scattered amplitudes.

Before we make our discussion we mention the following remarks on equation (V.3-1).

(i) The first term stands for p- wave contribution, the second for f- wave, whereas the last term is a mixture of p- and f- waves.

(ii) All interference terms between p- and f- waves have been cancelled as a result of summation over all rotational states allowed by the symmetry relations.

(iii) From the symmetry relations of the Clebsch-Gordan coefficients, summation runs over even values of  $L$ . So, the Legendre polynomial contains only even powers of  $\cos \theta$  and we get an angular distribution which is always symmetric around  $90^\circ$ .

(iv) The integrated cross sections are obtained by integrating

equation (V.3-1) over all the electronic scattering angles.

In figures (43a-43d) we show the variation of the individual eigenphases with the internuclear distance, at four incident electron energies. It is clear that the p-wave eigenphase changes minimally as a function of  $R$  as compared with the change of the f-wave eigenphase, confirming that the f-partial wave dominates the resonance. Also, it is shown the region where there is a strong mixing between p- and f-partial waves at each incident electron energy. This is again manifested on figures (44a-44d) where the mixing parameter is plotted as a function of  $R$  at fixed values of energy. The rapid variation of  $\beta$

with  $R$  contradicts the assumption made by Chang<sup>89</sup> that is the mixing parameter can be taken to be independent of the energy and the internuclear distance.

Table (3) gives the integrated cross sections for  $v_i = 0 \rightarrow v_f = 1, 2$  transitions, compared with other theoretical calculations and experimental data. In general the calculations are in reasonable accord with each other.

We present in figures (45-47) our numerical calculations for the vibrational excitation,  $v_i = 0 \rightarrow v_f = 1$ , angular distribution at incident energies 20, 25 and 30 eV. Some other theoretical calculation and experimental data are included for comparison. The circled curves are taken from Chang,<sup>90</sup> equation (3) with a fixed  $\beta = 60^\circ$ , after normalization to the experimental data of Tanaka et al<sup>93</sup> at 20, 25 and 30 eV by multiplying by  $7.8 \times 10^{-19}$ ,  $4.1 \times 10^{-19}$  and  $1.6 \times 10^{-19}$  ( $\text{cm}^2/\text{sr}$ ), respectively.

Our calculation, of angular distribution, exhibits a minimum at  $40^\circ$ , followed by a local maximum at  $61^\circ$  and another deeper minimum at  $90^\circ$ . The present calculation shows, in general, a fairly good agreement with Onda and Truhlar<sup>94</sup> calculation. At incident electron

energy 20 eV, the present calculation is agreeable with measurements by Tanaka et al<sup>93</sup> and Pavlovic et al<sup>50</sup> in shape but not in magnitude. At 25 eV a good agreement is shown with Tanaka et al<sup>93</sup> data, whereas there is a disagreement with the data of Pavlovic et al<sup>50</sup> (this disagreement is explained by Chang<sup>90</sup> as the resolution, in Pavlovic et al<sup>50</sup> experiment, was high enough to resolve the rotational states). At 30 eV our calculation is again agreeable with measurements by Tanaka et al<sup>93</sup> and Truhlar et al<sup>95</sup> in shape but not in magnitude.

## REFERENCES

1. Fano U (1957): *Rev Mod Phys*, 29 74.
2. Messiah A (1965): Quantum Mechanics (North Holland, Amsterdam).
3. Blum K (1981): Density Matrix Theory and Applications (Plenum Press, New York and London).
4. McMaster W (1954): *Am J Phys*, 22 357.
5. Born M and Wolf E (1970): Principles of Optics (Pergamon Press, New York).
6. Fano U and Racah G (1959): Irreducible Tensorial Sets (Academic Press INC, New York).
7. Fano U (1953): *Phys Rev*, 90 577.
8. Blum K and Kleinpoppen H (1979): *Phys Rep*, 52 203.
9. Bartschat K, Blum K, Hanne G F and Kessler J (1981): *J Phys B: At Mol Phys*, 14 3761.
10. Sommerfeld A (1916): *Ann Phys (Leipzig)* [4], 51 1.
11. Dirac P A M (1928): *Proc Roy Soc, Ser, A* 117 610.
12. Dirac P A M (1930): The Principles of Quantum Mechanics (Oxford University Press).
13. Breit G (1929): *Phys Rev*, 34 553.
14. Breit G (1930): *Phys Rev*, 36 383.
15. Breit G (1932): *Phys Rev*, 39 616.
16. Doyle H T (1969): *Adv Atom Mol Phys*, 5 337.
17. Grant I P (1970): *Adv Phys*, 19 747.
18. Armstrong Jr L and Feneuille S (1974): *Adv Atom Mol Phys*, 5 1.
19. Armstrong Jr L (1971): Theory of the Hyperfine Structure of Free Atoms (John Wiley & Sons, New York).
20. Walker D W (1974): *J Phys B: At Mol Phys*, 7 97.
21. Chang J J (1975): *J Phys B: At Mol Phys*, 8 2327.
22. Glass R and Hibbert A (1976): *Comp Phys Commun*, 11 125.
23. Hibbert A (1979): *J Phys B: At Mol Phys*, 12 L661.
24. Scott N S, Bartschat K, Burke P G, Nagy O and Eissner W B (1984): *J Phys B: At Mol Phys*, 17 3755.

25. Scott N S, Bartschat K, Burke P G, Eissner W B and Nagy O (1984): J Phys B: At Mol Phys, 17 L 191.
26. Burke P G and Robb W D (1975): Adv Atom Mol Phys, 11 143.
27. Glass R and Hibbert A (1978): Comp Phys Commun, 16 19.
28. Burke P G and Seaton M J (1971): Meth Comp Phys, 10 1.
29. Hibbert A (1975): Comp Phys Commun, 9 141.
30. Burke P G and Schey H M (1962): Phys Rev, 126 147.
31. Norcross D W and Seaton M J (1969): J Phys B: At Mol Phys, 2, 731.
32. Mott N F (1929): Proc Roy Soc (London), A124 425.
33. Massey H S W and Mohr C B O (1941): Proc Roy Soc (London), A177 341.
34. Farago P S (1971): Rep Prog Phys, 34 1055.
35. Kleinpoppen H (1971): Phys, Rev, A3 2015.
36. Kessler J (1976): Polarized Electrons (Springer, Berlin).
37. Burke P G and Mitchell J F B (1973): J Phys B: At Mol Phys, 6 L161.
38. Burke P G and Mitchell J F B (1974): J Phys B: Atom Mol Phys, 7 214.
39. Scott N S (1980): Ph D Thesis (The Queens Univ of Belfast).
40. Taylor J R (1972): Scattering Theory (John Wiley, New York)
41. Percival I C and Seaton M J (1957): Philos Trans Roy Soc, A251 113.
42. Fano U and Macek J (1973): Rev Mod Phys, 45 553.
43. Khalid S M and Kleinpoppen H (1984): J Phys B: At Mol Phys, 17 243.
44. Nagy O, Bartschat K, Blum K, Burk P G and Scott N S (1984): J Phys B: At Mol Phys, 17 L527.
45. Bartschat K, Scott N S, Blum K and Burke P G (1984): J Phys B: At Mol Phys, 17 269.
46. Macek J and Jaacks D H (1971): Phys Rev, A4 2288.
47. Blum K (1978): in Progress in Atomic Spectroscopy (edt: Hanle W and Kleinpoppen H, Plenum Press, New York and London) p 71.
48. Brink D M and Satchler G R (1968): Angular Momentum (clarendon Press, Oxford).

49. King G W (1965): Spectroscopy and Molecular Structure (Holt, Rinehart and Winston, INC, New York).
50. Pavlovic Z, Boness M J W, Herzenberg A and Schulz G T (1972): Phys Rev, A6 676.
51. Tronc M, Azria R and Coat Y L (1980): J Phys B: At Mol Phys, 13 2327.
52. Mott N F and Massey H S W (1965): The Theory of Atomic Collisions (3 rd edition, Clarendon, Oxford).
53. Burke P G (1977): X ICPEAC, Electronic and Atomic Collisions, Invited Papers and Progress Reports (edt: Watel G, North Holland, Amsterdam) P201.
54. Chang E S and Fano U (1972): Phys Rev, A6 173.
55. Burke P G (1979): Adv Atom Mol Phys, 15 471.
56. Chang E S and Temkin A (1969): Phys Rev Lett, 23 399.
57. Lane N F (1980): Rev Mod Phys, 52 29.
58. Chase D M (1956): Phys Rev, 104 838.
59. Chandra N and Temkin A (1976a): Phys Rev, A13 188.
60. Chandra N and Temkin A (1976b): Phys Rev, A14 507.
61. Hara S (1967): J Phys Soc jpn, 22 710.
62. Riley M E and Truhlar D G (1975): J Chem Phys, 63 2182.
63. Baille P and Darewych J W (1977): J Chem Phys, 67 3399.
64. Burke P G and Chandra N (1972): J Phys B: At Mol Phys, 5 1696.
65. Nagy O, Burke P G and Noble C J (1985): to be published in J Phys B: At Mol Phys.
66. Buckley B D and Burke P G (1977): J Phys B: At Mol Phys, 10 725.
67. Raseev G, Giusti-Suzor A and Lefebvre-Brion H (1978): J Phys B: At Mol Phys, 11 2735.
68. Morrison M A, Lane N F and Collins L A (1977): Phys Rev, A15 2186.
69. Morrison M A (1979): Electron-Molecule and Photon-Molecule Collisions (edt: Rescigno T N, McKoy V and Schneider B I, Plenum Press, New York and London).
70. Collins L A, Robb W D and Morrison M A (1980): Phys Rev, A21 488.
71. Collins L A, Robb W D and Morrison M A (1978): J Phys B: At Mol Phys, 11 L777.

72. Temkin A (1966): Autoionization (edt: Temkin A, Mono Book Corporation, Baltimore).
73. Hazi A U and Taylor H S (1970): Phys Rev, A1 1109.
74. Rescigno T N, McCurdy C W and McKoy V (1974a): Chem Phys Lett, 27 401.
75. Rescigno T N, McCurdy C W and McKoy V (1974b): Phys Rev, A10 2240.
76. Burke P G; McChy I and Shimamura I (1977): J Phys B: At Mol Phys, 5 2497.
77. Bloch C (1957): Nucl Phys, 4 503.
78. Gehenn W and Reichert E (1977): J Phys B: At Mol Phys, 10 3105.
79. Hanne G F (1984): Private Communication.
80. Kleinpoppen H (1985): Private Communication.
81. Scott N S and Burke P G (1980): J Phys B: At Mol Phys, 13 4299.
82. Scott N S and Taylor K T (1982): Comp Phys Commun, 25 347.
83. Scott N S, Burke P G and Bartschat K (1983): J Phys B: At Mol Phys, 16 L 361.
84. Eissner W, Jones M and Nussbaummer H (1974): Comp Phys Commun, 8 270.
85. Nesbet R K (1980): Variational Methods in Electron-Atom Scattering Theory (Plenum Press, New York).
86. Hanne G F (1983): Phys Rep, 95 95.
87. Measurements by Nass P (1985): Institut fur Physik, Mainz, Germany (Private Communication).
88. Moore C E (1970): Atomic Energy Levels NSRDS-NBS3 (Washington, D C: US Govt Printing Office).
89. Chang E S (1977): Phys Rev, A16 1841.
90. Chang E S (1983): Phys Rev, A27 709.
91. Burke P G, Noble C J and Salvini S (1983): J Phys B: At Mol Phys, 16 L113.
92. Salvini S and Thompson D G (1981): Comp Phys Commun, 22 49.
93. Tanaka H, Yamamoto T and Okada T (1981): J Phys B: At Mol Phys, 14 2081.
94. Onda K and Truhlar D G (1980): J Chem Phys, 72 5249.

95. Truhlar D G, Brandt M A, Srivastava S K, Trajmar S and Chutjian A (1977): J Chem Phys, 66 655.
96. Onda K and Truhlar D G (1979): J Chem Phys, 71 5107.
97. Rumble J R, Truhlar D G and Morrison M A (1981): J Phys B: At Mol Phys, 14 L301.
98. Dehmer J L, Siegel J, Welch J and Dill D (1980): Phys Rev, A21 101.

## TABLE AND FIGURE CAPTIONS

- Table 1 Adjustable parameters used in the model potential defined in equation (V.1A-3). For  $\ell > 3$  the values for  $\ell = 3$  were used. Also shown are the corresponding eigenenergies of equation (V.1A-4). The experimental energies are taken from Moore<sup>88</sup>.
- Table 2 Definition of the configuration assignments used in figures 5-14.
- Table 3 Integrated cross sections ( $a^2$ ) for electron-N<sub>2</sub> scattering in  $v(0 \rightarrow 1,2)$  vibrational excitation at several impact energies.
- Figure 1 Collision and detector frames.
- Figure 2 Reflection in the scattering plane.
- Figure 3 Precession of L and S about the axis of a diatomic molecule.
- Figure 4 Partitioning of space according to the frame transformation theory<sup>54</sup>.
- Figures 5-9 The odd parity eigenphase sums for the symmetries  $J = 0, 1, 2, 3$  and  $4$  in  $e^- + Cs$  scattering. The  ${}^2P_{\frac{1}{2}}, {}^2P_{\frac{3}{2}}, {}^2D_{\frac{3}{2}}$  and  ${}^2D_{\frac{5}{2}}$  thresholds are indicated by arrows at 1.39, 1.46, 1.80 and 1.81 eV, respectively.
- Figures 10-14 The even parity eigenphase sums for the symmetries  $J = 0, 1, 2, 3$  and  $4$  in  $e^- + Cs$  scattering. The  ${}^2P_{\frac{1}{2}}, {}^2P_{\frac{3}{2}}, {}^2D_{\frac{3}{2}}$  and  ${}^2D_{\frac{5}{2}}$  thresholds are indicated by arrows at 1.39, 1.46, 1.80 and 1.81 eV, respectively.
- Figure 15 Total cross section for the  ${}^2S_{\frac{1}{2}} \rightarrow {}^2S_{\frac{1}{2}}$  transition in Cs. The  ${}^2P_{\frac{1}{2}}, {}^2P_{\frac{3}{2}}, {}^2D_{\frac{3}{2}}$  and  ${}^2D_{\frac{5}{2}}$  thresholds at 1.39, 1.46, 1.80 and 1.81 eV, respectively, are indicated by arrows.

- Figure 16 The same as fig 15 for  $2S_{\frac{1}{2}} \rightarrow 2P_{\frac{1}{2}}$  transition.
- Figure 17 The same as fig 15 for  $2S_{\frac{1}{2}} \rightarrow 2P_{\frac{3}{2}}$  transition.
- Figure 18 Differential cross sections,  $\sigma(\theta_e)$ , for the transition  $2S_{\frac{1}{2}} \rightarrow 2S_{\frac{1}{2}}$  at the energies 0.816 eV(---), 1.632 eV(—) and 2.04 eV(---).
- Figure 19 Scattering asymmetry,  $A_S(\theta_e) = P_Y(\theta_e)$ , for the transition  $2S_{\frac{1}{2}} \rightarrow 2S_{\frac{1}{2}}$  at the energies 0.816 eV(~~—~~), 1.632 eV(-o-) and 2.04 eV(-O).
- Figure 20 Spin polarization,  $P_Y(\theta_e)$  and the asymmetry function  $A_S(\theta_e)$  for the transition  $2S_{\frac{1}{2}} \rightarrow 2P_{\frac{1}{2}}$  at energy 1.632 eV,  $P_Y(\theta_e)$ (-o-) and  $A_S(\theta_e)$ (-●-).
- Figure 21 As fig 20 at the energy 2.04 eV.
- Figure 22 As fig 20 for the transition  $2S_{\frac{1}{2}} \rightarrow 2P_{\frac{3}{2}}$ .
- Figure 23 As fig 21 for the transition  $2S_{\frac{1}{2}} \rightarrow 2P_{\frac{3}{2}}$ .
- Figure 24 Differential cross section,  $\sigma(\theta_e)$ , for the transition  $2S_{\frac{1}{2}} \rightarrow 2P_{\frac{1}{2}}$  at the energies 1.632 eV(-●-) and 2.04 eV(-o-).
- Figure 25 The same as fig 24 for the transition  $2S_{\frac{1}{2}} \rightarrow 2P_{\frac{3}{2}}$ .
- Figure 26-29 The differential cross section for the transition  $2S_{\frac{1}{2}} \rightarrow 2S_{\frac{1}{2}}$  in Cs, at the scattering angle  $\theta_e = 10^\circ, 30^\circ, 50^\circ, 70^\circ, 90^\circ, 110^\circ, 130^\circ$  and  $150^\circ$ .
- Figures 30-33 The polarization vector,  $P_Y(\theta_e)$ , of the scattered electrons for the transition  $2S_{\frac{1}{2}} \rightarrow 2S_{\frac{1}{2}}$  in Cs at the scattering angle  $\theta_e = 10^\circ, 30^\circ, 50^\circ, 70^\circ, 90^\circ, 110^\circ, 130^\circ$  and  $150^\circ$ . The incident electron beam was initially unpolarized.
- Figures 34-37 The polarization vector,  $P_Y(\theta_e)$ , of the scattered electrons for the transition  $2S_{\frac{1}{2}} \rightarrow 2S_{\frac{1}{2}}$  in Cs at the scattering angle  $\theta_e = 10^\circ, 30^\circ, 50^\circ, 70^\circ, 90^\circ, 110^\circ, 130^\circ$  and  $150^\circ$ . The incident beam was initially fully transversally polarized.
- Figure 38 Stokes' parameter  $\eta_{1/p_y}$  for the transition  $2P_{\frac{3}{2}} \rightarrow 2S_{\frac{1}{2}}$  in

Cs as a function of the Collision energy. The arrows mark the excitation thresholds  $2P_{\frac{1}{2}}$ ,  $2P_{\frac{3}{2}}$ ,  $2D_{\frac{3}{2}}$  and  $2D_{\frac{5}{2}}$  at 1.39, 1.46, 1.80 and 1.81 eV, respectively. The incident electrons were initially fully transversally polarized in the y-direction.

Figure 39 As fig 38 for  $\eta_2/P_y$ .

Figure 40 As fig 38 for  $\eta_3$ .

Figure 41 Stokes' parameter  $\eta_2/P_y$  for the transition  $2P_{\frac{1}{2}} \rightarrow 2S_{\frac{1}{2}}$  in Cs. Further details as in figure 38.

Figure 42 Stokes' parameter  $\eta_2/P_z$  for the transition  $2P_{\frac{1}{2}} \rightarrow 2S_{\frac{1}{2}}$  in Cs. The incident electrons were initially fully longitudinally polarized in the z-direction.

Figures 43a-43d SEP p- and f- wave eigenphases as a function of the internuclear distance at incident electron energies:

a - 20 eV	b - 25 eV
c - 27.21 eV	d - 30 eV

Figures 44a-44d As figs 43a-43d for the mixing parameter.

Figure 45 SEP differential cross sections in  $10^{-19}(\text{cm}^2/\text{Sr})$  for  $v_i = 0 \rightarrow v_f = 1$  transition at incident electron energy 20 eV.—, present calculations; ---, Onda and Truhlar<sup>94</sup>; -.-, Pavlovic et al<sup>50</sup>; o-o-o, Tanaka et al<sup>93</sup>; ooo, Chang<sup>90</sup>.

Figure 46 As fig 45 at energy 25 eV.

Figure 47 As fig 45 at energy 30 eV.♦♦♦, Truhlar et al<sup>95</sup>.

TABLE 1

	$\alpha_d$	$\alpha_q$	$r_c$	Eigenenergy (Ryds)	Experimental energy (Ryds)
$l = 0$	15.0	64.0	0.9		
6s				-0.286723	-0.286482
7s				-0.117355	-0.117578
8s				-0.064640	-0.064746
$l = 1$	15.0	38.3	0.9		
6p				-0.181068	-0.181262
7p				-0.086804	-0.086922
8p				-0.034097	-0.034126
$l = 2$	15.0	34.4	0.9		
5d				-0.153620	-0.153789
6d				-0.080163	-0.080646
7d				-0.048745	-0.049025

TABLE 2

A	$6p \overline{ns} \ ^3P_{0,1,2}$
B	$6p \ 5d \ ^3D_{1,2,3}$
C	$6s \ 6p \ ^1P_1$
D	$6p \ 5d \ ^3F_{2,3,4}$
E	$6p \ 5d \ ^1D_2$
F	$6p \ 5d \ ^1F_3$
G	$6p \ 5d \ ^3D_{1,2,3}$
H	$6p^2 \ ^1S_0$
I	$6p^2 \ ^3P_{0,1,2}$
J	$6s \ 5d \ ^3D_{1,2,3}$
K	$6p \ \overline{np} \ ^3D_{1,2,3}$

TABLE 3

Energy (ev)	v (0 - 1)	v (0 - 2)
20	0.0933 <sup>a</sup>	0.0060 <sup>a</sup>
	0.268 <sup>b</sup>	0.0082 <sup>b</sup>
	0.076 <sup>c</sup>	0.00132 <sup>c</sup>
	0.16 <sup>d</sup>	
	0.471 <sup>e</sup>	
	0.6963 <sup>f</sup>	
25	0.3453 <sup>a</sup>	0.0331 <sup>a</sup>
	0.26 <sup>c</sup>	0.0178 <sup>c</sup>
	0.58 <sup>d</sup>	
	0.2935 <sup>f</sup>	
30	0.2711 <sup>a</sup>	0.0447 <sup>a</sup>
	0.39 <sup>b</sup>	0.0531 <sup>b</sup>
	0.364 <sup>c</sup>	0.0492 <sup>c</sup>
	0.45 <sup>d</sup>	
	0.0852 <sup>e</sup>	
	0.0949 <sup>f</sup>	

- a - Present results
- b - Rumble et al.<sup>97</sup>
- c - Onda and Truhlar.<sup>94</sup>
- d - Dehmer et al.<sup>98</sup>
- e - Truhlar et al, Heizenberg - Schulze and other data from Trajmar's laboratory as reanalyzed by Onda.<sup>94,96</sup>
- f - Tanaka et al.<sup>93</sup>

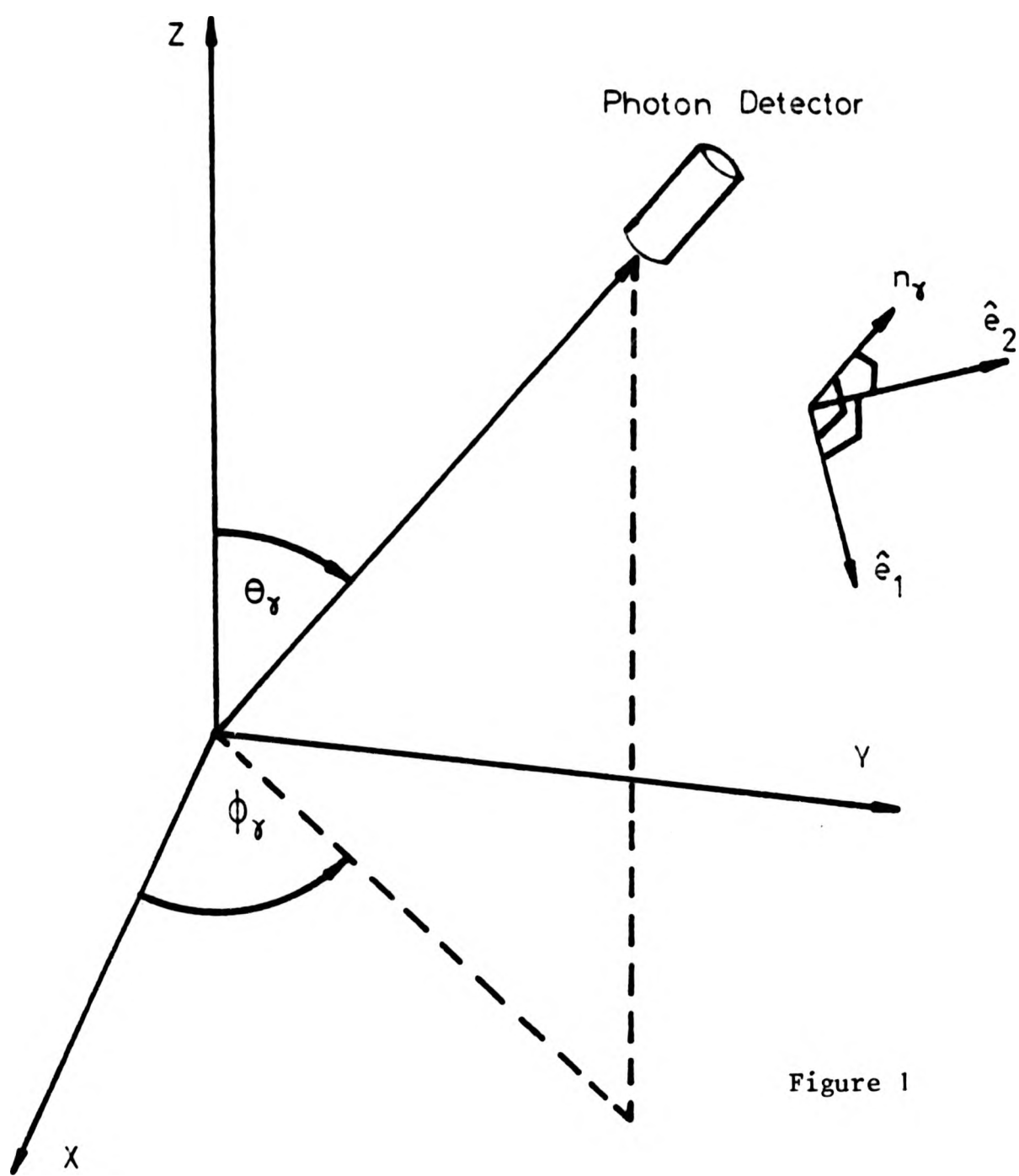


Figure 1

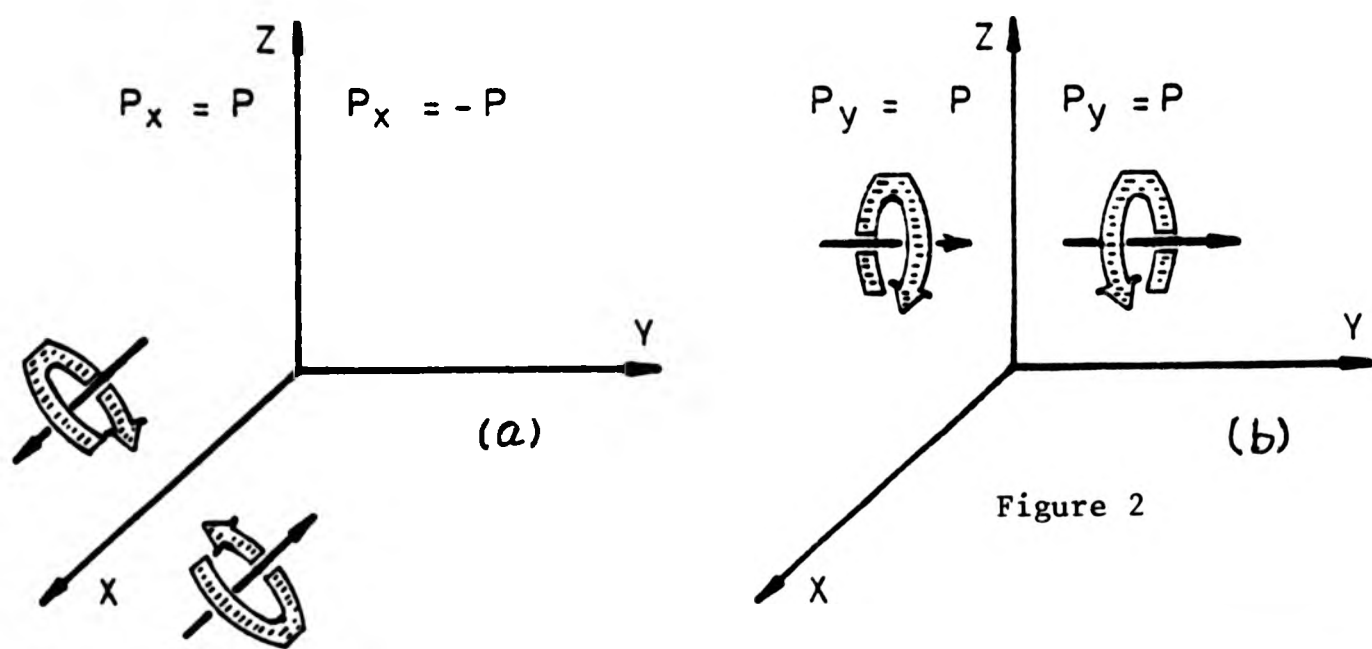


Figure 2

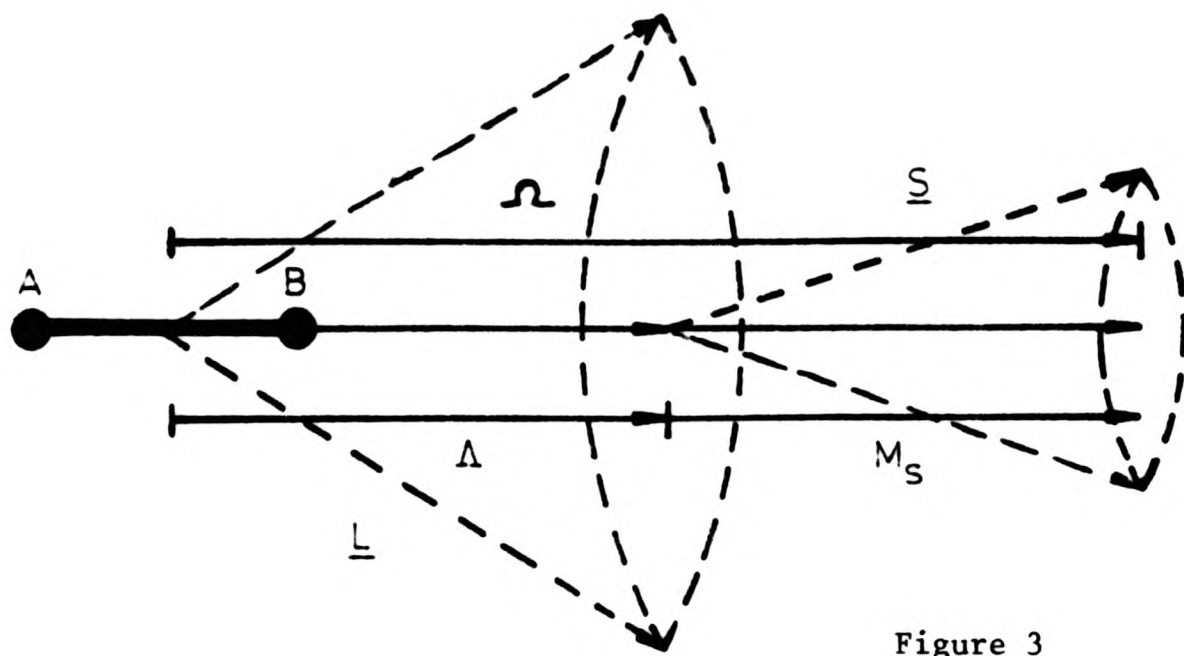


Figure 3

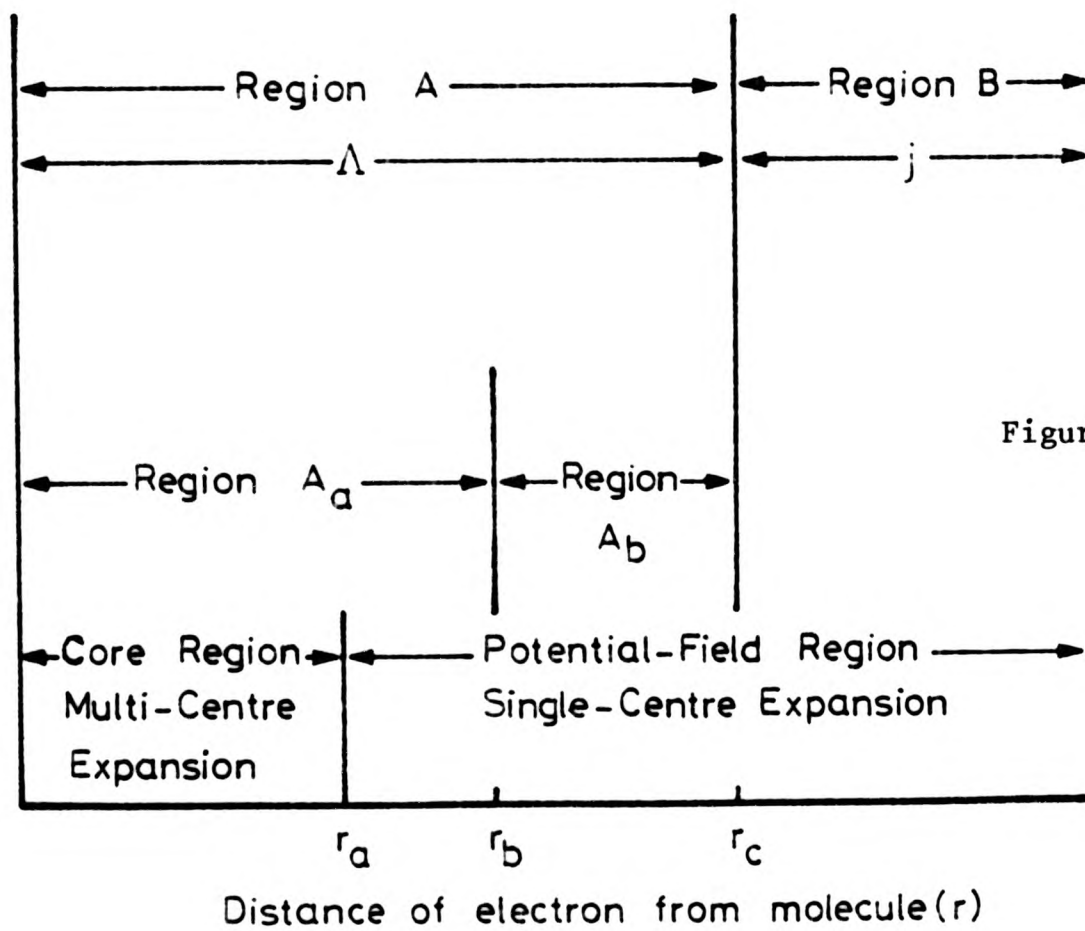


Figure 4

Figure 5

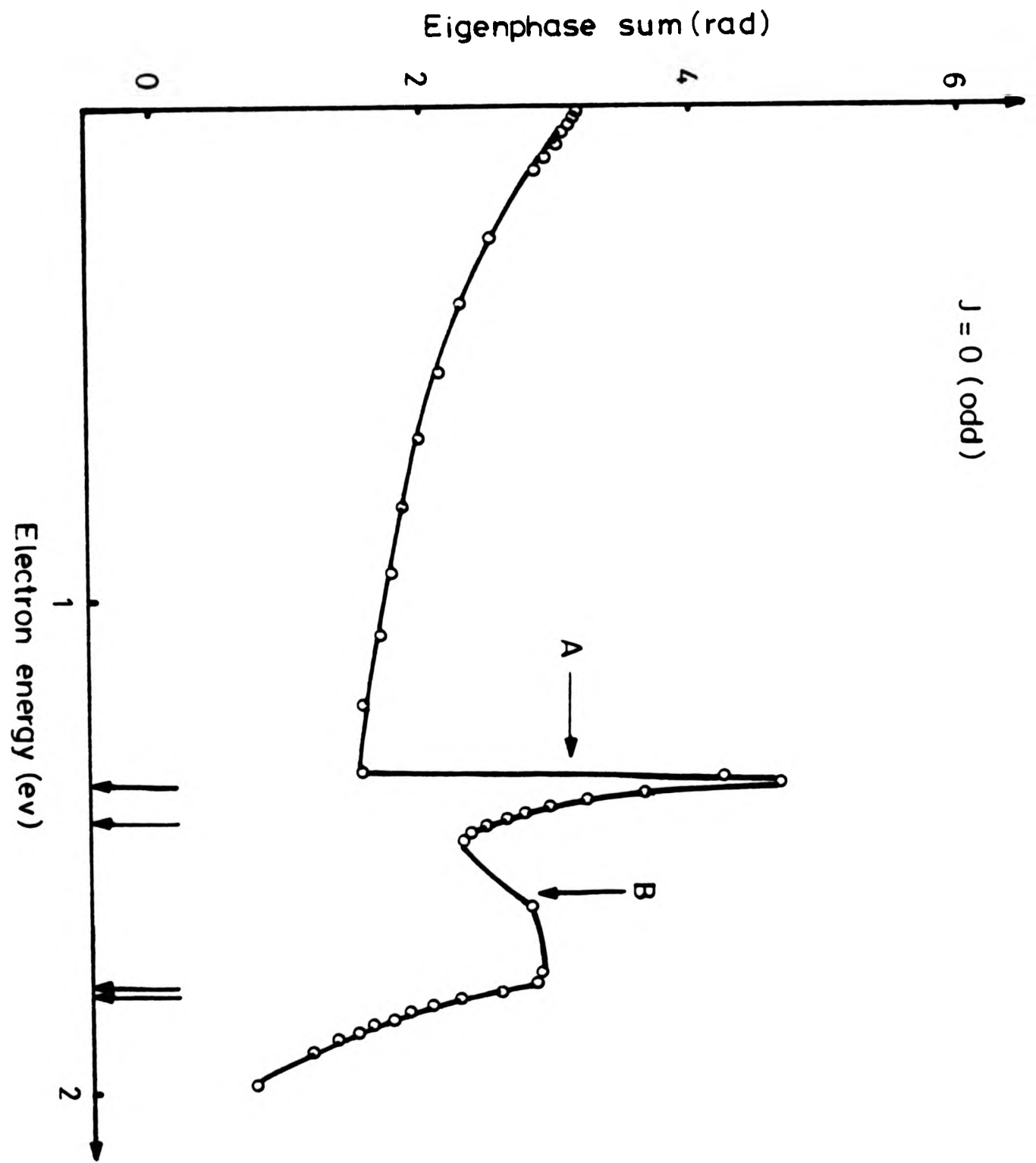


Figure 6

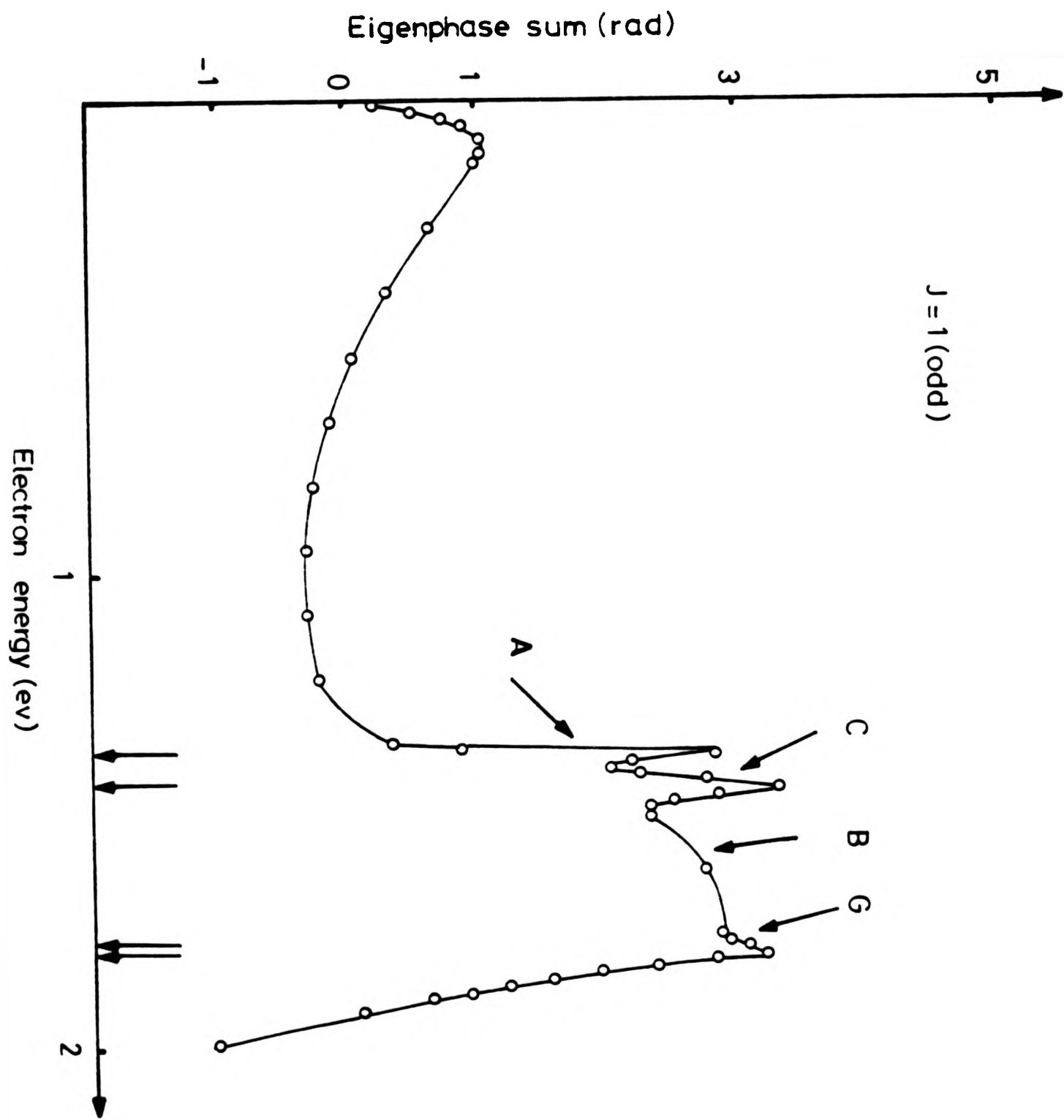


Figure 7

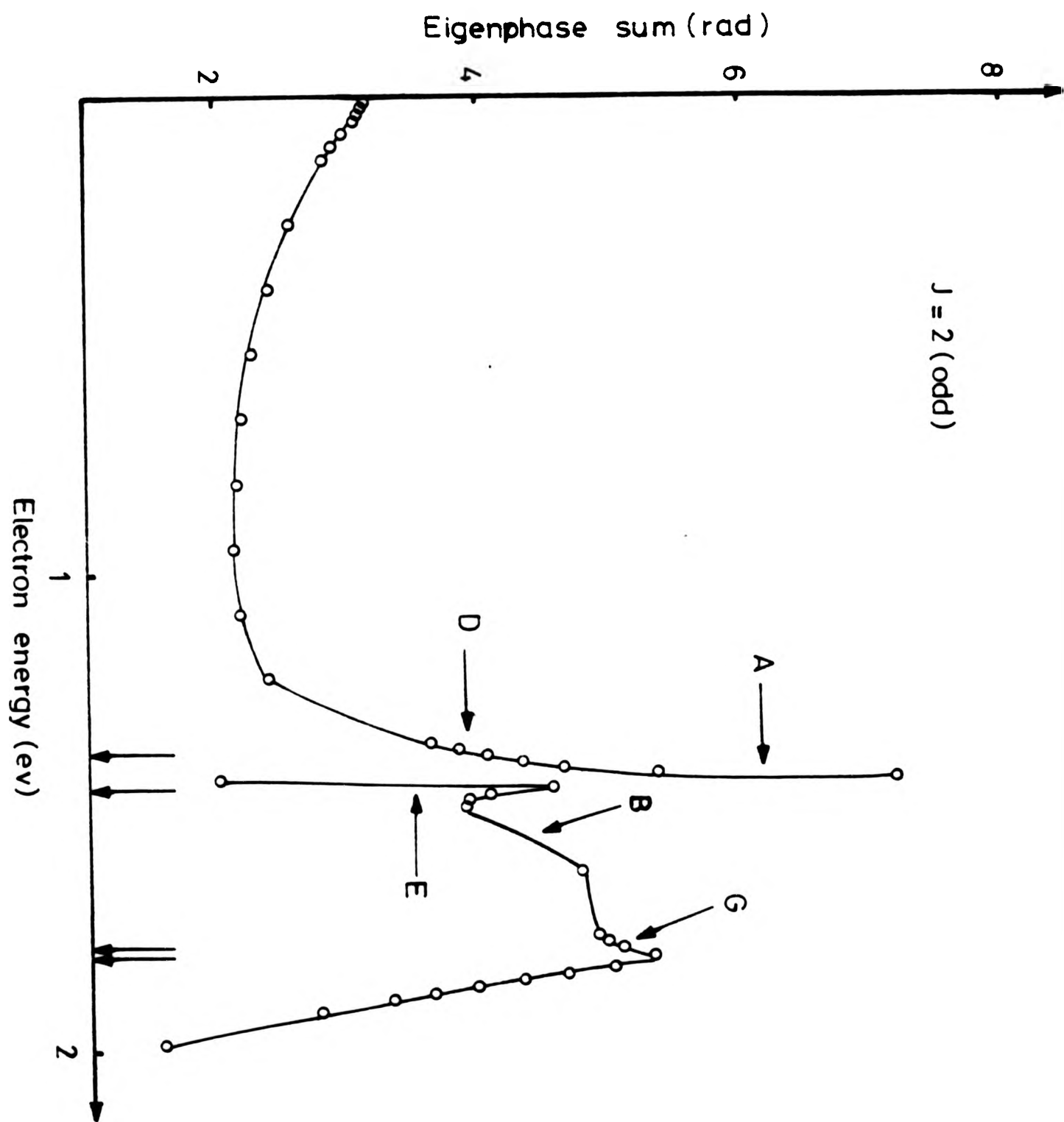


Figure 8

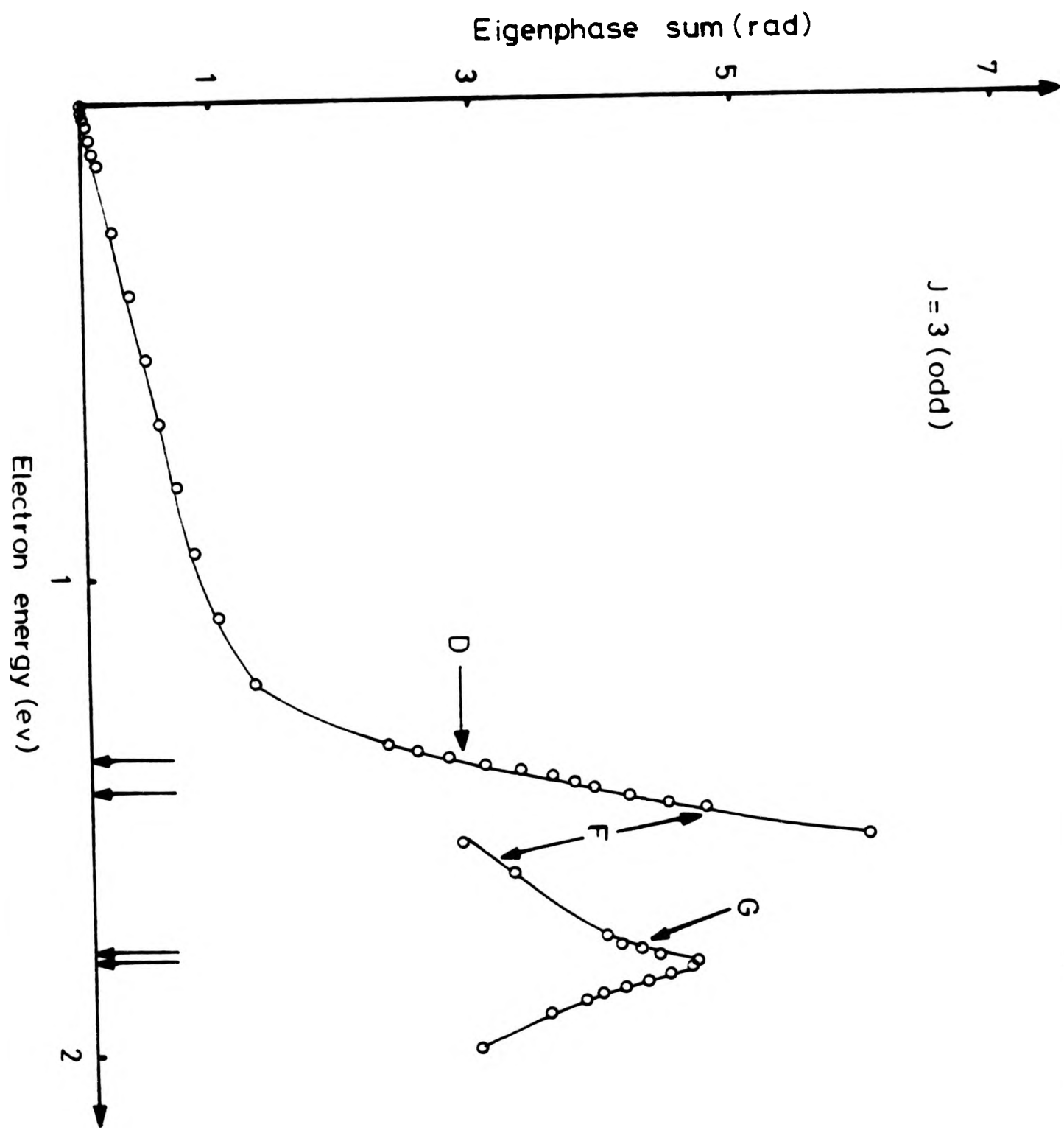


Figure 9

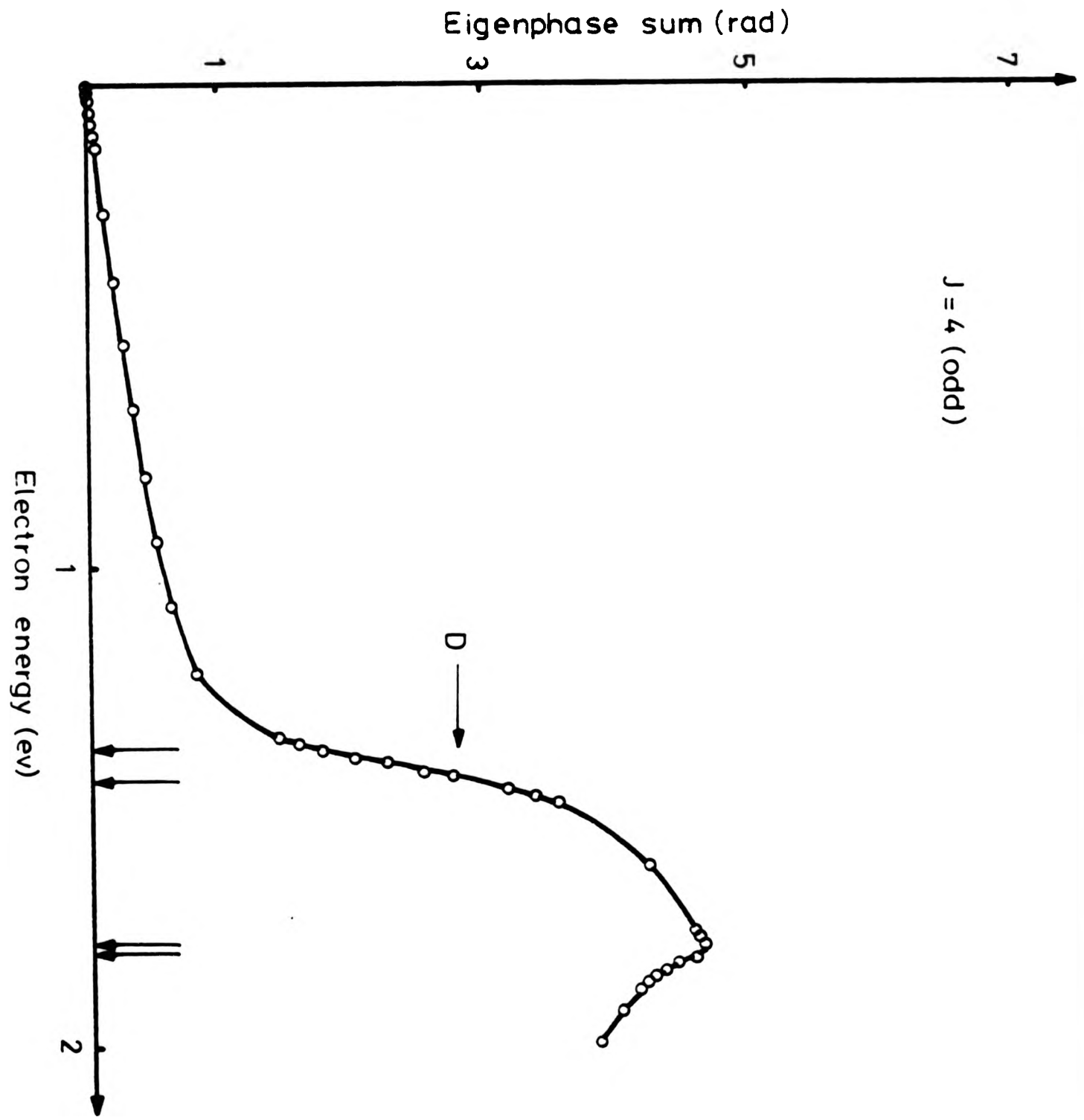


Figure 10

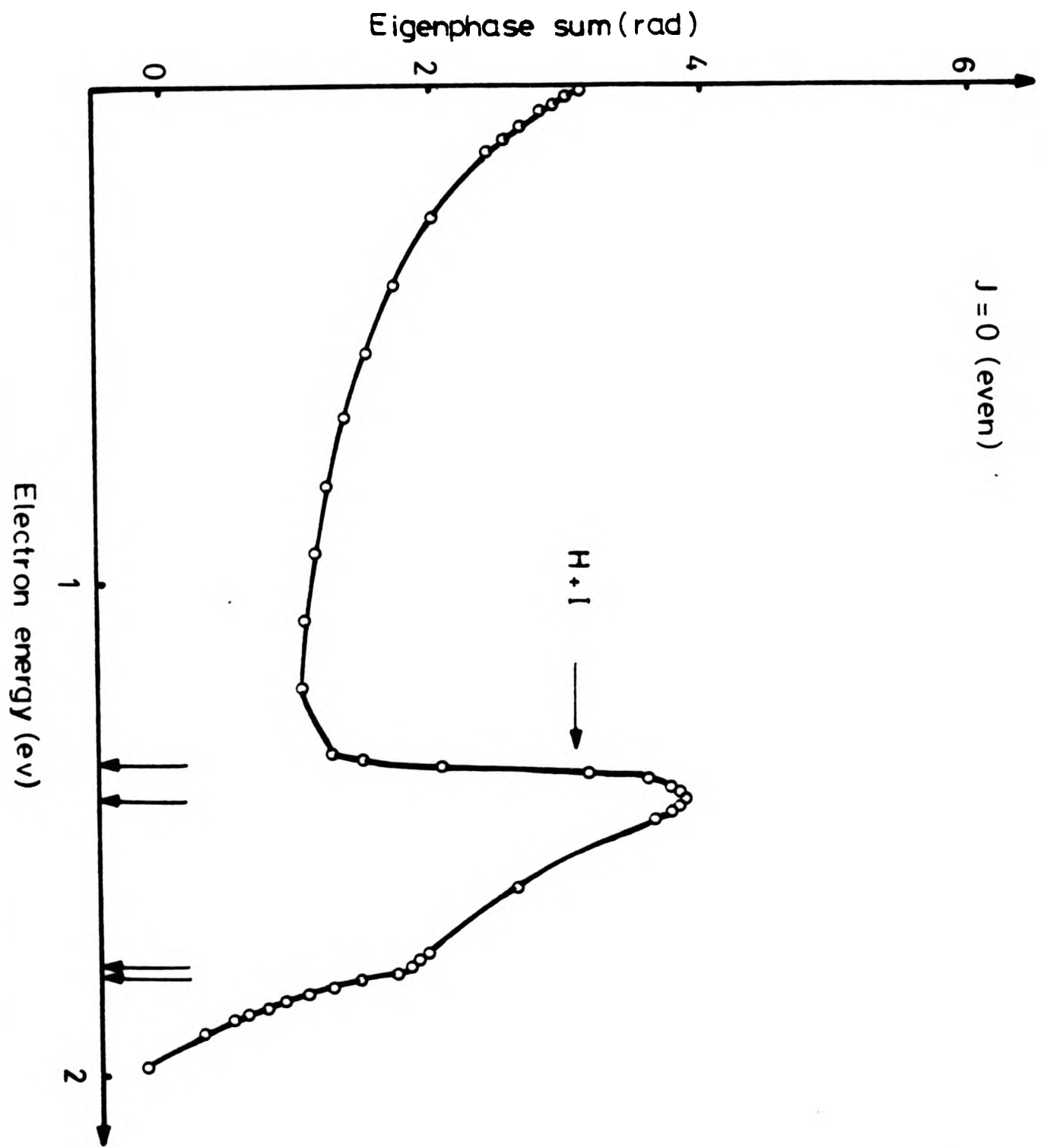


Figure 11

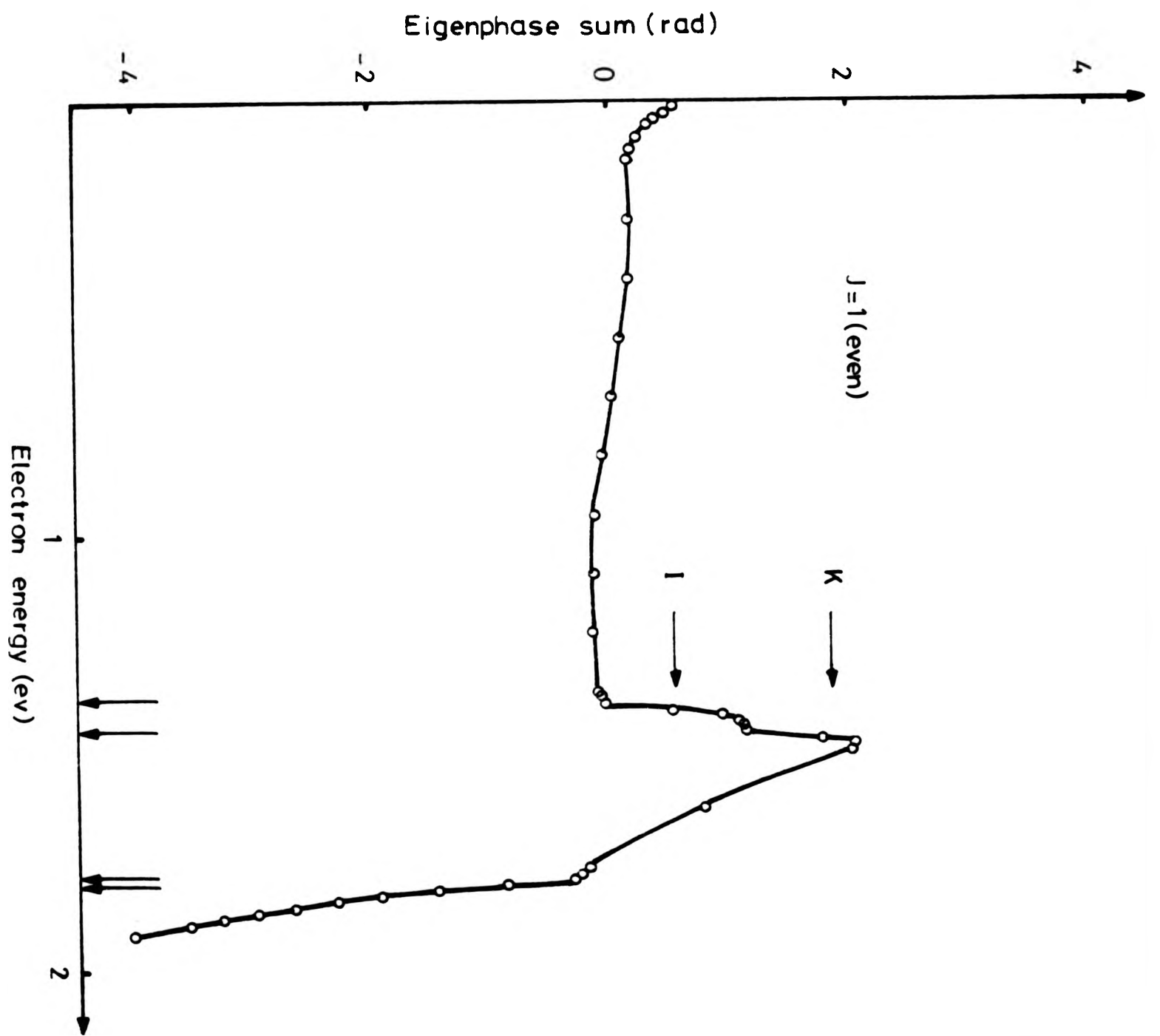


Figure 12

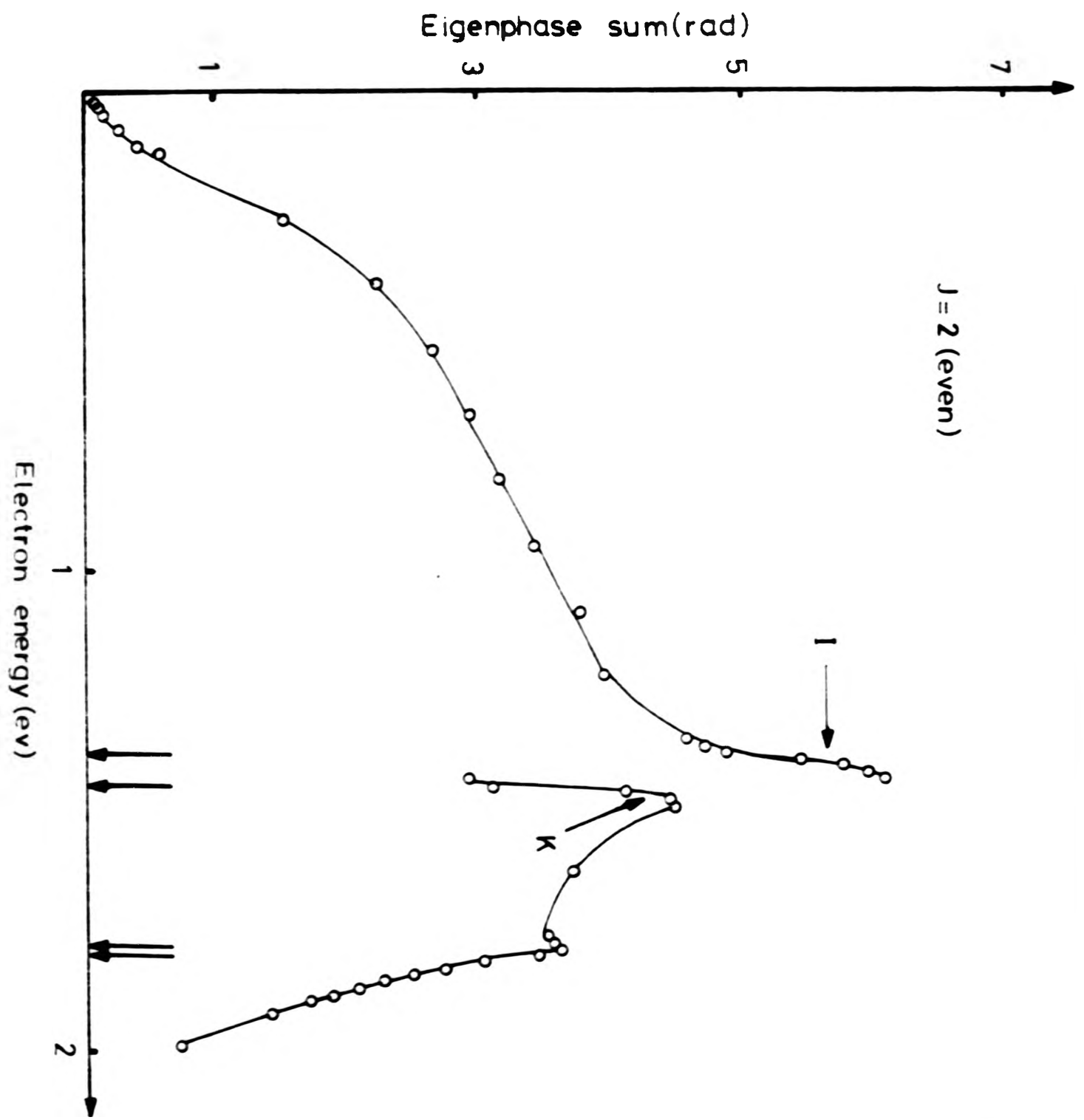


Figure 13

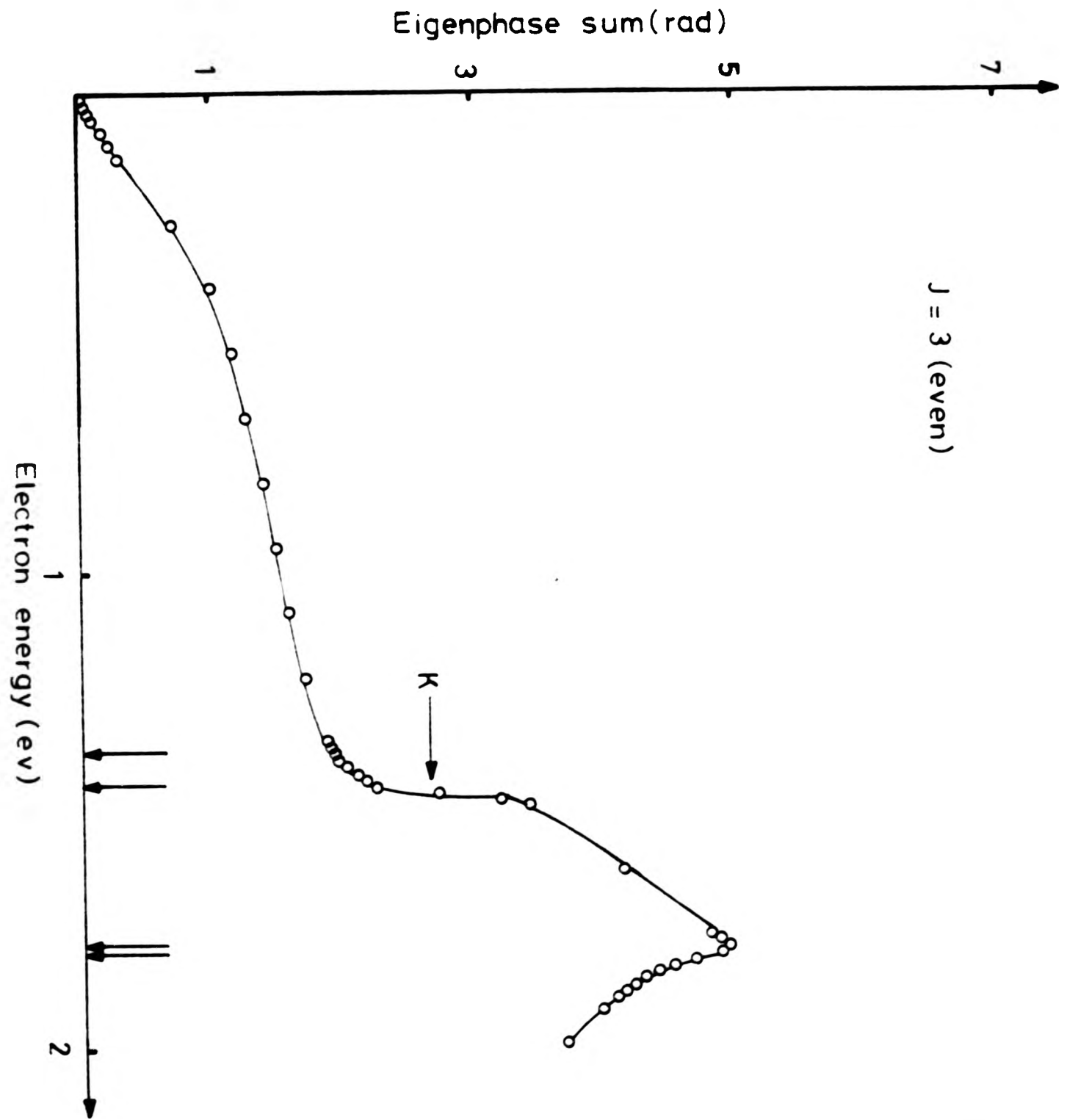


Figure 14

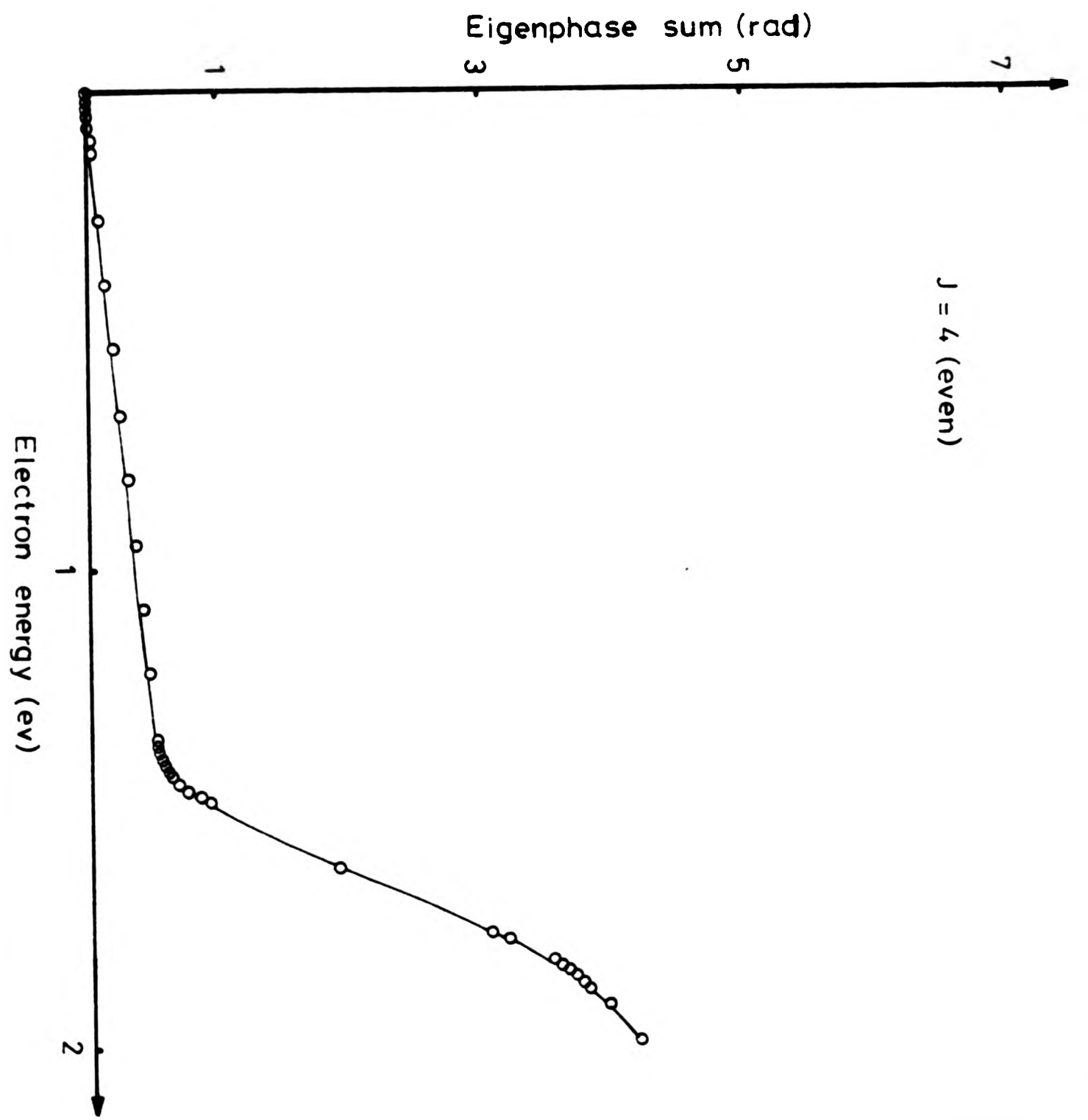


Figure 15

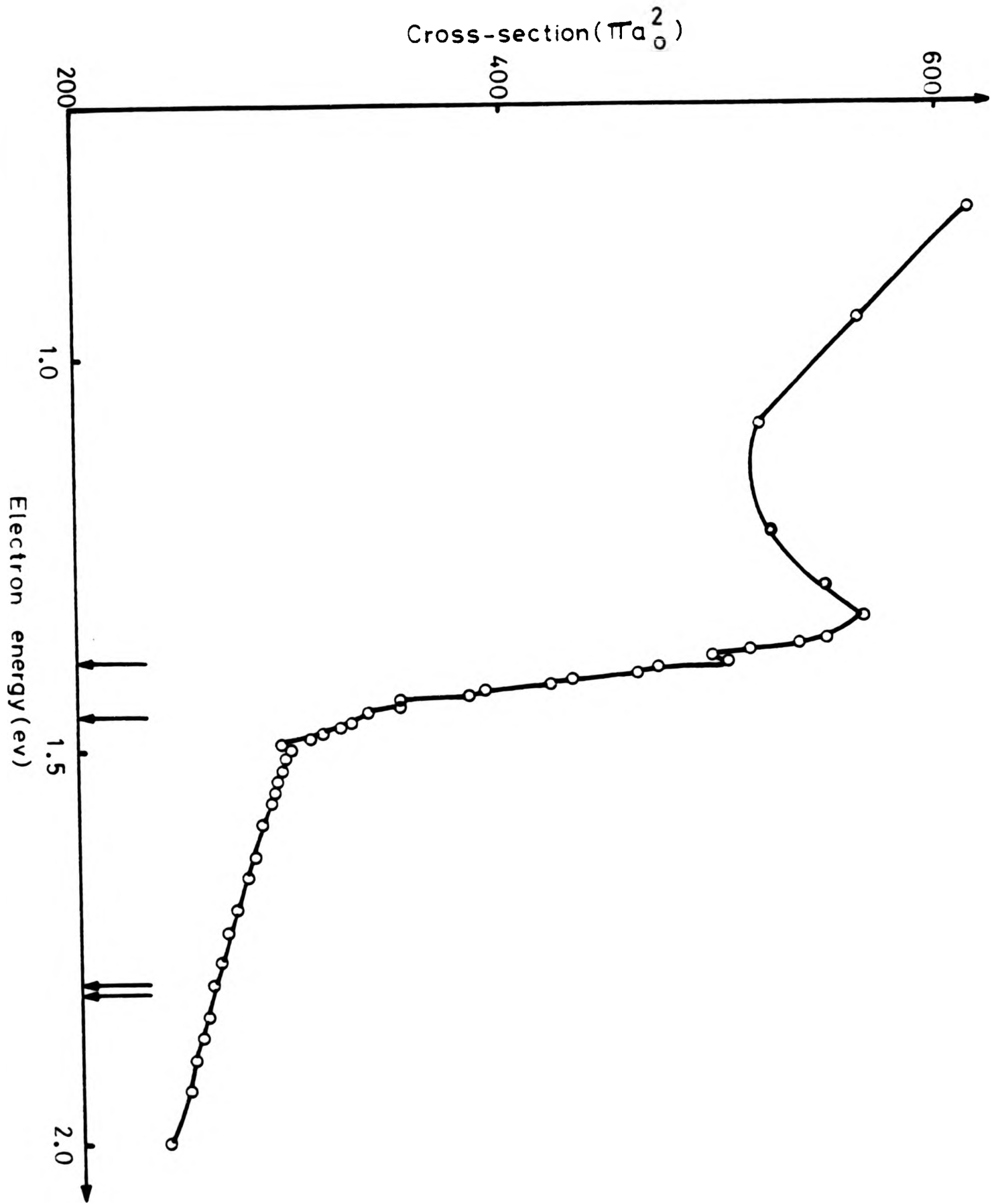


Figure 16

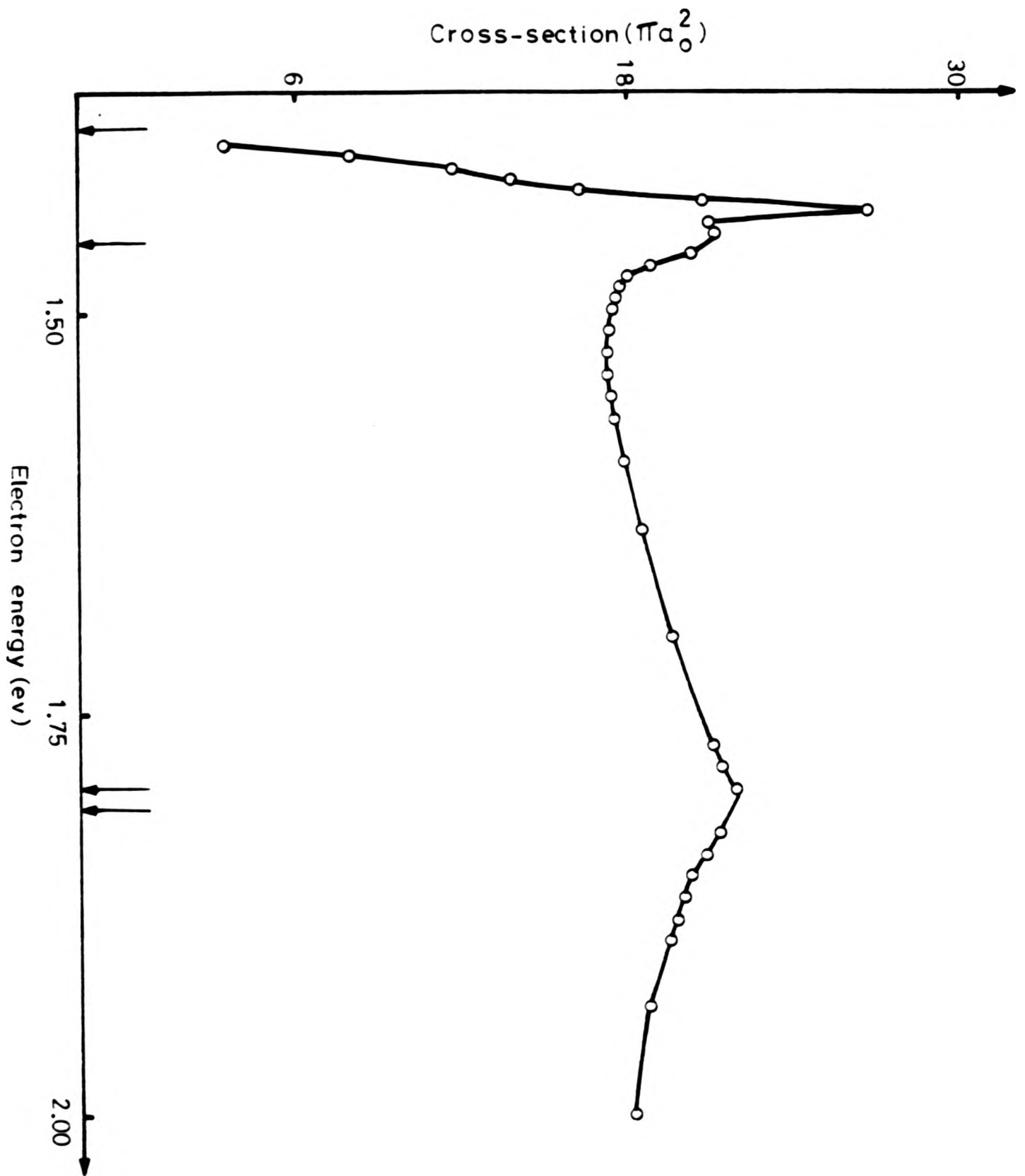


Figure 17

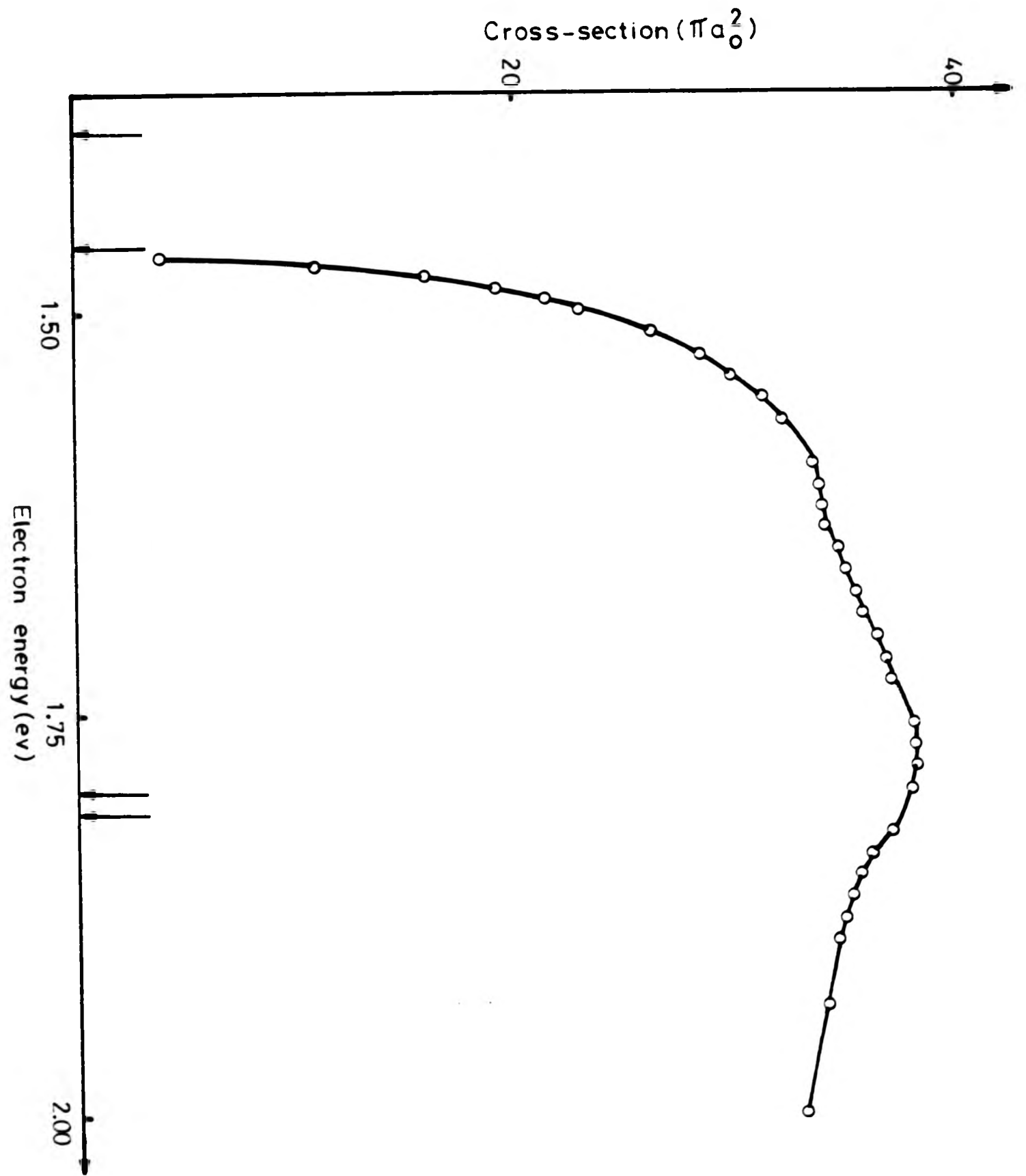


Figure 18

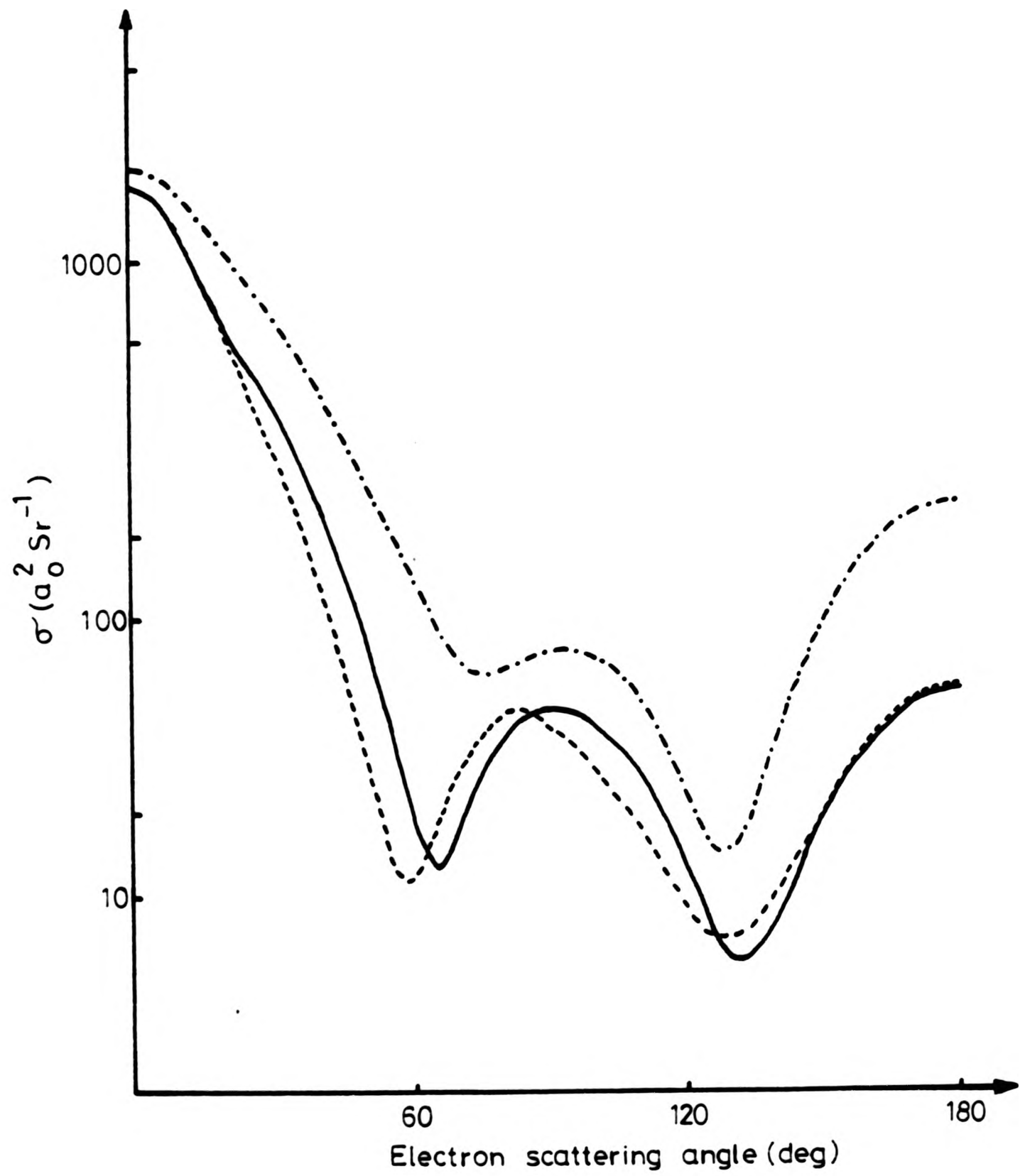


Figure 19

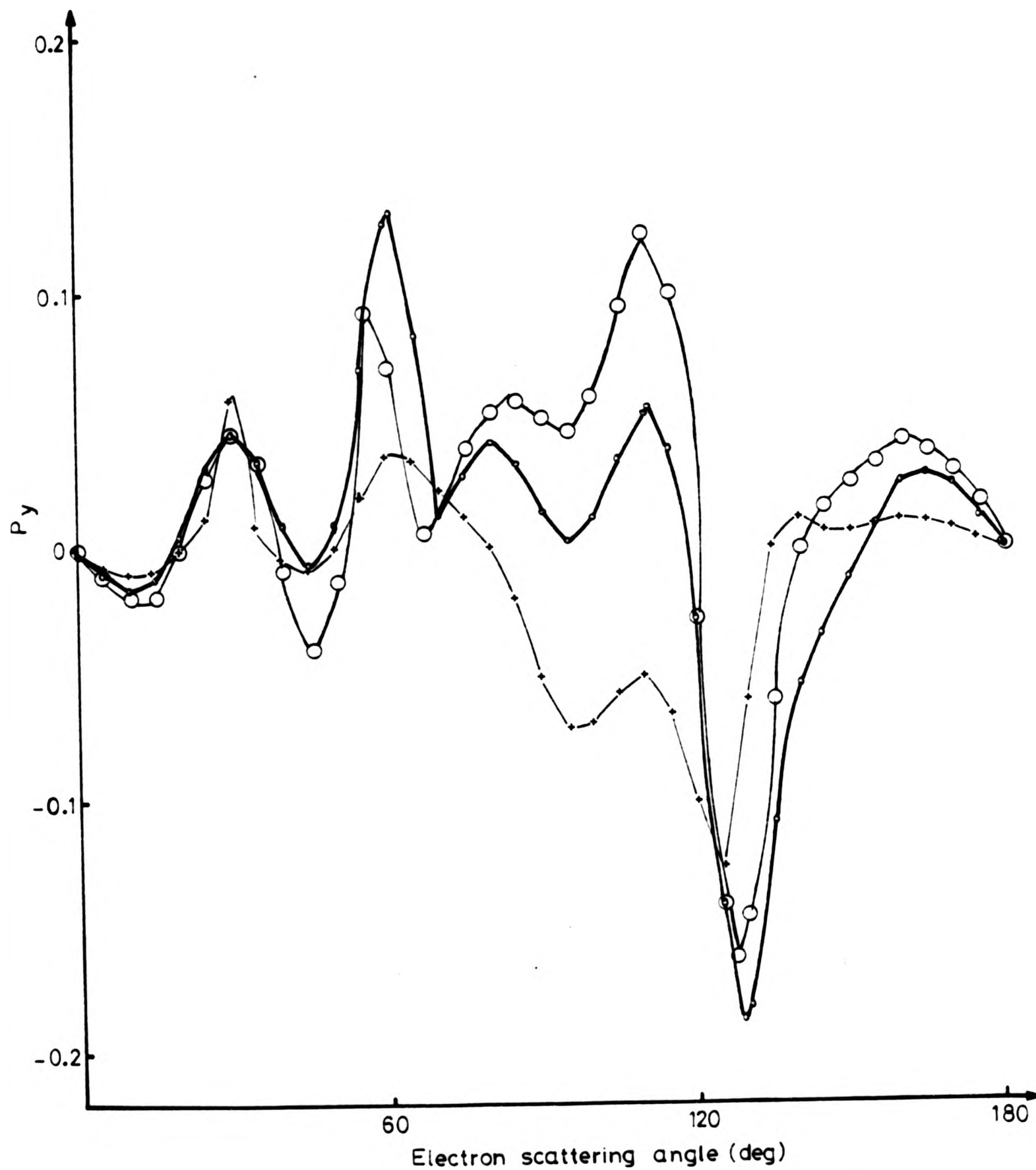


Figure 20

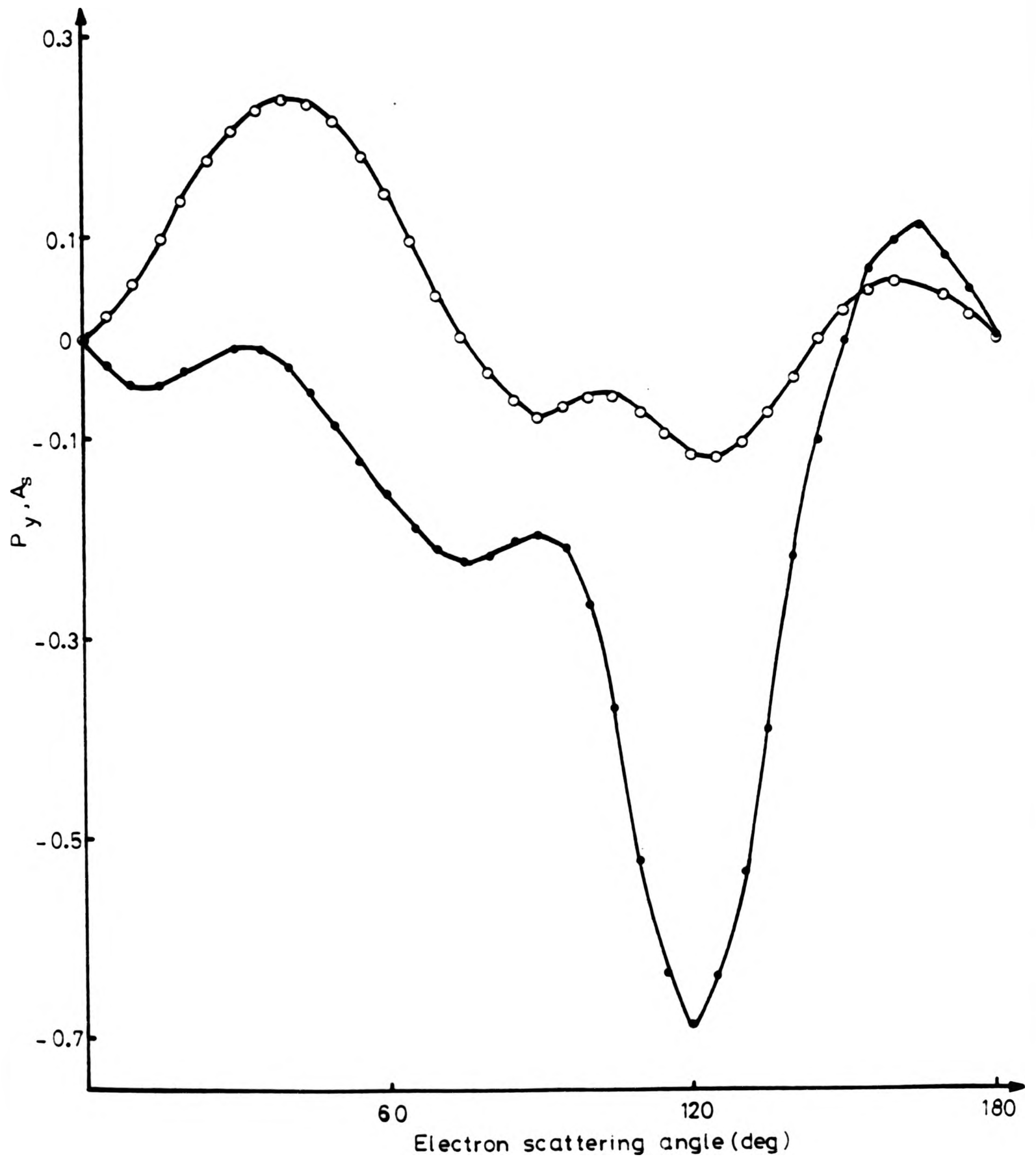


Figure 21

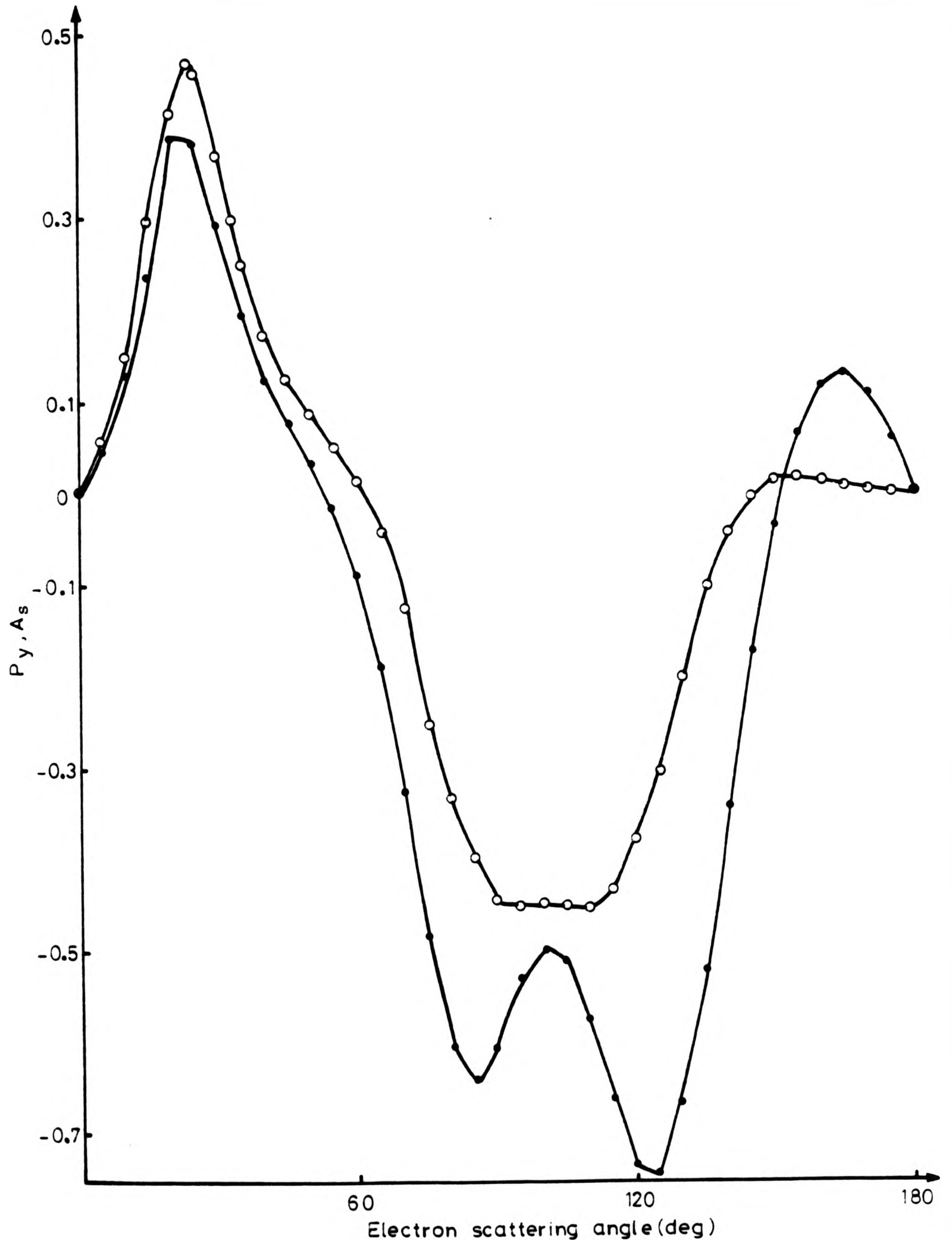


Figure 22

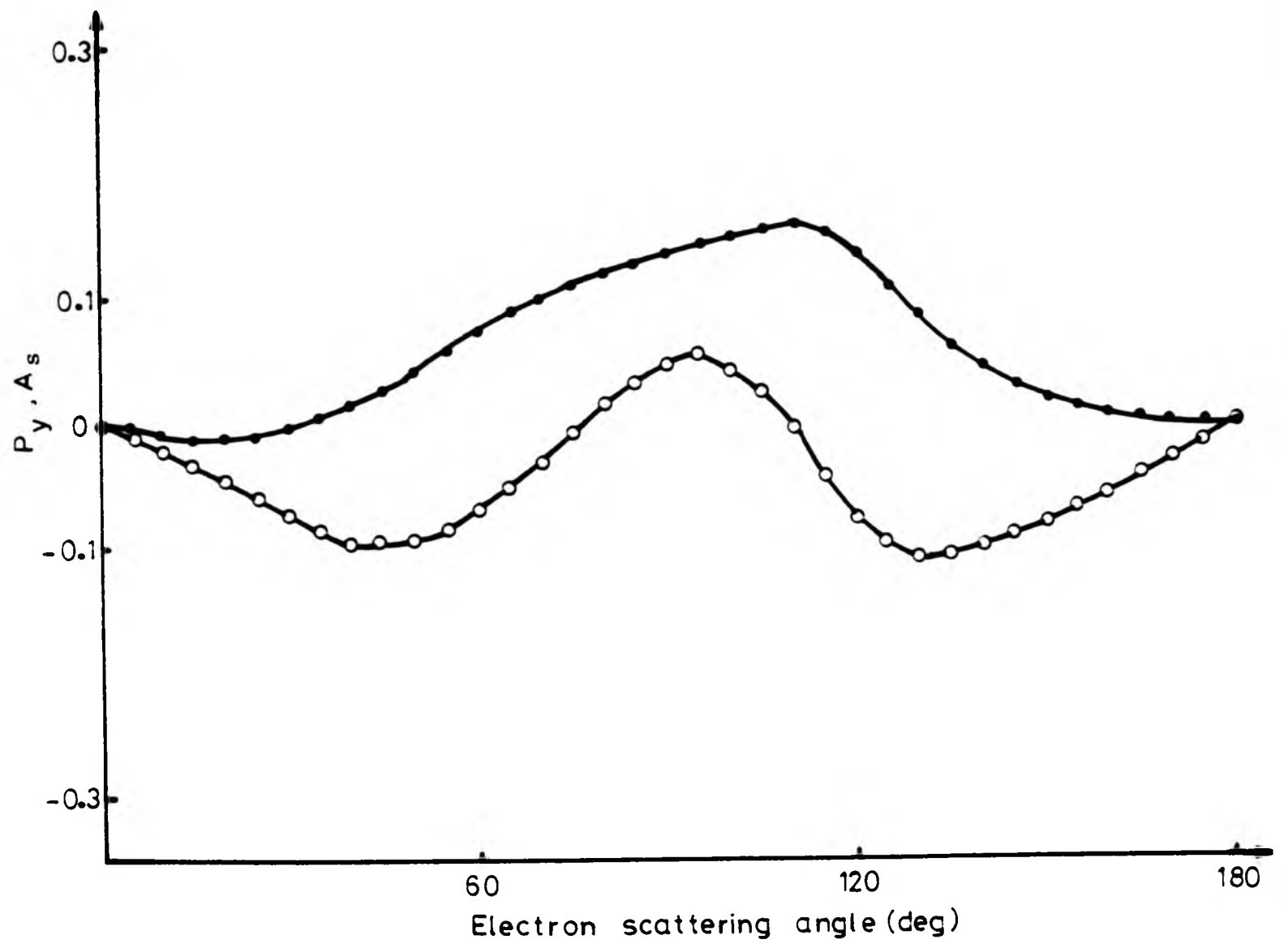


Figure 23

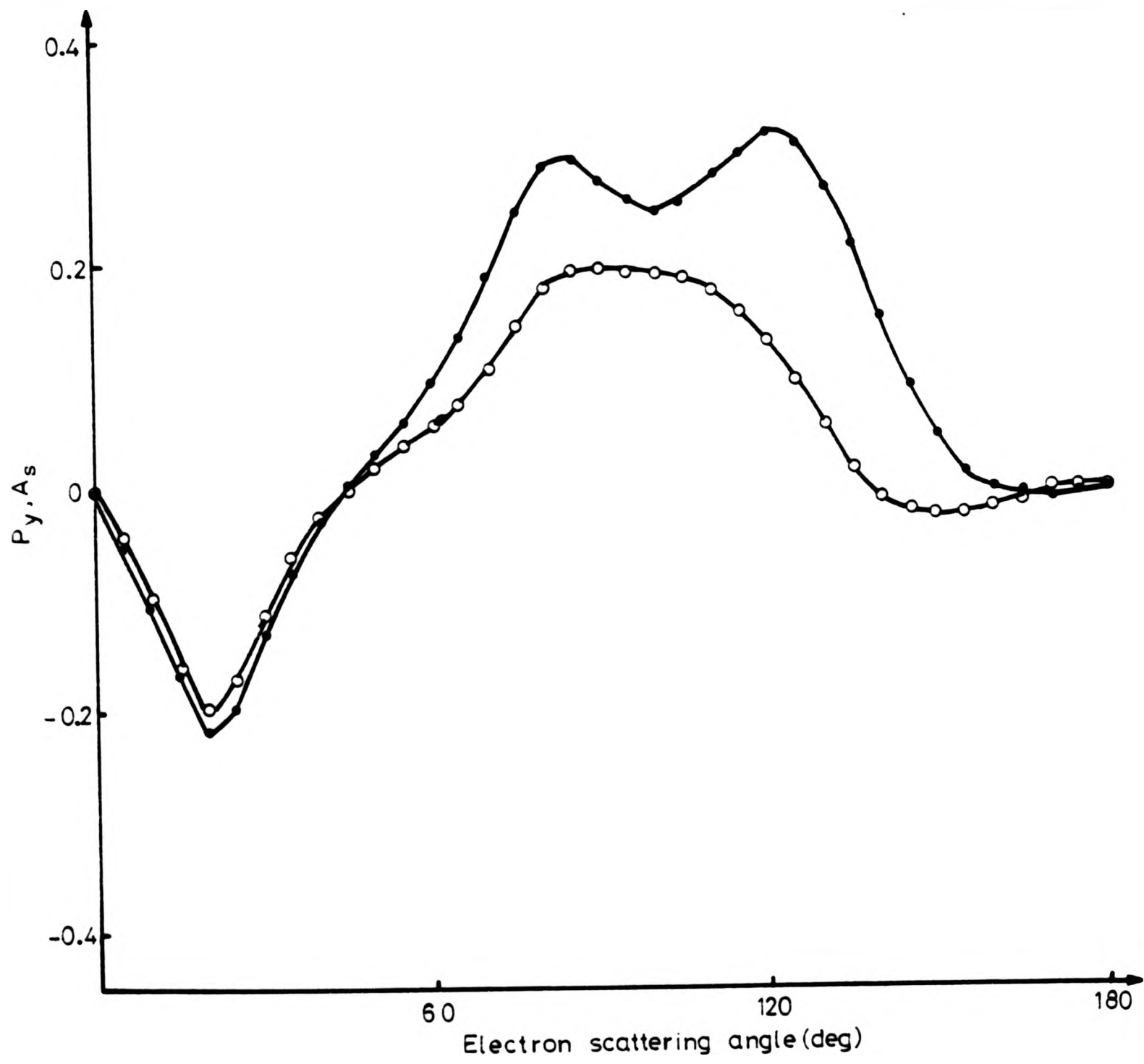


Figure 24

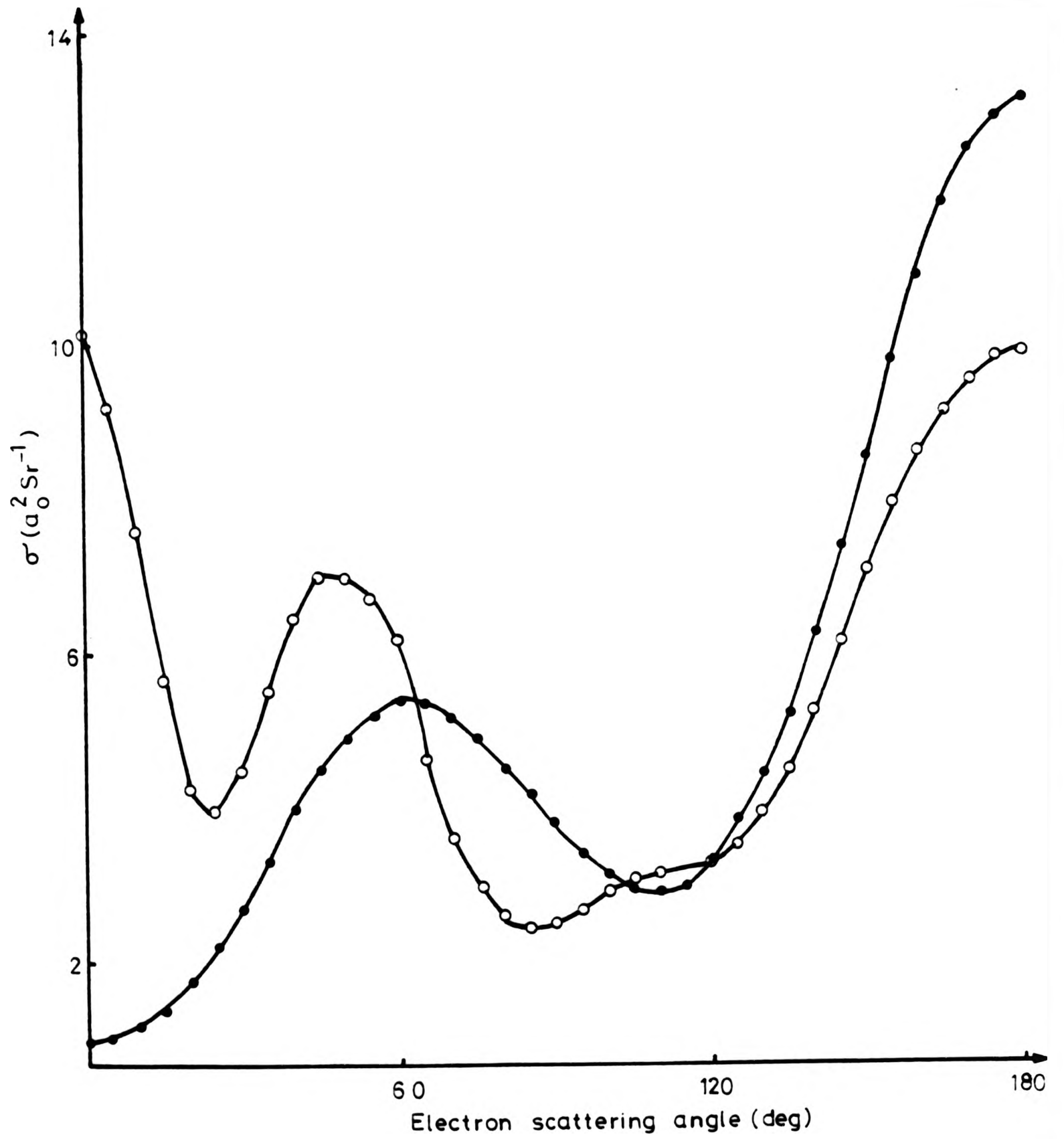


Figure 25

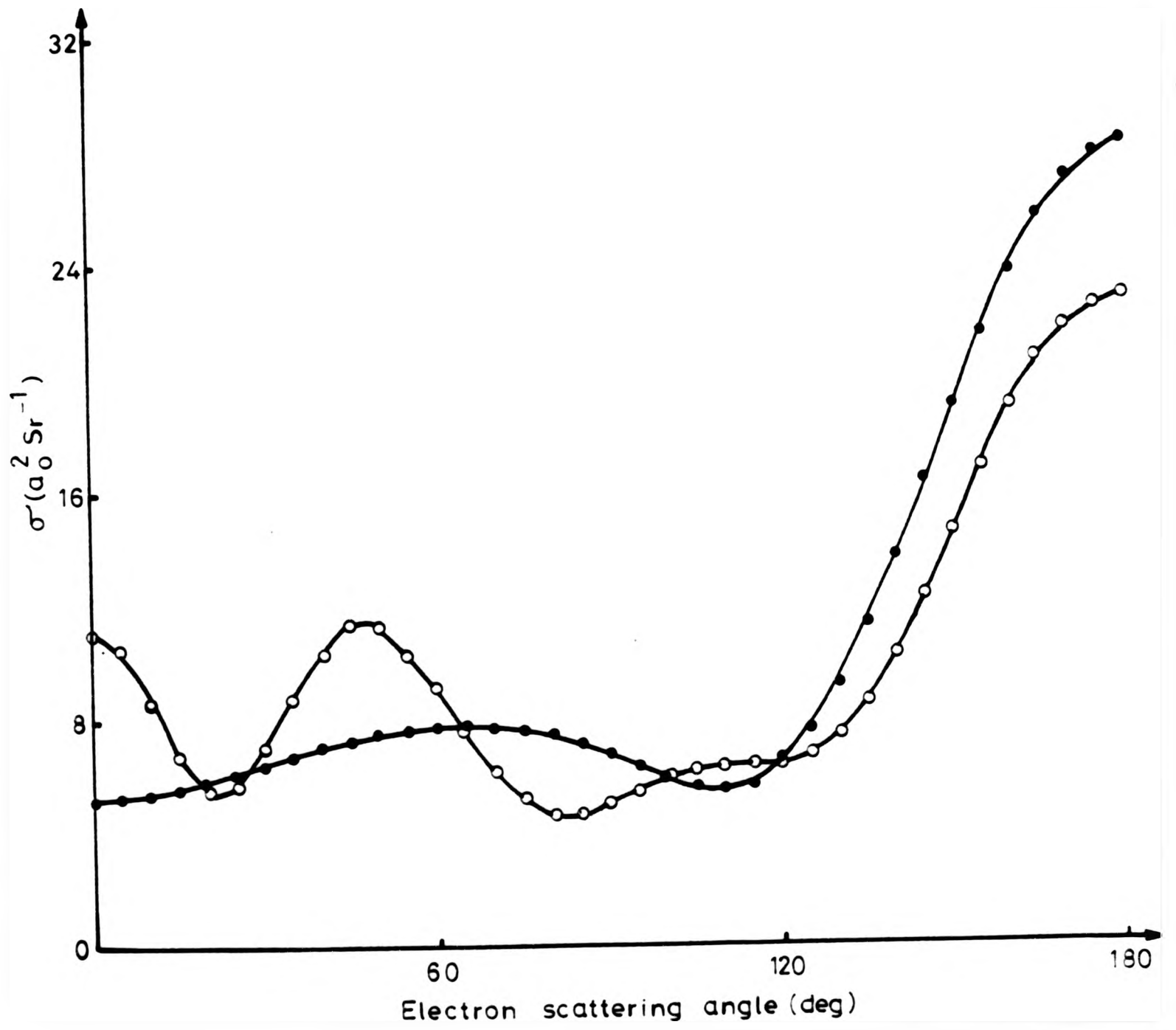


Figure 26

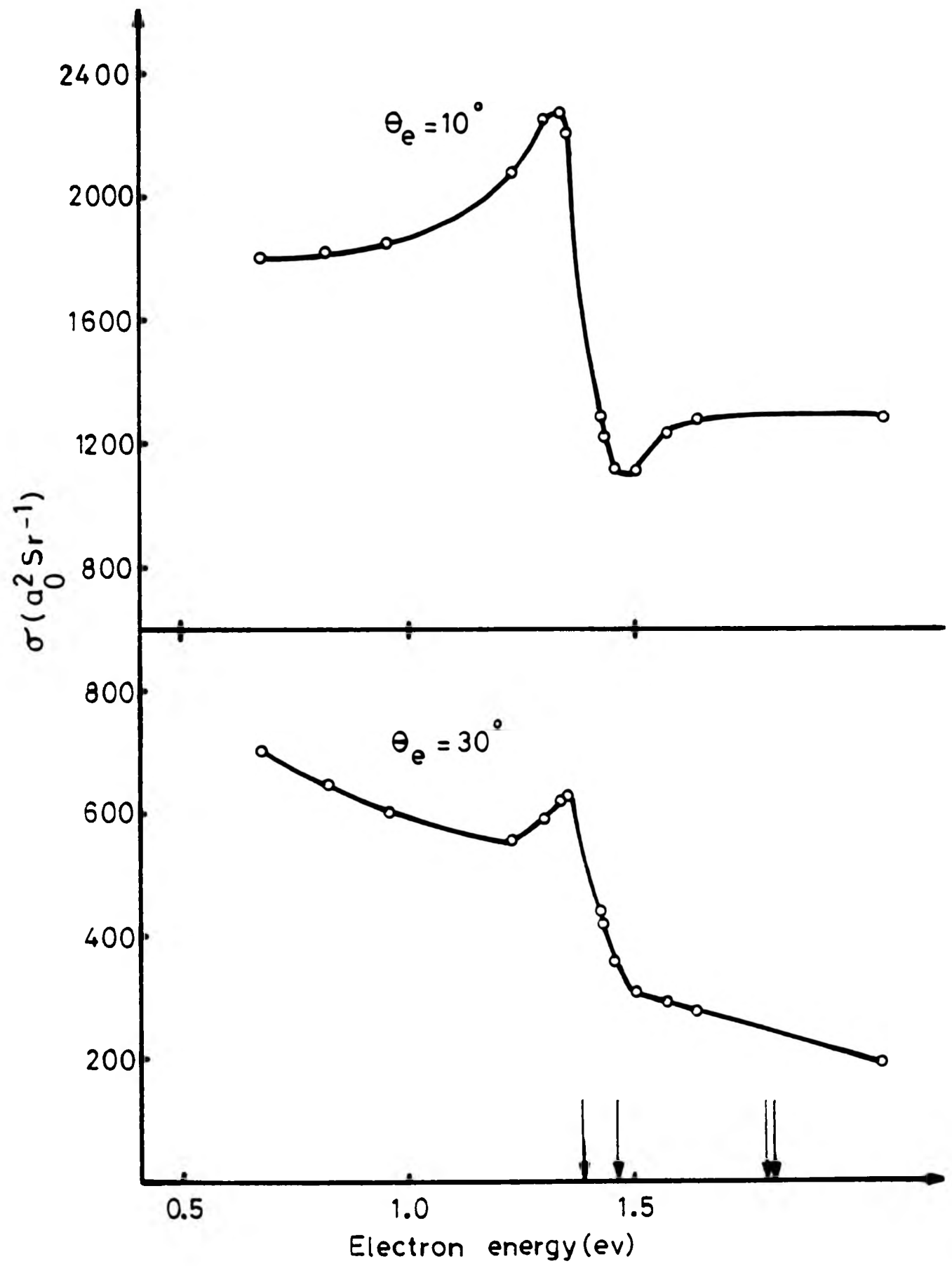


Figure 27

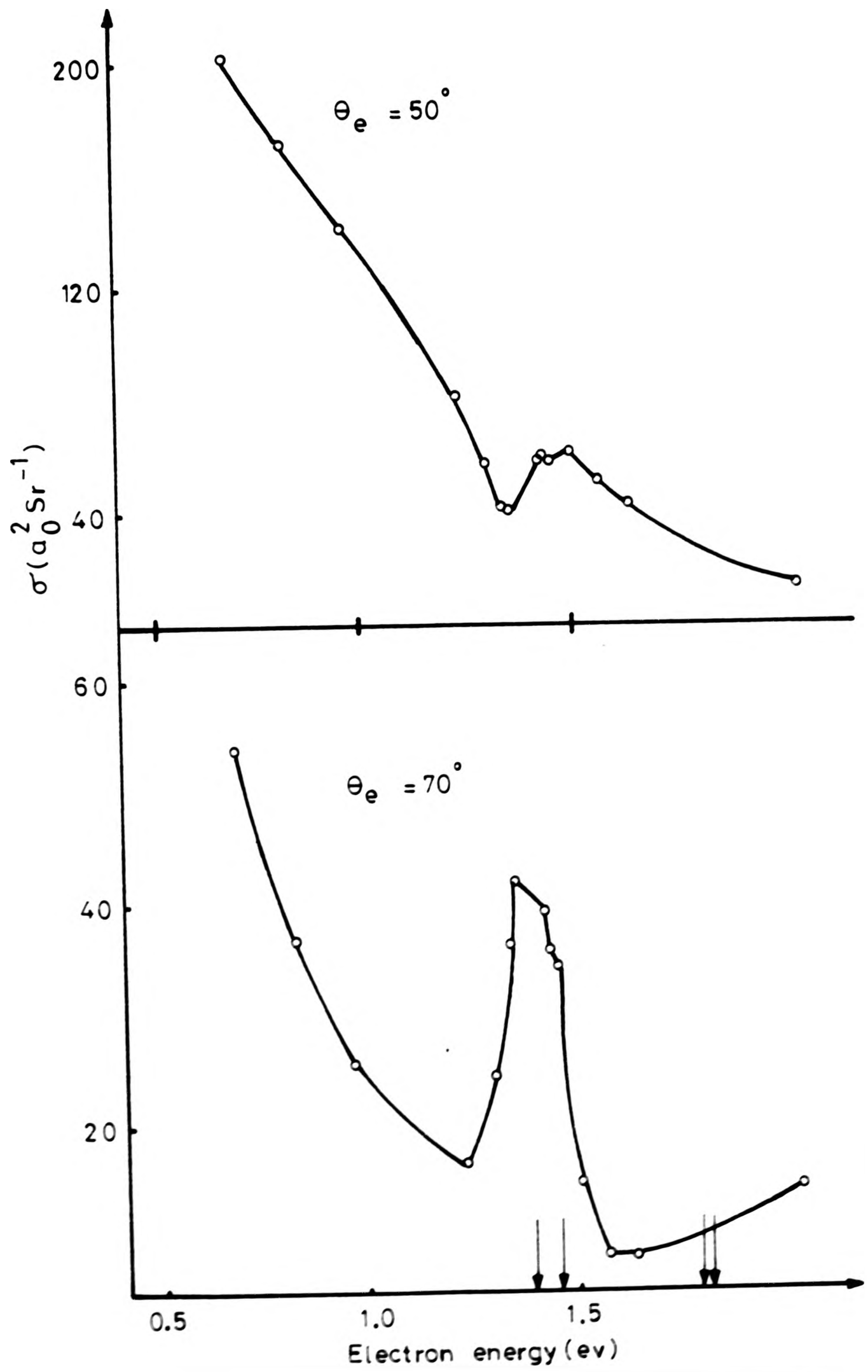


Figure 28

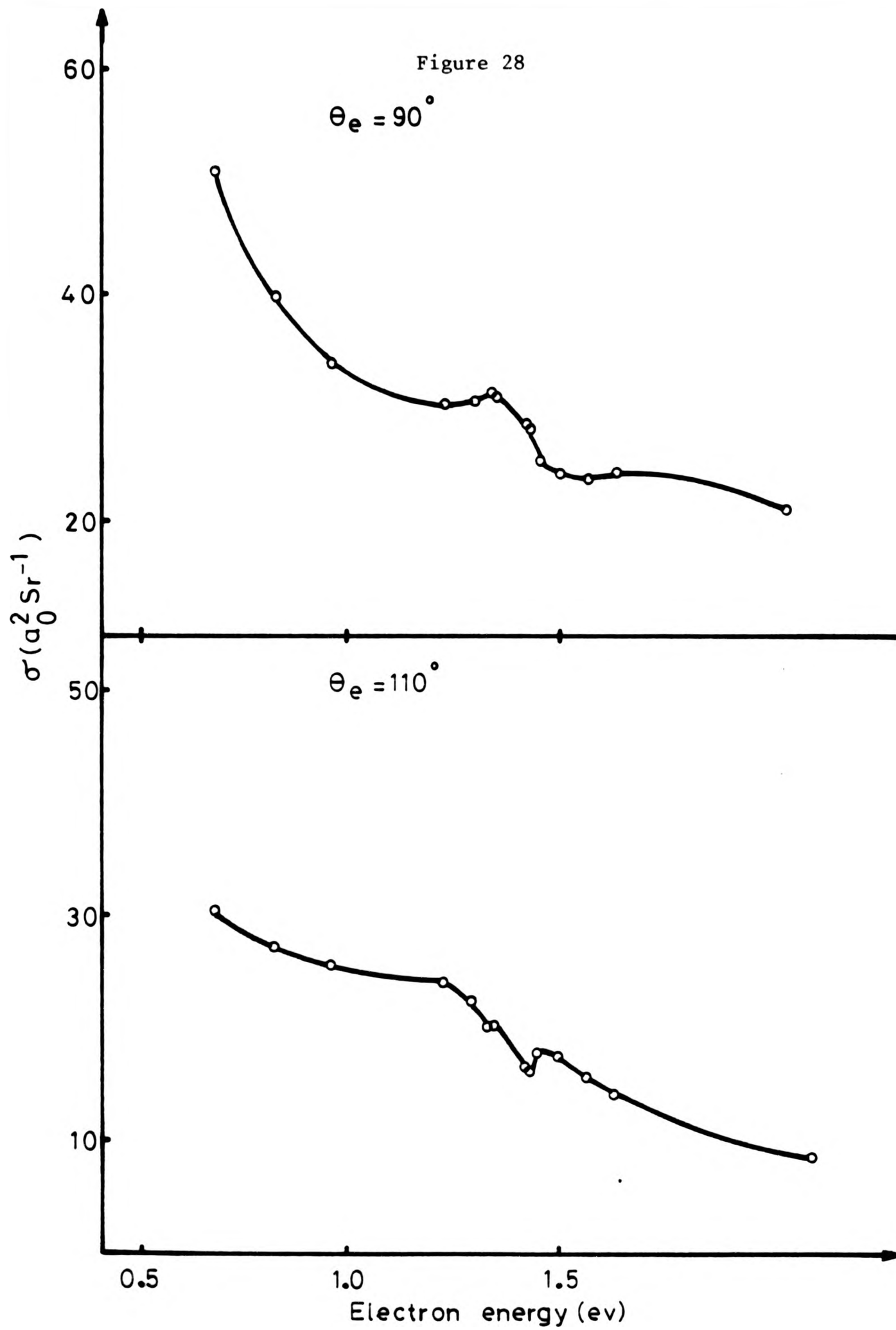


Figure 29

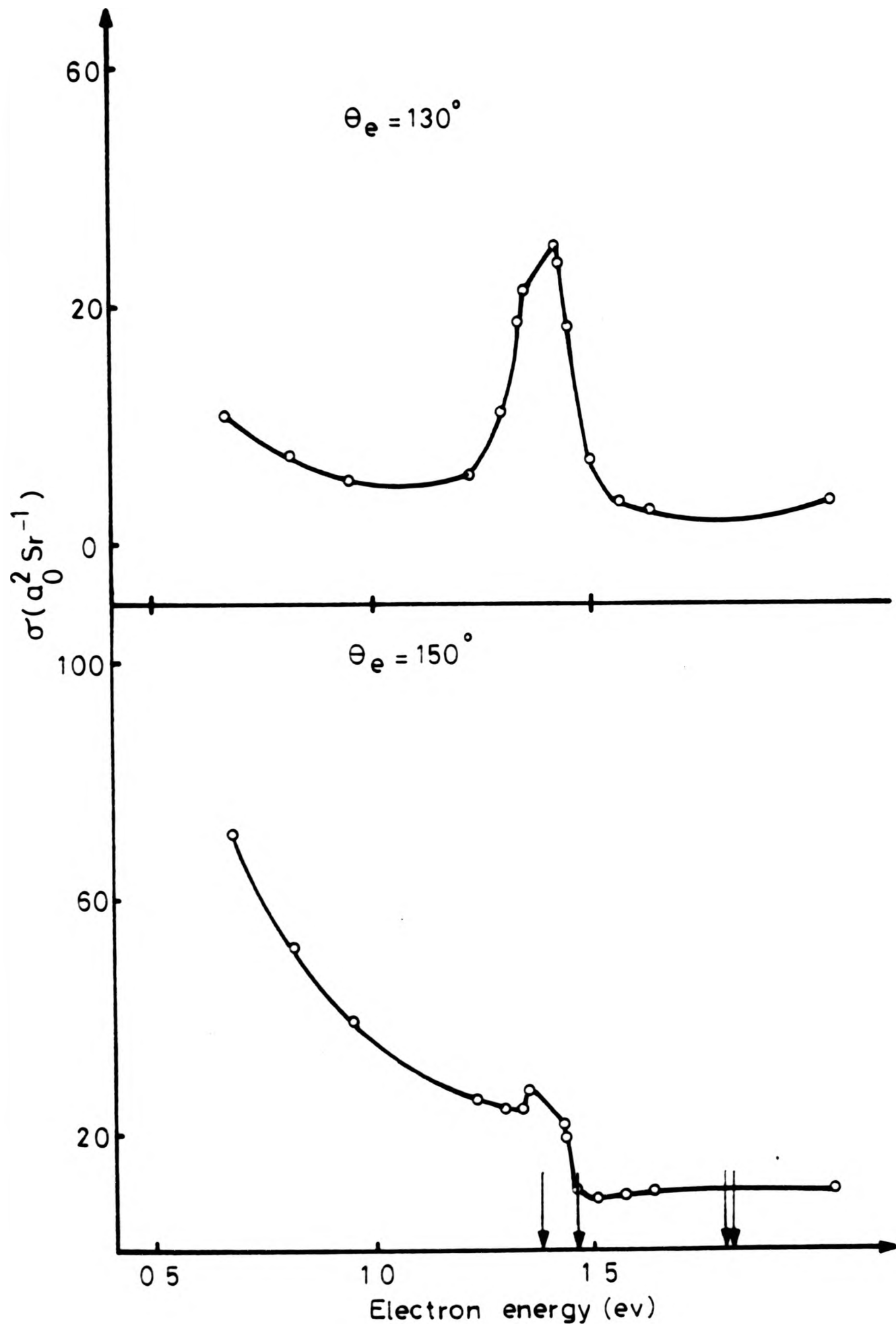


Figure 30

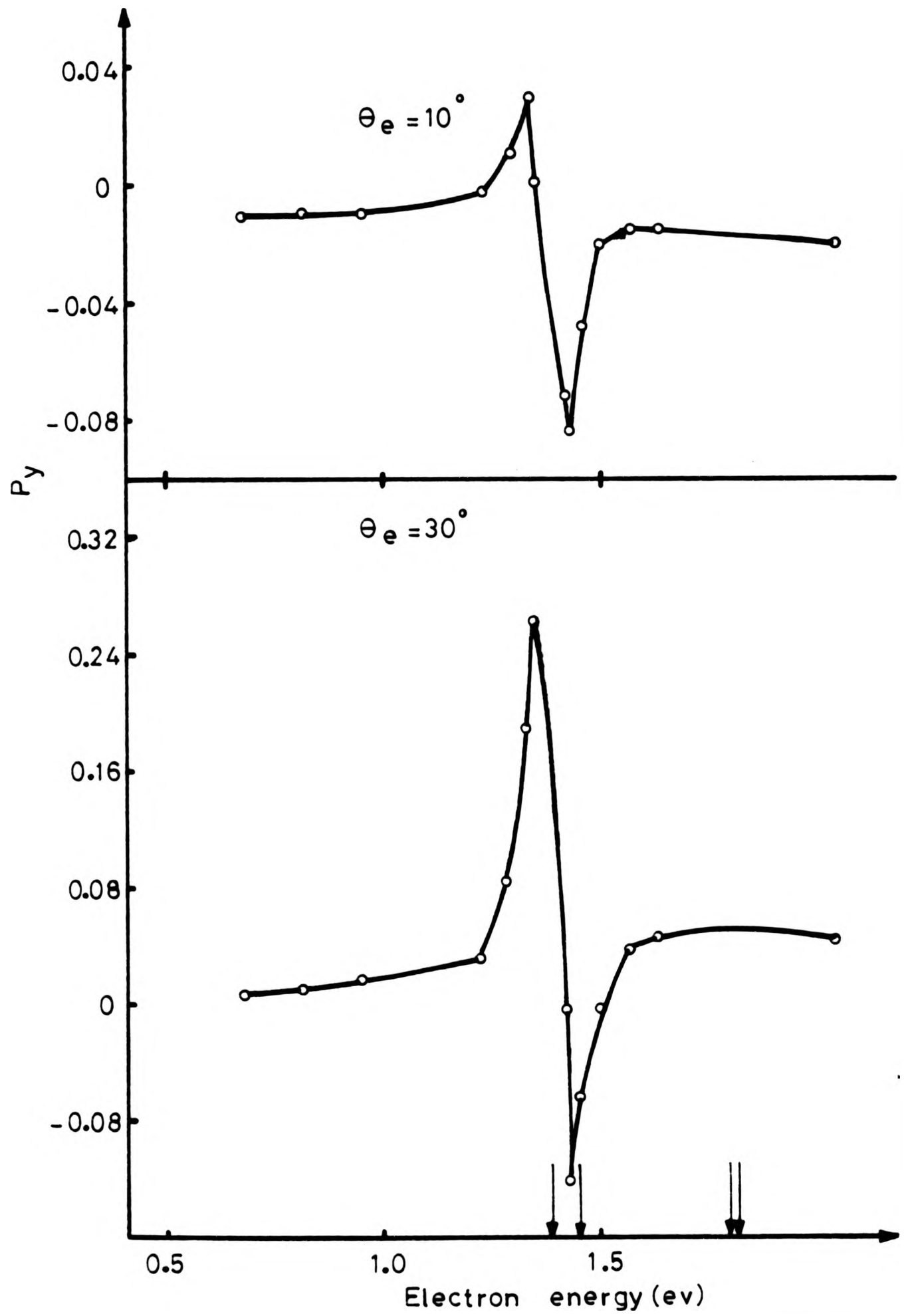


Figure 31

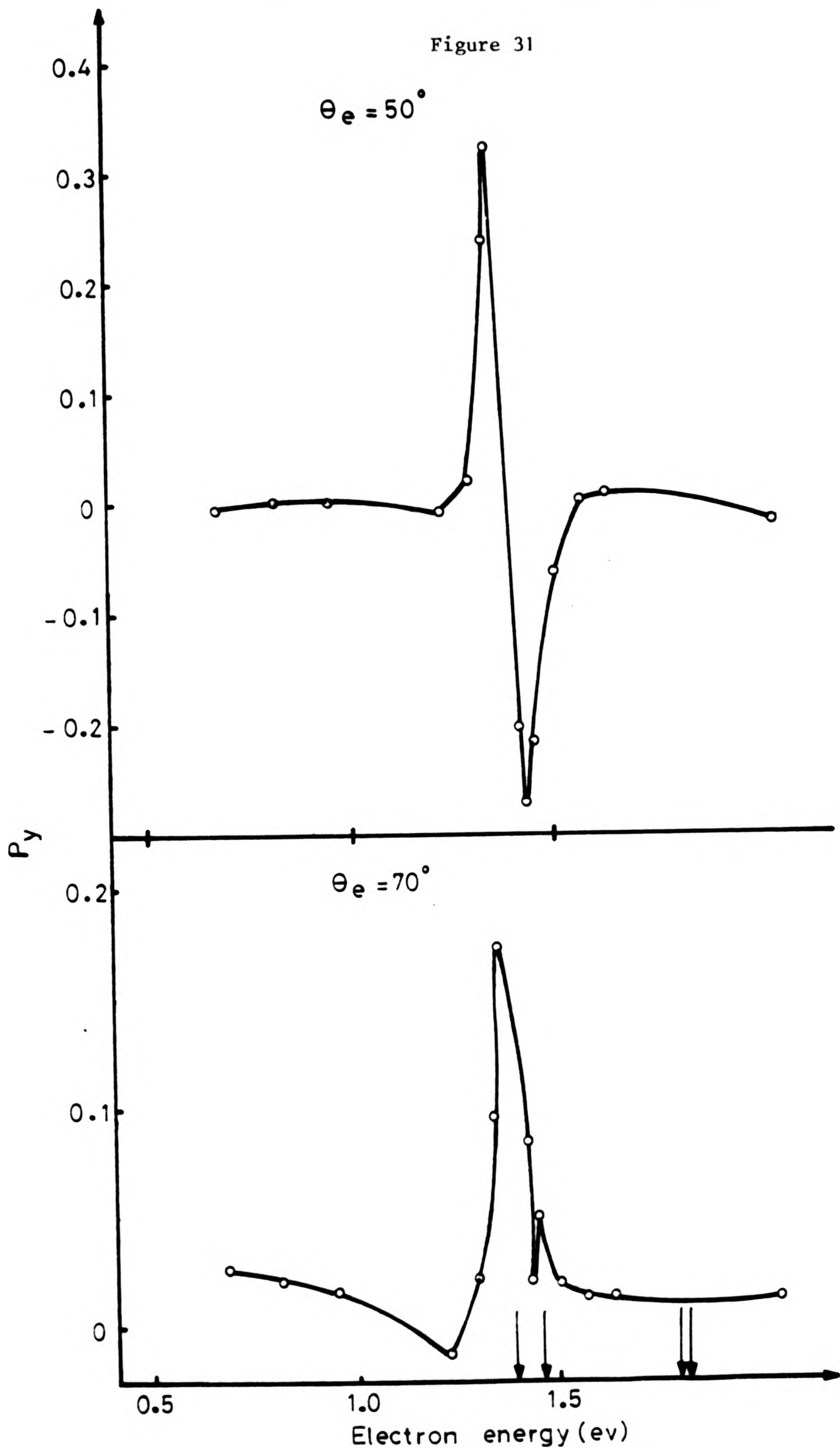


Figure 32

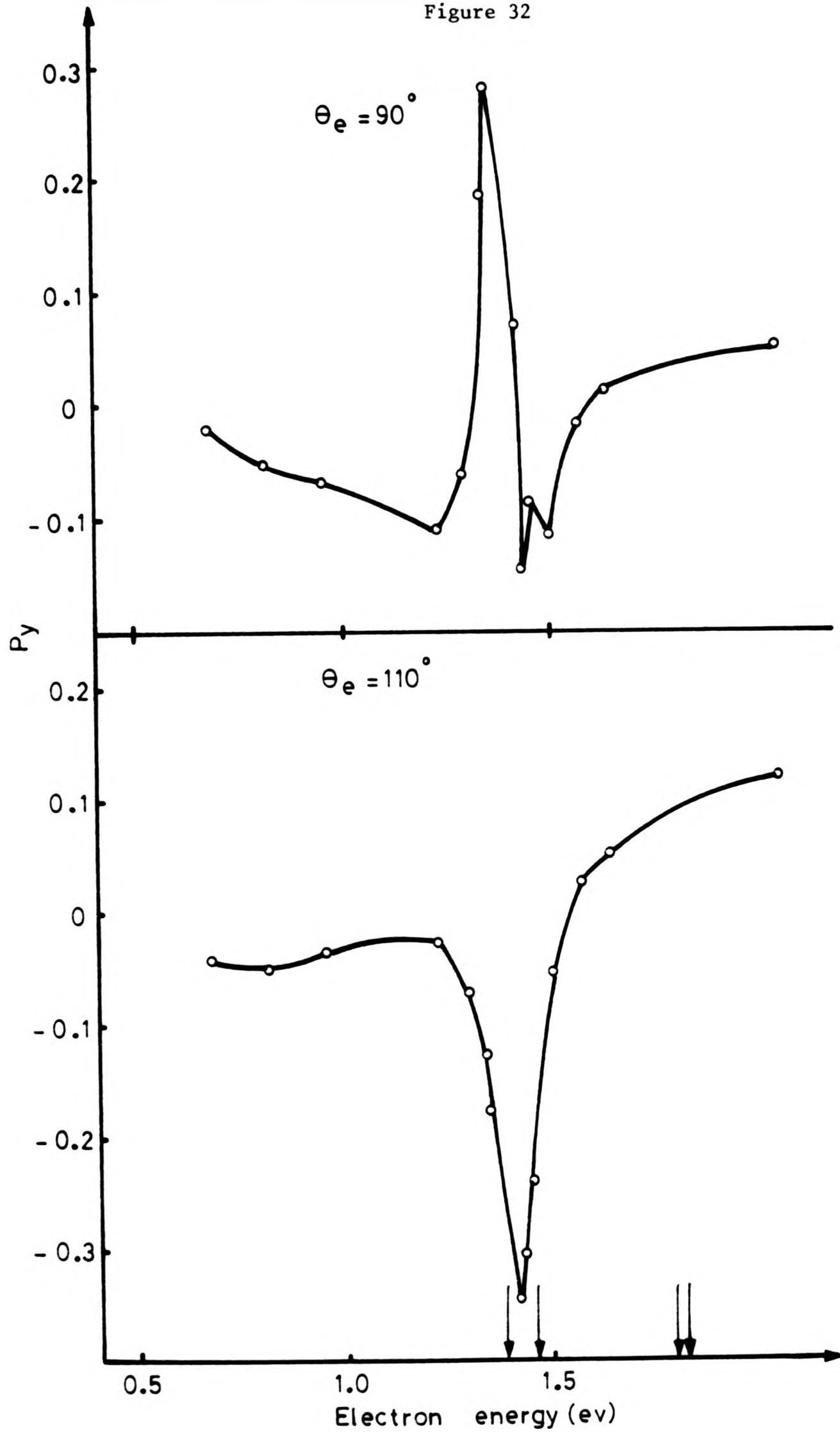


Figure 33

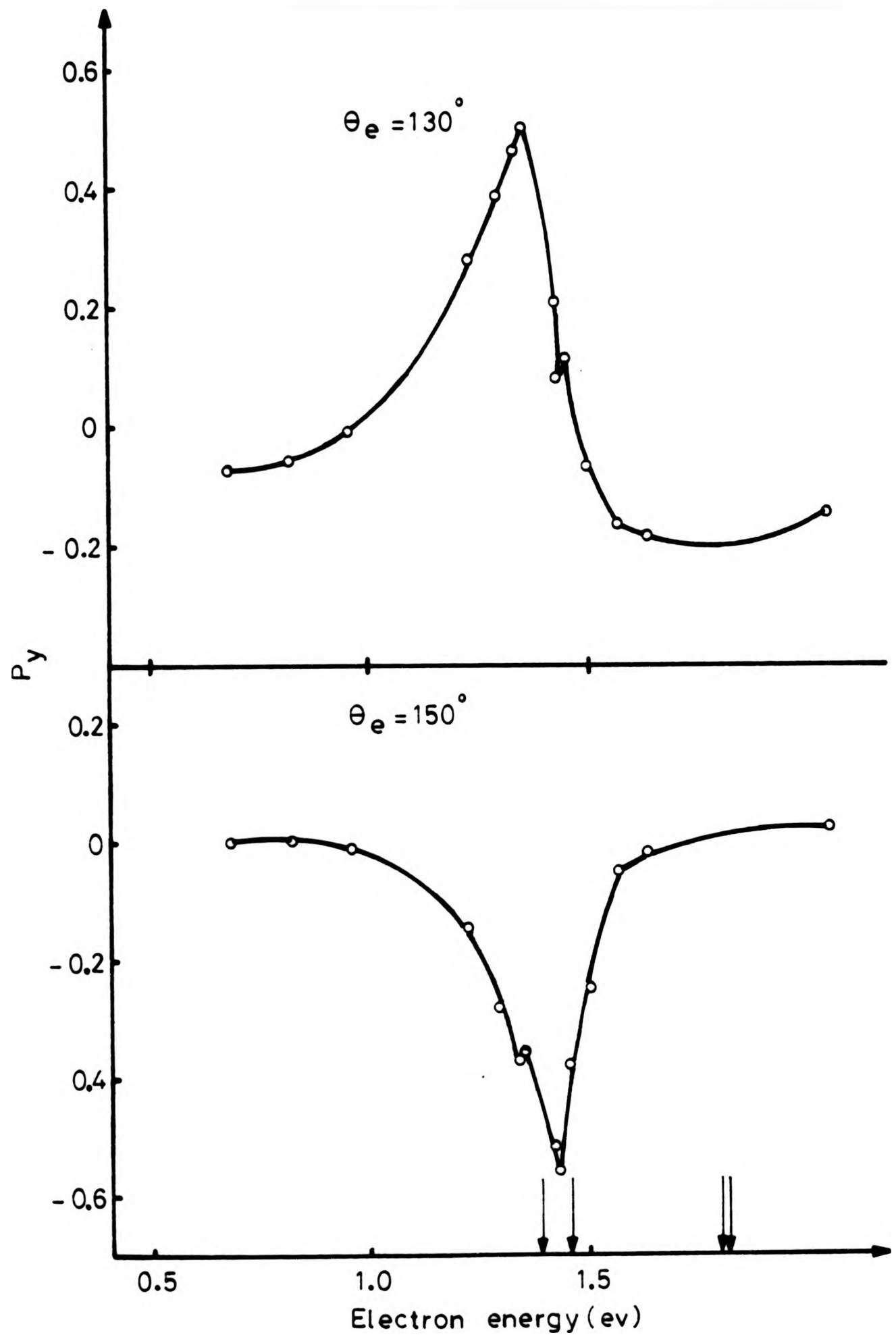


Figure 34

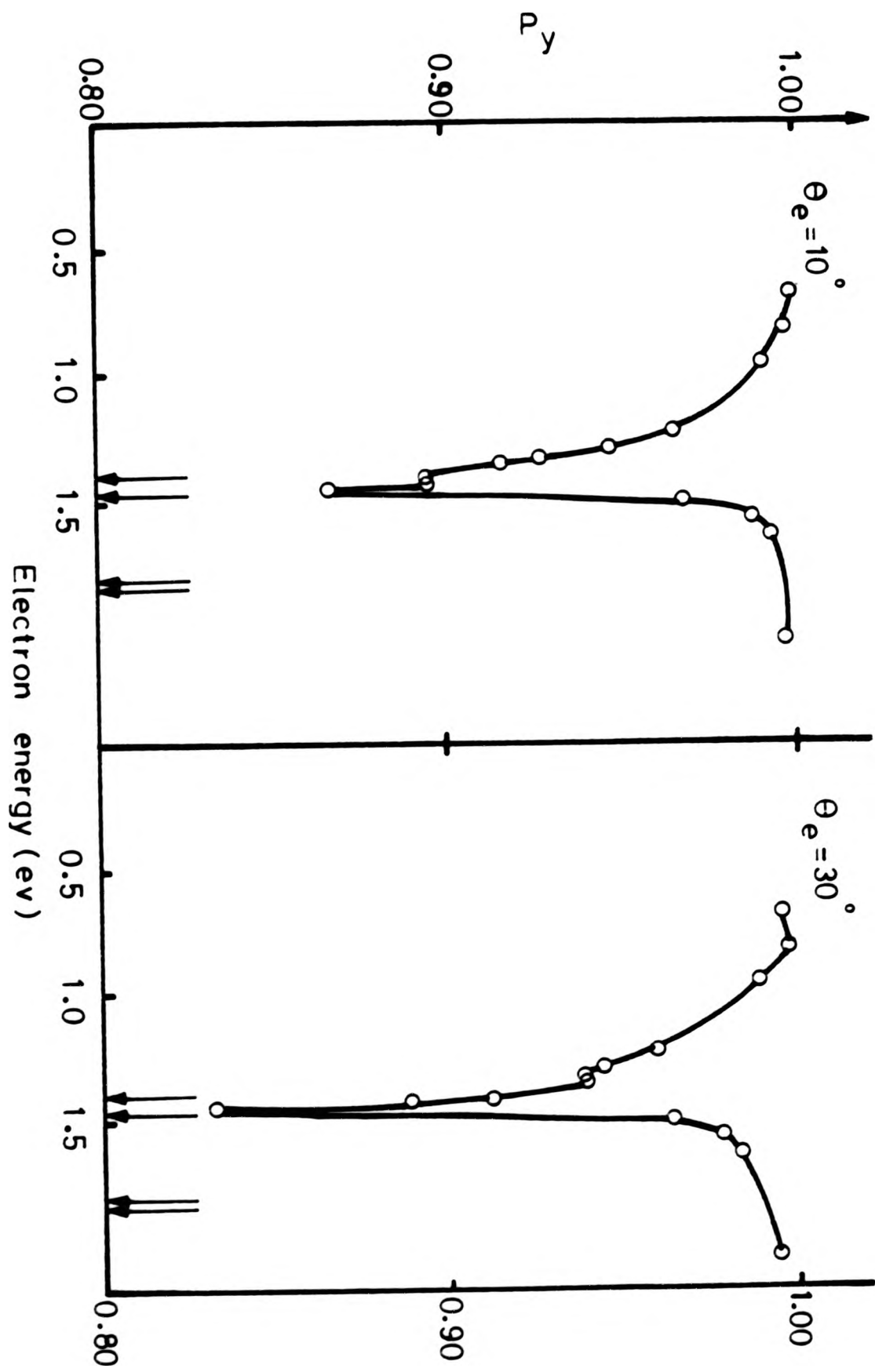


Figure 35

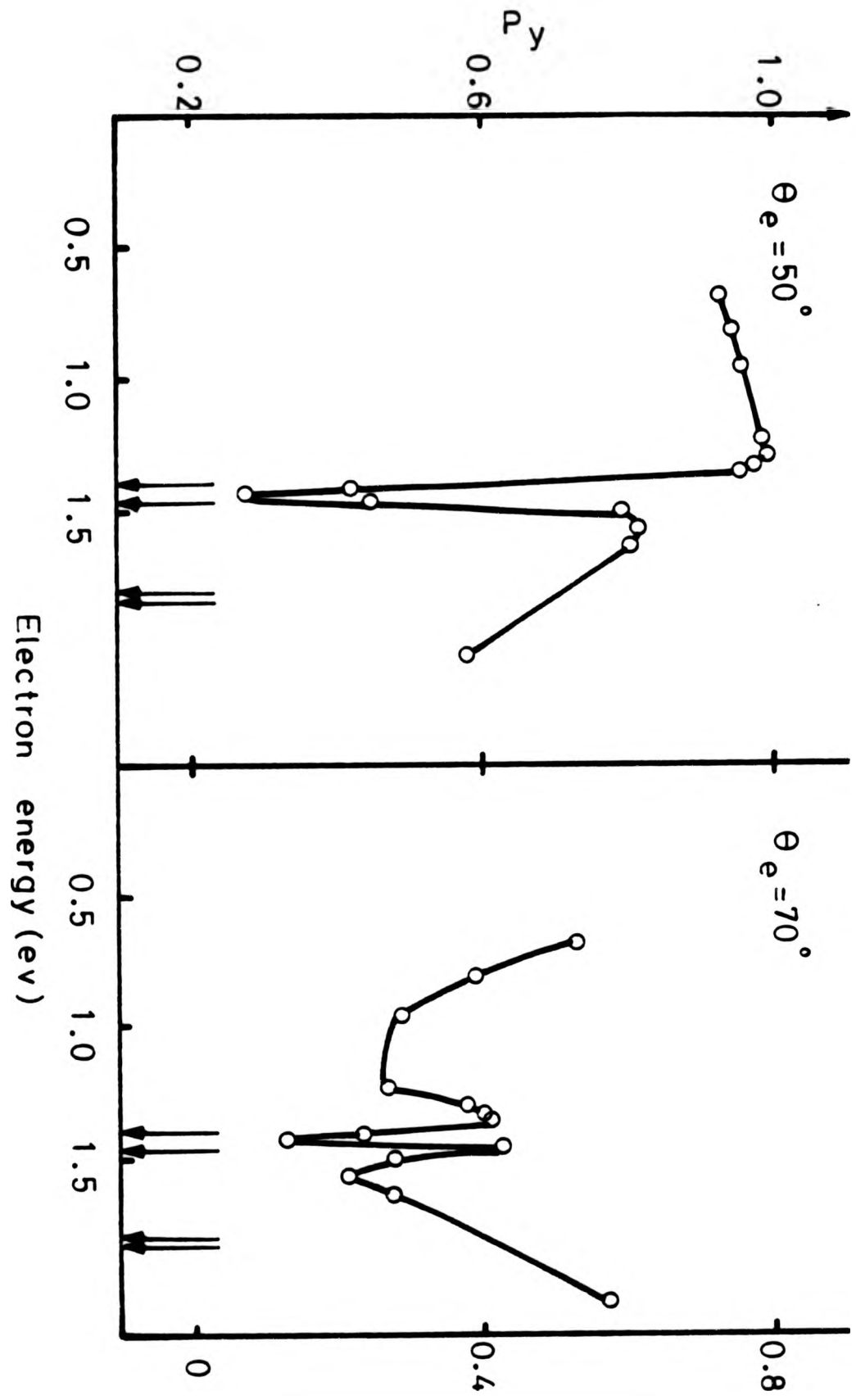


Figure 36

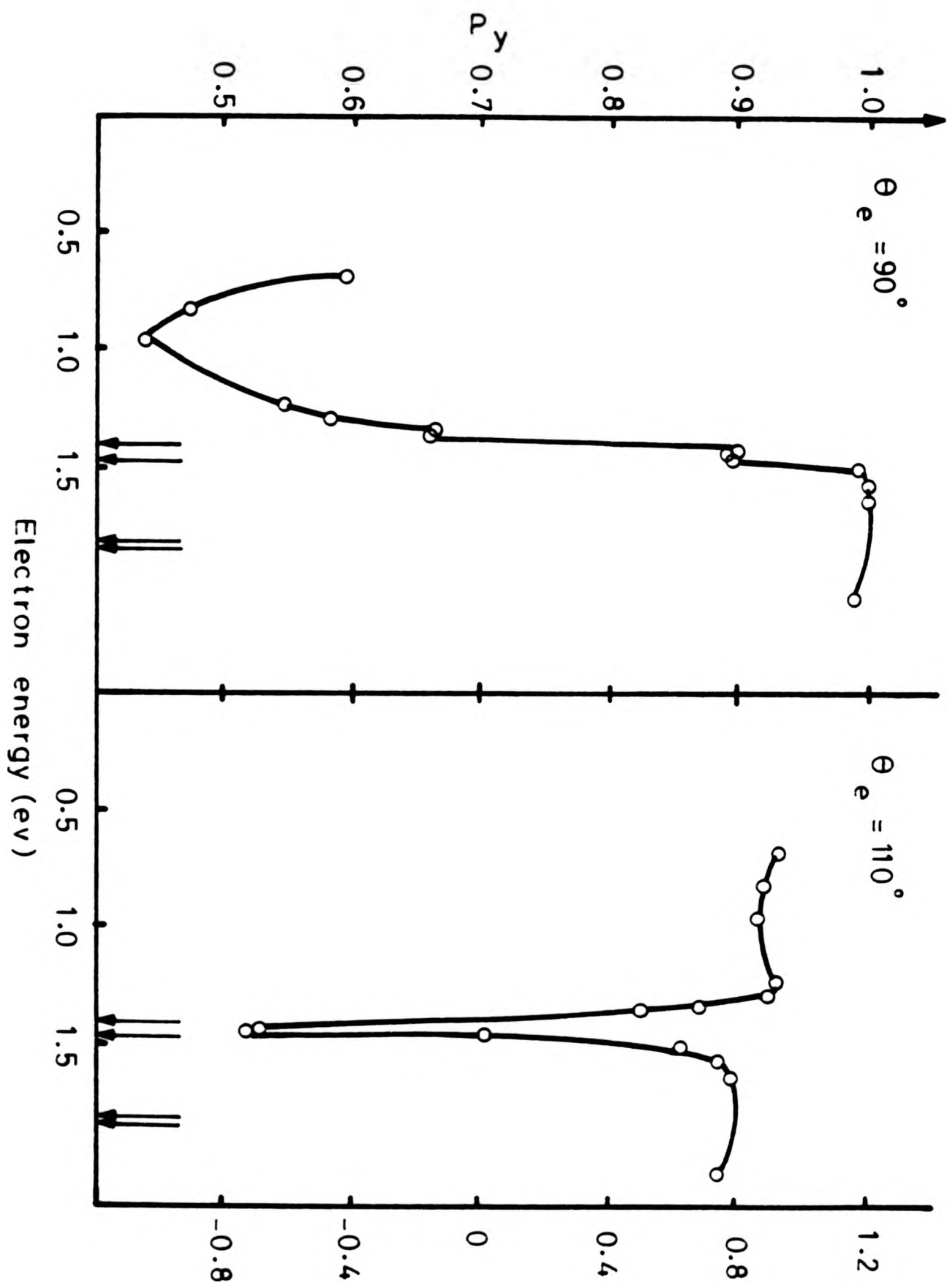


Figure 37

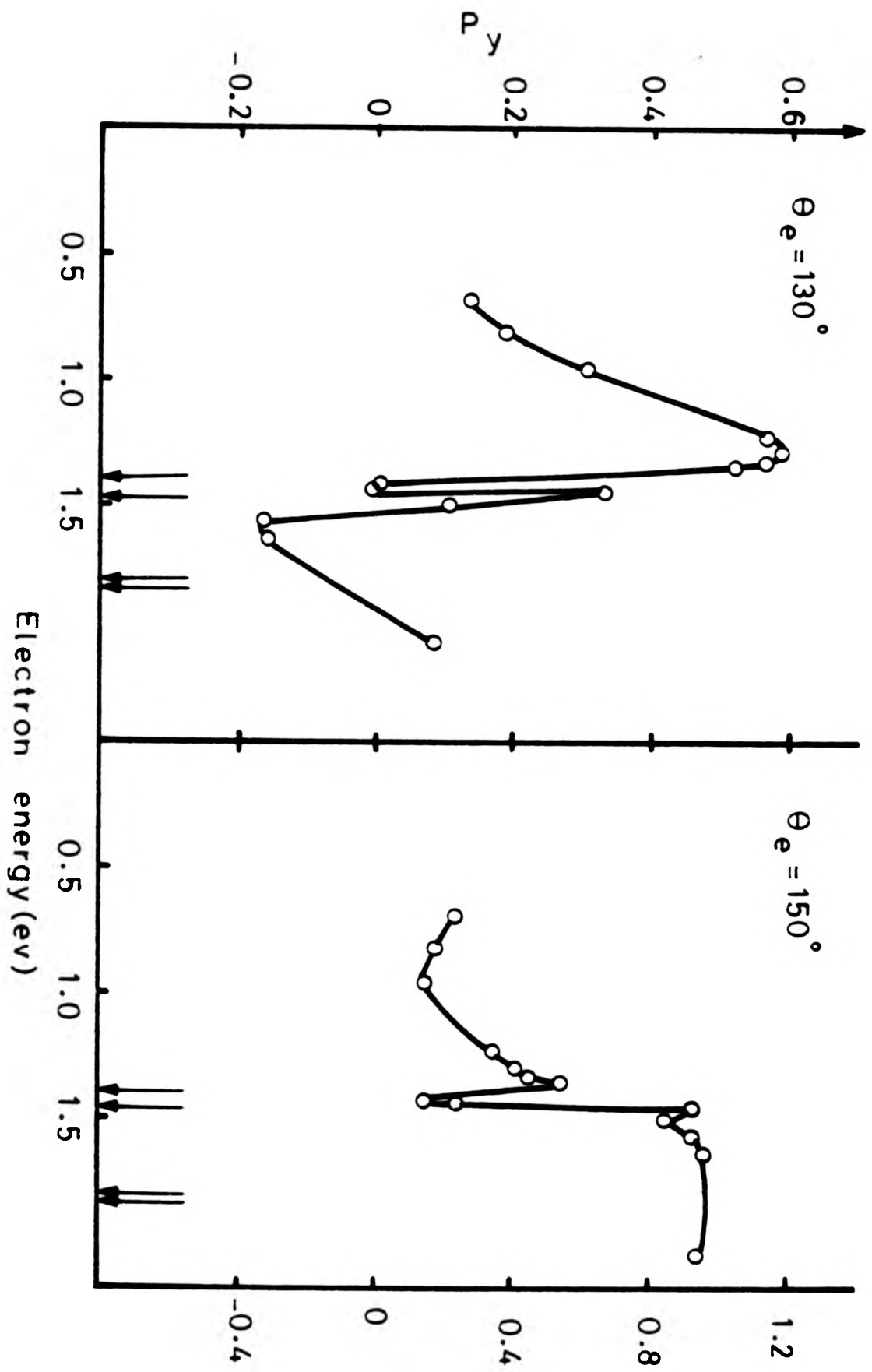


Figure 38

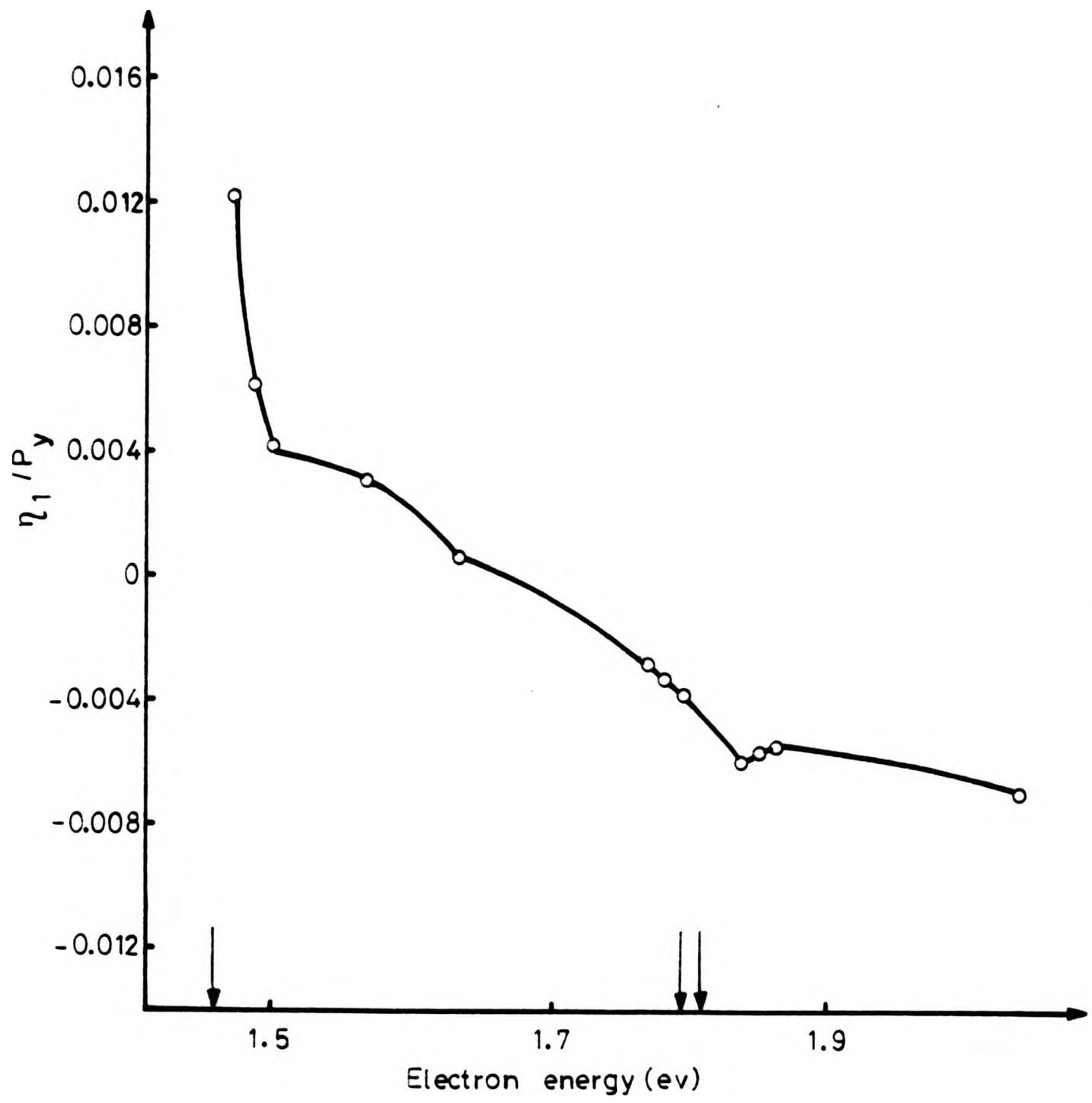


Figure 39

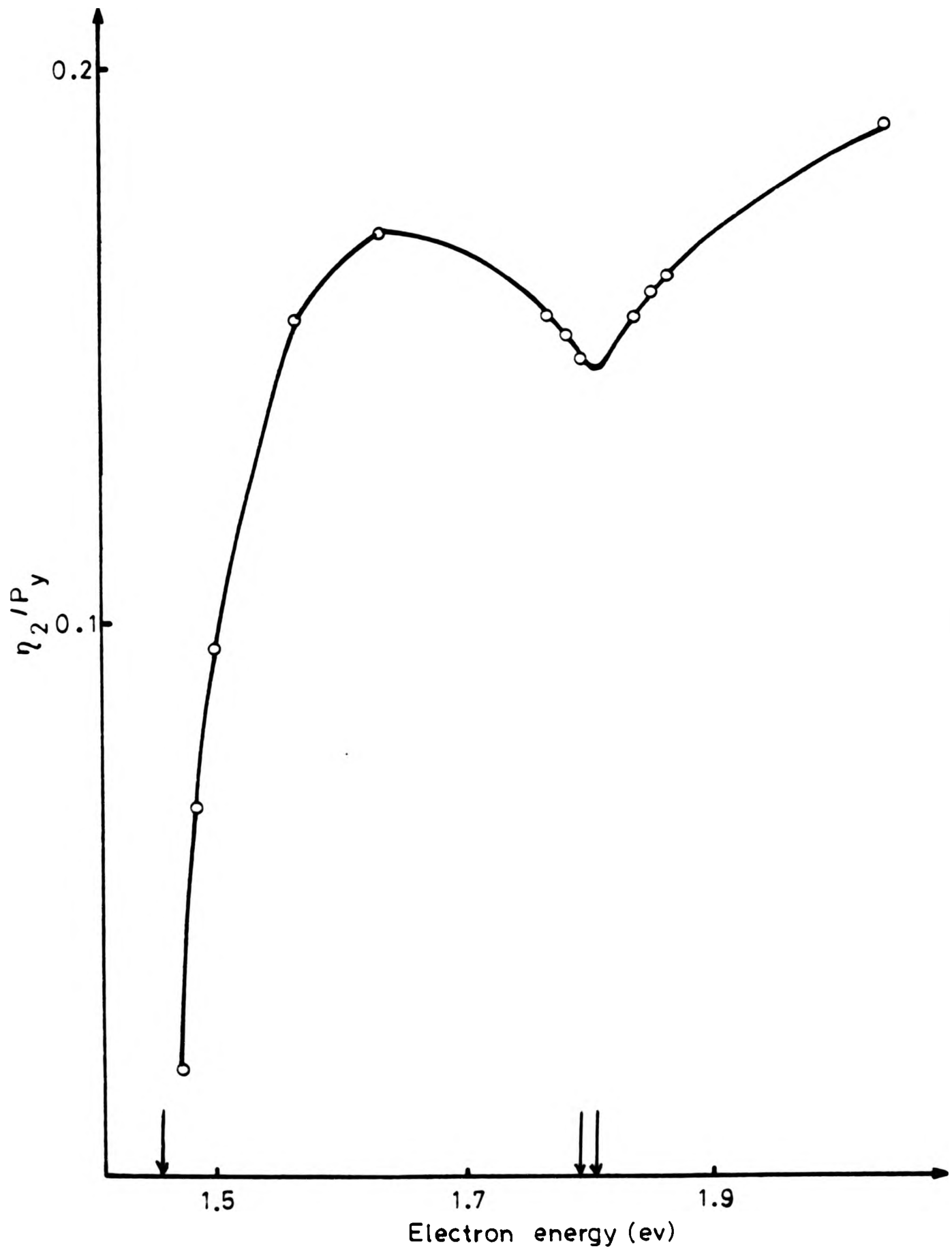


Figure 40

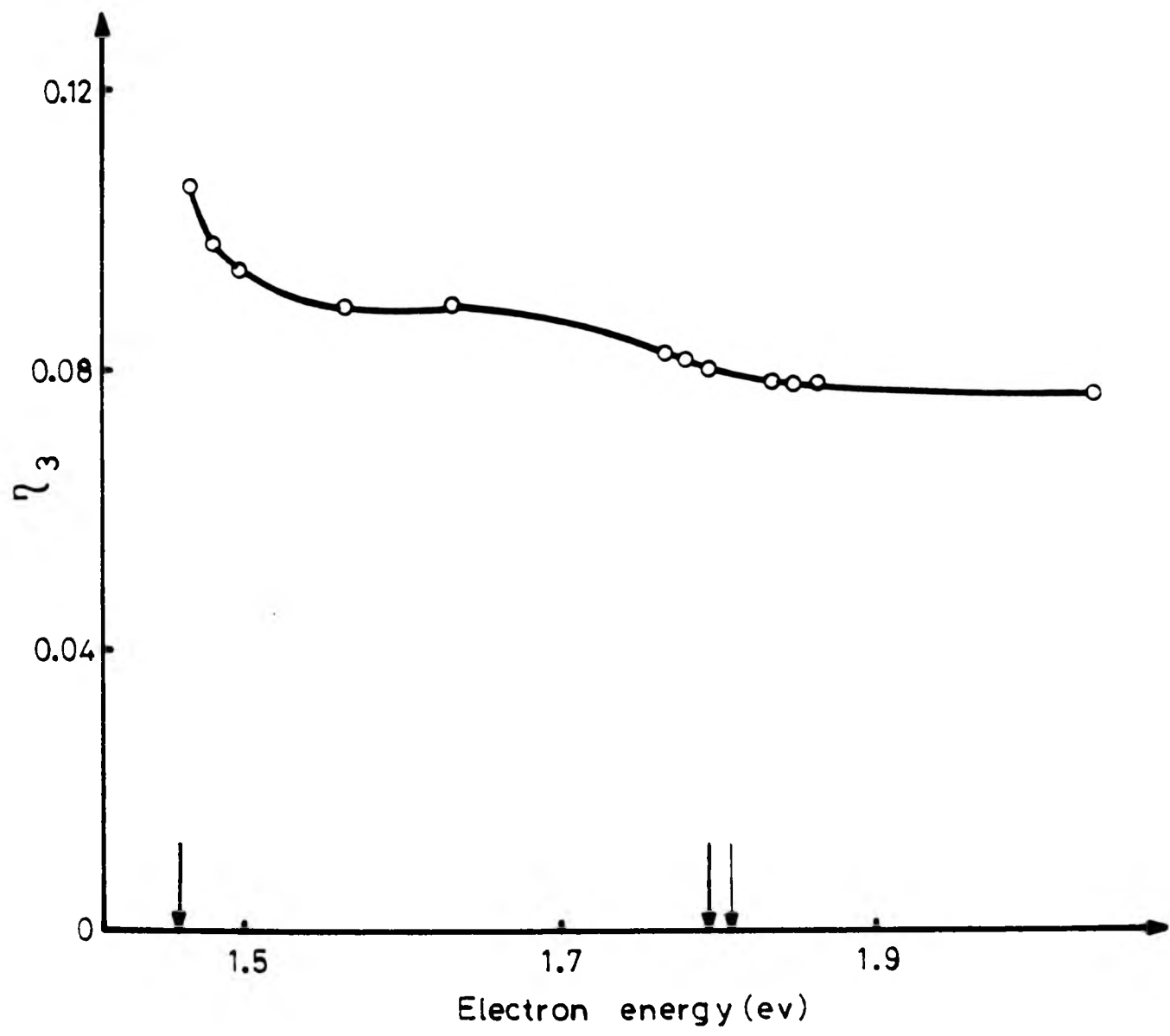


Figure 41

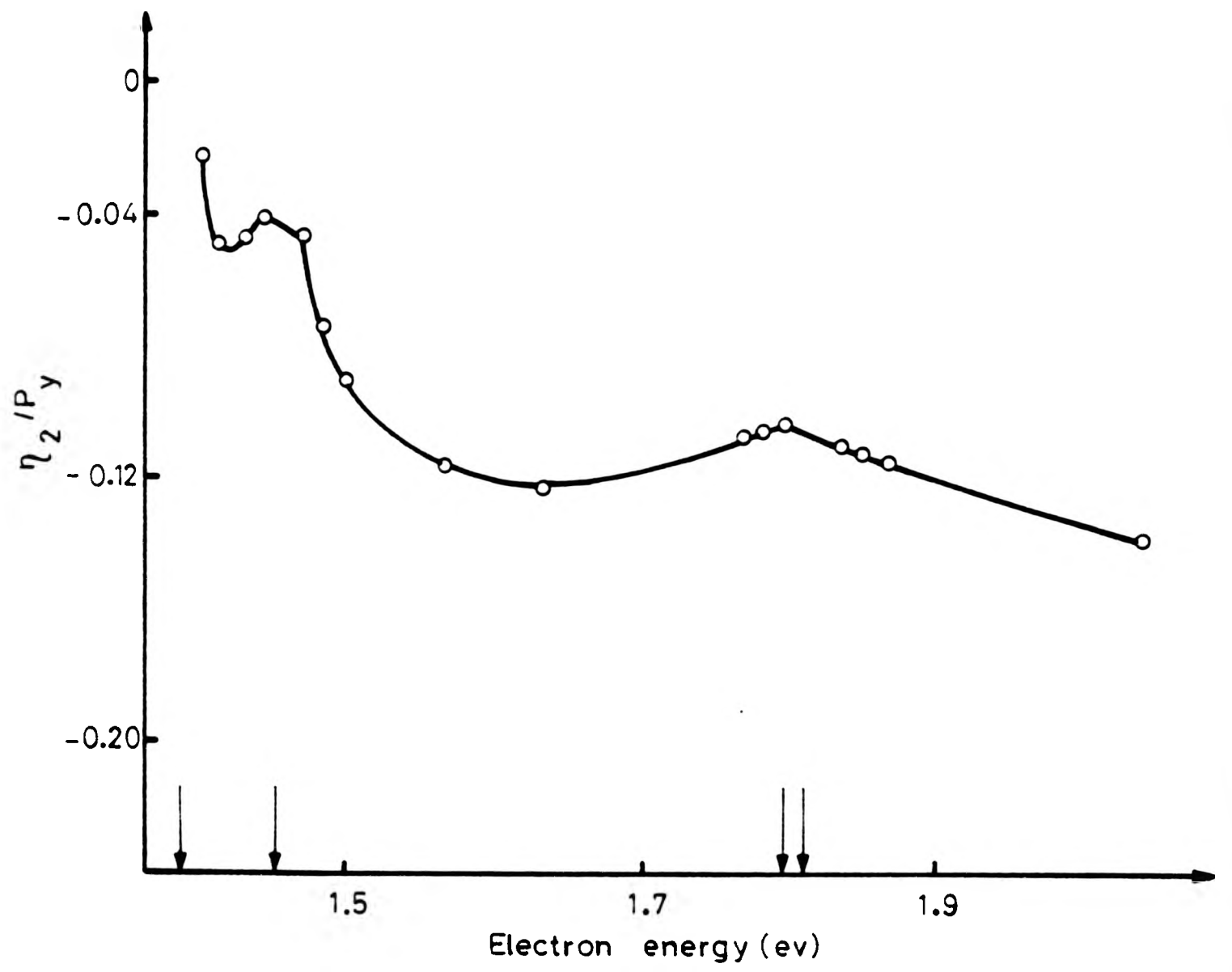


Figure 42

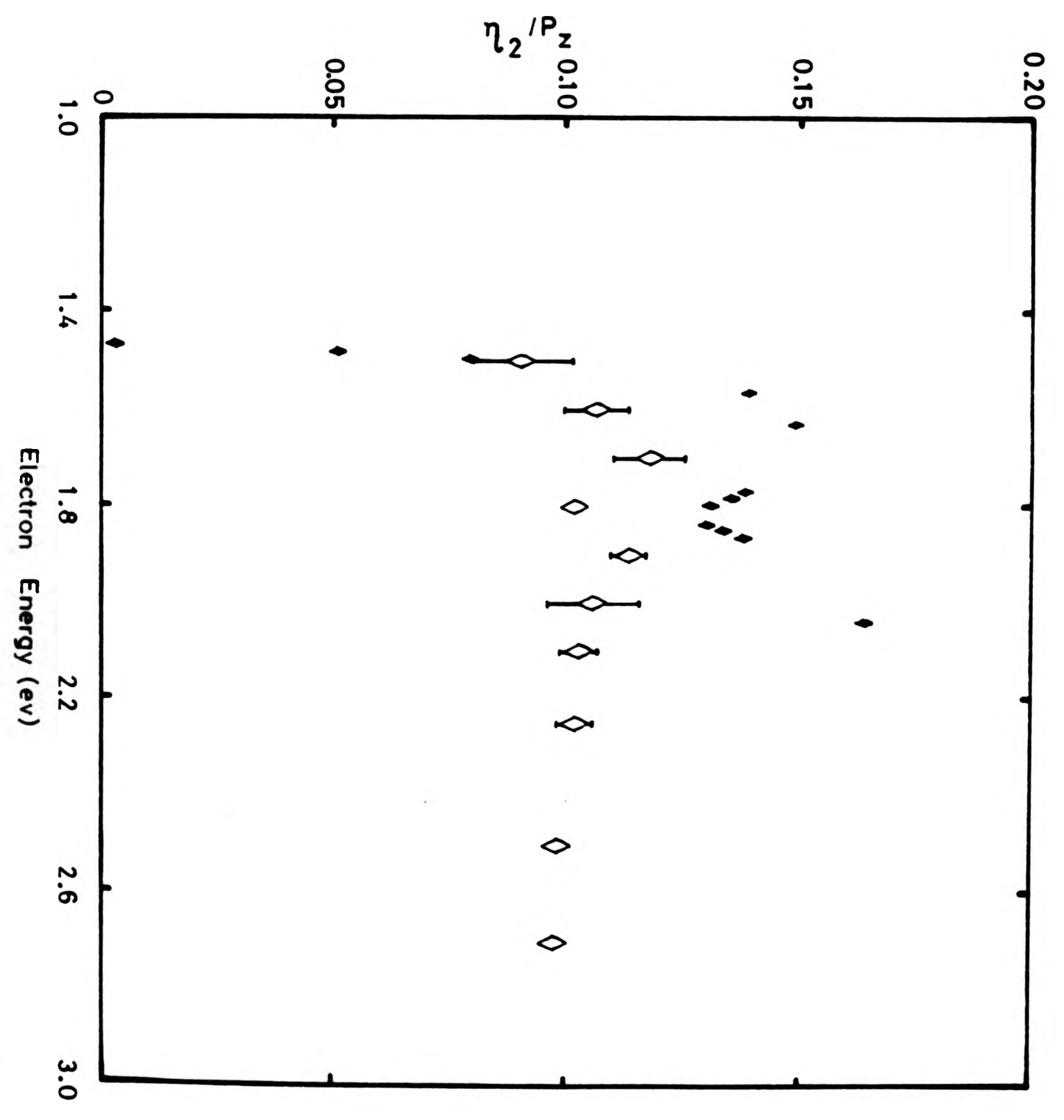


Figure 43

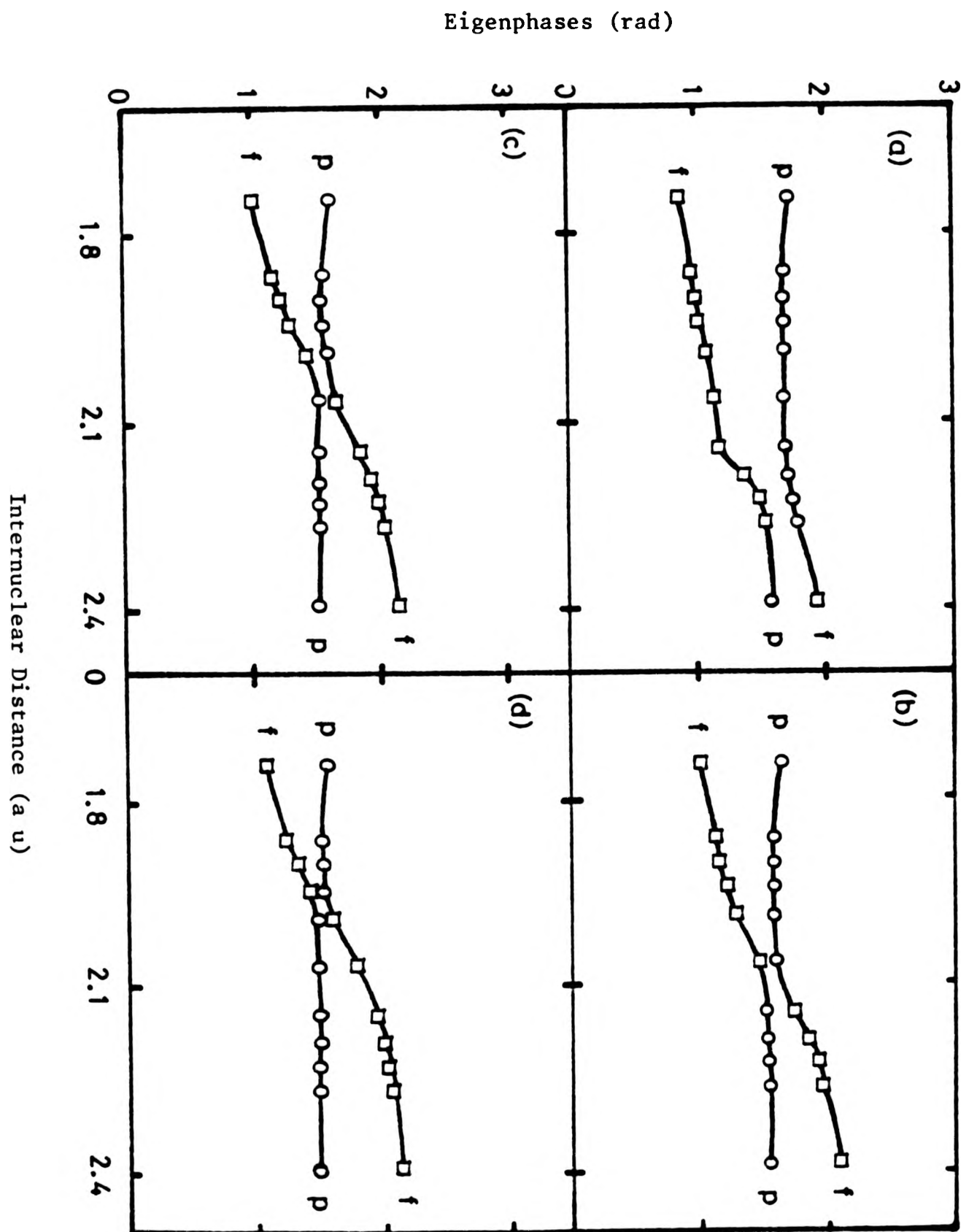


Figure 44

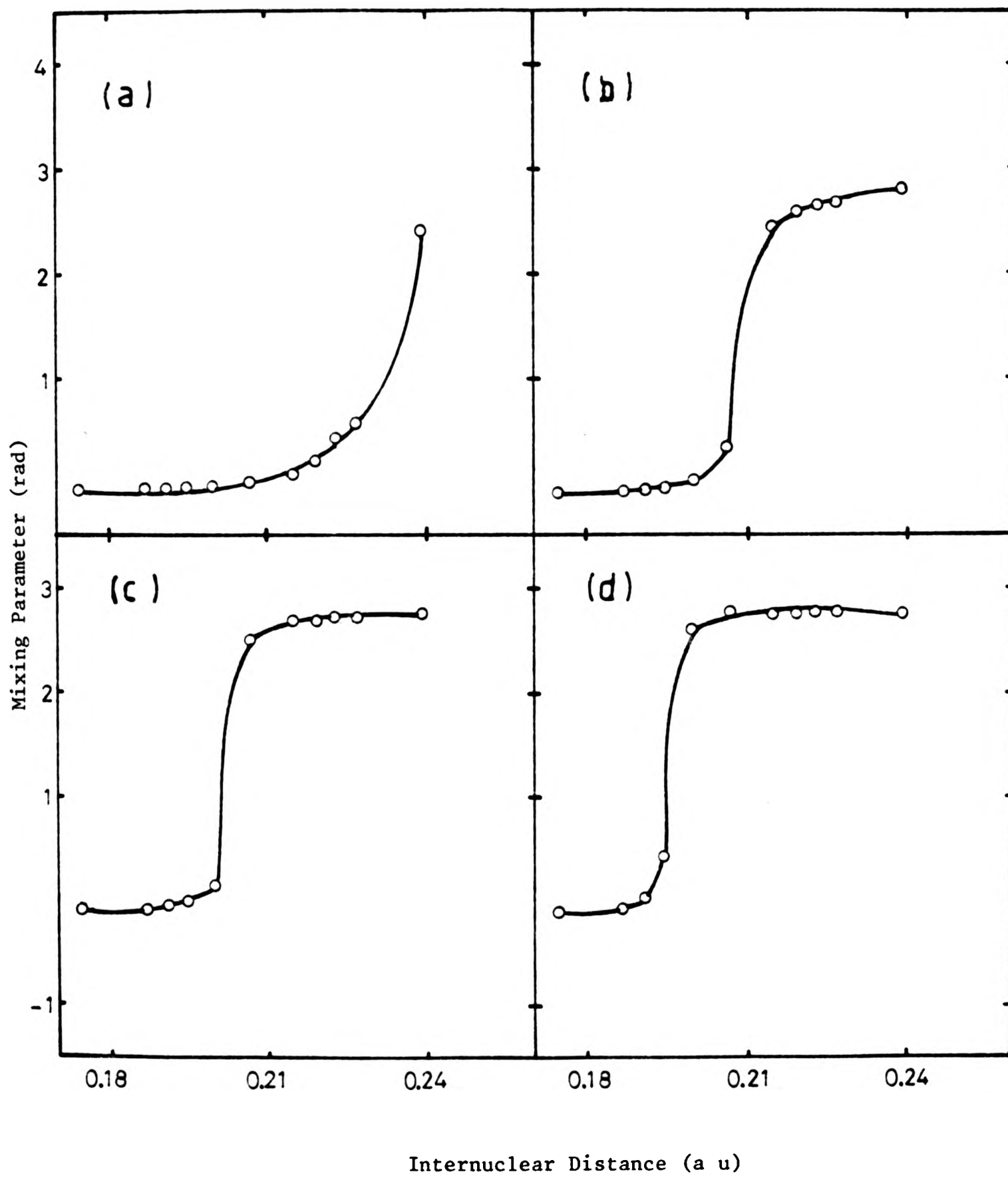


Figure 45

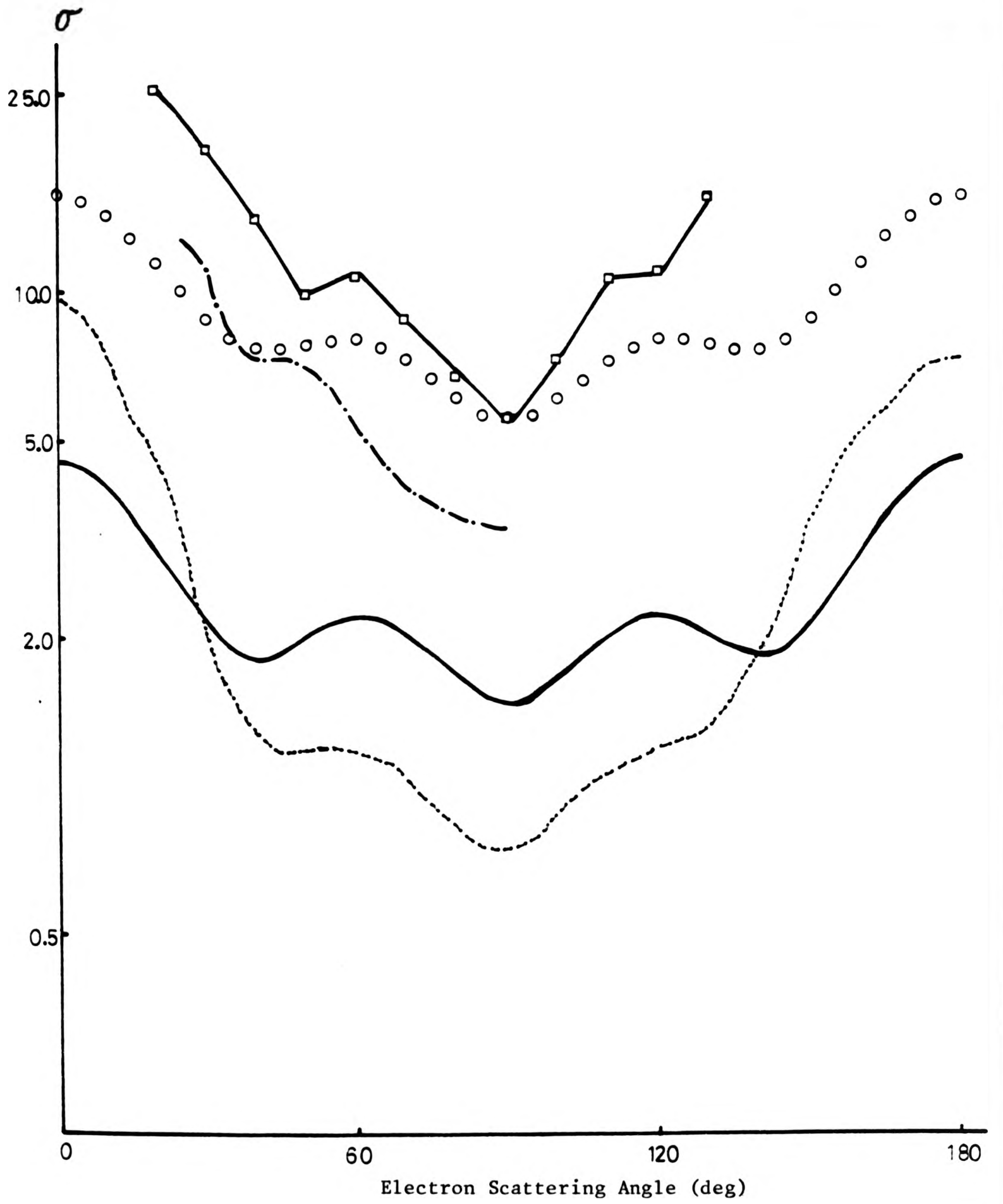


Figure 46

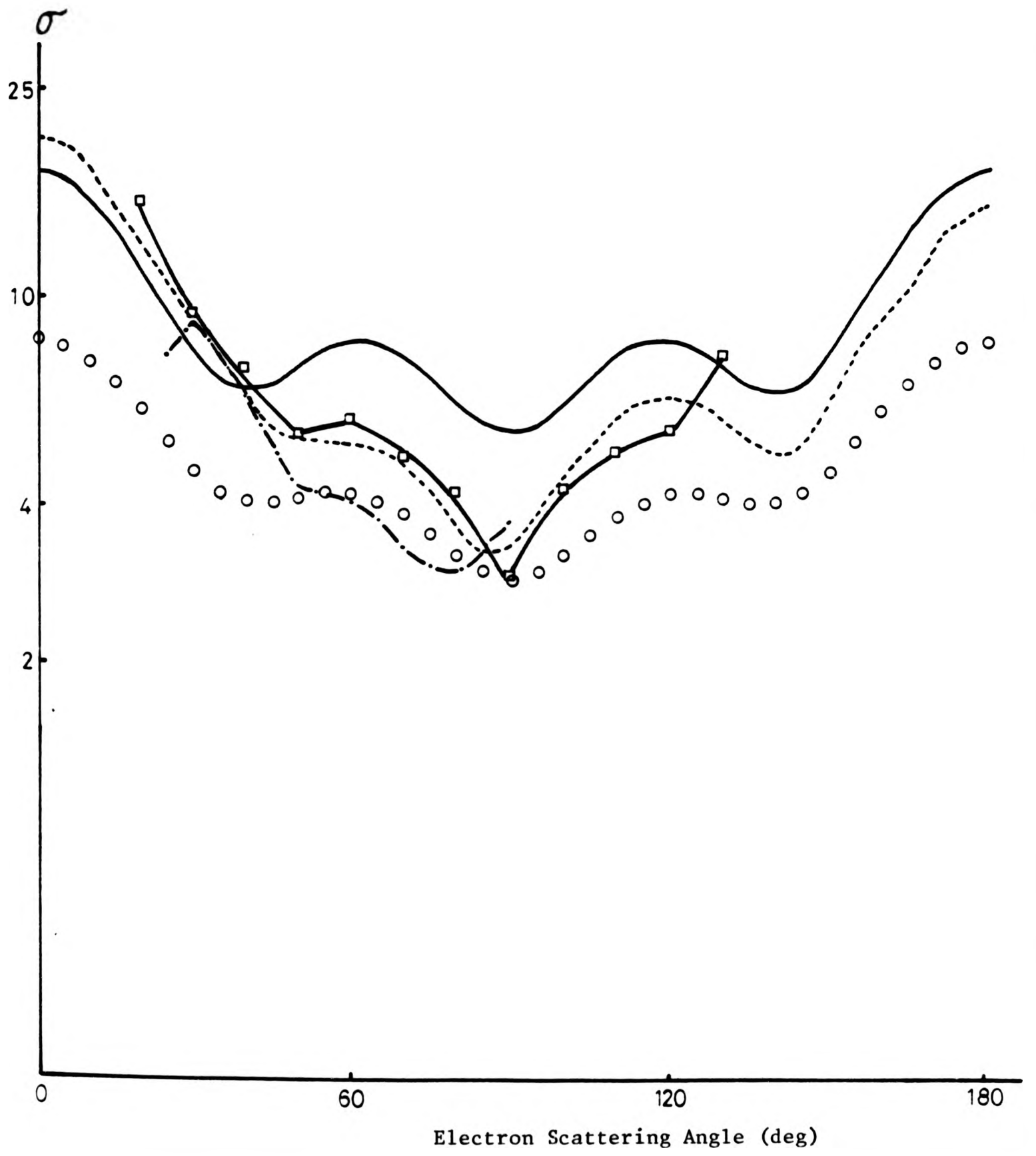


Figure 47

